

Eternal traversable wormhole

Juan Maldacena¹ and Xiao-Liang Qi^{2,1}

¹Institute for Advanced Study, Princeton, NJ 08540, USA

²Stanford University, CA 94305, USA

Abstract

We construct a nearly- AdS_2 solution describing an eternal traversable wormhole. The solution contains negative null energy generated by quantum fields under the influence of an external coupling between the two boundaries. In parallel, we discuss two SYK systems coupled by a relevant interaction. The physics of the two cases is very similar. They both share a “gravitational” subsector which is identical. The solution within this subsector sets the stage for dynamics which is almost conformal invariant. We study this system in detail, both in gravity and in the SYK model. The coupled SYK models have an interesting phase diagram at finite temperature, displaying the usual Hawking-Page transition between the thermal AdS phase at low temperature and the black hole phase at high temperature. Interestingly, these two phases are continuously connected in the microcanonical ensemble.

*Dedicated to the memory of Joe Polchinski,
an outstanding colleague in many dimensions.*

Contents

1	Introduction and motivation	2
2	Nearly AdS_2 gravity with a global time isometry	4
2.1	Global AdS_2	4
2.2	Nearly AdS_2 gravity	5
3	Two coupled SYK models	8
3.1	Review of the SYK model	8
3.2	Two coupled SYK models	10
3.3	Low energy analysis	11
4	Low energy analysis of the coupled theory	13
4.1	Classical solution	13
4.2	Quantum version	17
4.3	Getting the thermofield double from a quench	19
4.4	Computing the leading correction to the overlap	20
4.5	Finite temperature	22
4.5.1	Lower temperatures	22
4.5.2	Higher temperatures	24
4.6	Some properties of correlation functions	26
4.7	The three generators of $SL(2)$	28
5	The two coupled SYK models beyond the low energy limit	29
5.1	Large N equations	29
5.2	Numerical analysis	31
5.3	Large q analysis. Zero temperature	35
5.4	Large q at finite temperature	38
5.5	Overlap of the ground state and the TFD at large q	45
5.6	Different microscopic couplings	50
6	Conclusions and discussion	51
A	Thermodynamics of the two coupled SYK models at large q	54
A.1	Inverse temperature of order $q \log q$	54
A.2	Inverse temperature of order $\beta \sim q$	56
A.3	Inverse temperatures of the form $\beta \sim \sqrt{q}$	58
A.4	Inverse temperatures of order one	60
B	$SL(2)$ charges	61

C	Boundary conditions and negative energy for a CFT in the bulk	63
C.1	Negative energy on the strip goes to zero energy in AdS_2	63
C.2	Negative energy for a free fermion AdS_2 plus a boundary interaction . . .	64
C.3	Profile for the bulk dilaton	65
D	Derivation of the Liouville effective action	66
E	The two-time solution	68

1 Introduction and motivation

AdS_2 is a very simple two dimensional spacetime that has two asymptotic boundaries. Furthermore, AdS_2 , viewed as a global spacetime, has two boundaries that are causally connected. We can send a signal from one boundary to the other. It behaves like a traversable wormhole! See figure 1(a).

In this paper we consider physical situations where a spacetime very similar to AdS_2 arises, in the framework of nearly- AdS_2 gravity [1, 2, 3, 4]. It involves a solution that balances classical and quantum effects. In order to get the computation under control one needs a large number of quantum fields. These quantum fields are in a state with negative null energy because we set up an interaction between the two boundaries. This is an interaction that looks non-local in the bulk, but could arise locally in a higher dimensional ambient space. This is like the interaction that makes wormholes traversables [5]. In this case, we get a traversable wormhole that is static and time independent, an eternal traversable wormhole.

We also analyze a closely related problem in the SYK model [6, 7, 8]. We consider two identical SYK models coupled by a simple bilinear term. When the coupling is small, the low energy physics of the model is nearly conformal and its features can be described by the reparametrization mode described in [7, 8, 9, 10]. In fact, the SYK model and the nearly- AdS_2 spacetime share a common subsector that is associated to gravitational physics. For this common subsector we can perform an analysis that is valid for both cases. This means that the basic mechanism that renders the wormhole traversable is common to both, and relies on the physics of the emergent spontaneously and explicitly broken time reparametrization symmetry. This common description is valid when the interaction between the two systems is relatively small, so that its effects become significant at the energy scales where the SYK model is nearly scale invariant. It is expected to be valid for any quantum mechanical system with an emergent approximate conformal symmetry in the IR. This version of coupled SYK model is also interesting purely from the quantum mechanical point of view. We get a gapped system, which in itself is not surprising, but we get an excitation spectrum that is largely controlled by an $SL(2)$ symmetry that is broken in a controlled way. The net result is that one can predict the spectrum of excitations of the model. The energy levels are set by the dimensions of operators of a single SYK model. A similar feature is present in higher dimensional CFT_d s where the spectrum of operators

of the theory is related to the spectrum of energies of the CFT_d on an $S^{d-1} \times (\text{time})$. In this case we have a nearly- CFT_1 and an S^0 consists of two points, which are the two copies of SYK. So, our construction can be a way to realize a form of the state/operator map in a nearly- CFT_1 . Of course, here we need to add an extra interaction between the two sides. So there are some similarities and differences with the higher dimensional situation. In this paper we spell them out in detail. It should be noted that various models with interplay of SYK interaction and bilinear terms have been studied in the literature, such as [11, 12, 13, 14, 15]. Gravity solutions describing weakly interacting CFTs were discussed in [16].

In the SYK model, we can also consider stronger couplings, which we can also analyze by solving the large N Schwinger-Dyson equations. These equations can be solved numerically. They can also be solved analytically in the large q limit (q is defined in (3.14)).

In writing this paper we have tried to separate a bit the gravity and the SYK discussions so that it can be read also by readers who are not familiar with one or the other. So the reader should feel free to skip some sections.

In section 2, we review AdS_2 and nearly- AdS_2 gravity. We explain the setup that leads to a solution where we preserve the global time translation symmetry of AdS_2 . We also describe the effective action that describes gravitational effects in this theory.

In section 3 we review a single SYK model and describe the system consisting of two coupled SYK models. We describe how the reparametrization mode encodes some important aspects of the physics. This action has the same form as the one describing the gravitational modes of nearly- AdS_2 gravity.

In section 4 we analyze the common effective action that appeared in the previous two sections. We find the equations that determine the size of the energy gap of the system and the overall scale of the spectrum. We also discuss some aspects of the quantization of this action. We describe how the approximate $SL(2)$ symmetry is realized on the spectrum. We also connect the ground state of this coupled system to the thermofield double state of the two decoupled systems. It turns out that both states are very close to each other and we quantify how close they are.

In section 5 we return to the analysis of the two coupled SYK models, but now beyond the low energy limit. This is done numerically for $q = 4$ and analytically in the large q limit. We describe some aspects of the thermodynamics of the coupled model. In the large q limit we also show that the ground state of the coupled model is equal to the thermofield double state of the decoupled model for a specific temperature. Finally we also discuss the solution in the case that the microscopic couplings of the two SYK models are not exactly equal.

2 Nearly AdS_2 gravity with a global time isometry

2.1 Global AdS_2

We start by recalling a few properties of AdS_2 and setting some notation. Two dimensional anti-de-Sitter space can be written in terms of global coordinates that cover the whole space-time

$$ds^2 = \frac{-dt^2 + d\sigma^2}{\sin^2 \sigma}, \quad \sigma \in [0, \pi] \quad (2.1)$$

Other coordinate systems that are also popular are

$$\text{Poincare : } ds^2 = \frac{-dt_P^2 + dz^2}{z^2}, \quad \text{Rindler/Thermal : } ds^2 = -dt_R^2 \sinh^2 \rho + d\rho^2 \quad (2.2)$$

These coordinate systems do not cover the full spacetime, see figure 1. The full spacetime has an $SL(2, R)$ group of isometries, but the above coordinate systems manifest only one of them, a different generator for each of the coordinate systems. This generator corresponds to the time translation symmetry for each of the choices of the time coordinate.

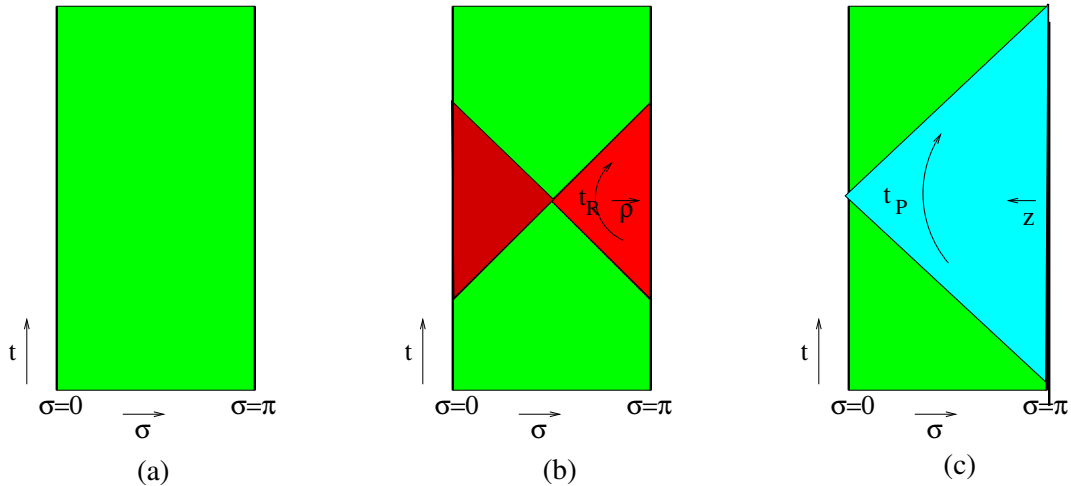


Figure 1: (a) Full AdS_2 Penrose diagram. It has two boundaries, one at $\sigma = 0$ and one at $\sigma = \pi$, see (2.1). (b) The right triangle is covered by the Rindler or Thermal coordinates in (2.2). (c) The full triangle is covered by the Poincare coordinates (2.2).

We can also describe AdS_2 in terms of global coordinates Y^M with the constraint $-(Y^{-1})^2 - (Y^0)^2 + (Y^1)^2 = -1$ (or, more precisely, its universal cover). It is also possible to describe the boundary in terms of projective coordinates X^M with the constraint $X \cdot X = 0$ and the identification $X^M \sim \lambda X^M$. We can introduce the boundary analogs of the previous time coordinates via

$$e^{it_r} = X^{-1} + iX^0, \quad \text{for } X^1 = 1, \quad e^{it_i} = X^{-1} + iX^0, \quad \text{for } X^1 = -1$$

$$\frac{X^0}{X^{-1} + X^1} = t_P, \quad , \quad e^{t_R} = X^1 + X^0, \quad \text{for } X^{-1} = 1 \quad (2.3)$$

Here t_l , t_r are the global time coordinates along each of the two boundaries, which are selected via the “gauge” choice $X^1 = \pm 1$ respectively. These equations enable us to find the relations between these times, for example,

$$\frac{X^0}{X^{-1} + X^1} = t_P = \tan \frac{t_r}{2} = -\frac{1}{\tan \frac{t_l}{2}} = \tanh \frac{t_R}{2} \quad (2.4)$$

These relations also arise by relating the bulk coordinates in (2.1) (2.2) and then moving close to the boundary.

2.2 Nearly AdS_2 gravity

Purely AdS_2 asymptotic boundary conditions are not consistent in a theory of quantum gravity with finite energy excitations [17] (see [18] for a recent related discussion). The next best possibility is to consider Nearly- AdS_2 boundary conditions [1, 3, 2, 4], which are described by Jackiw-Teitelboim gravity [19, 20]

$$S = \frac{\phi_0}{2} \left[\int R + 2 \int_{\text{Bdy}} K \right] + \frac{1}{2} \left[\int \phi(R + 2) + 2\phi_b \int_{\text{Bdy}} K \right] + S_{\text{matter}}[\chi, g] \quad (2.5)$$

with boundary conditions that fix the boundary value of the metric and the dilaton,

$$ds|_{\text{Bdy}} = \frac{du}{\epsilon}, \quad \phi|_{\text{Bdy}} = \phi_b = \frac{\phi_r}{\epsilon} \quad (2.6)$$

and taking ϵ to zero, see [3] for more details. The term proportional to ϕ_0 is a topological term that will not contribute to the main solutions we will describe here, which have the topology of a strip or a cylinder, so we will mostly ignore it. χ denotes the matter fields, and we assumed that ϕ does not appear in the matter action. This action is a good approximation to the dynamics of nearly extremal black holes [1, 21, 22].

In this theory, the only gravitational mode can be viewed as living at the boundary of the space. Since the metric is set to be exactly AdS_2 , the gravitational dynamics comes purely from the location of the physical boundary in that rigid AdS_2 space. There are a couple of different ways to think about this location. One is to first solve the dynamics of matter, then compute the dilaton from the (metric) equation of motion in (2.5), and finally find the location where the dilaton has the desired boundary value [1]. Alternatively, we can reduce the problem explicitly to a dynamical system at the boundary. There are different parametrizations for this dynamical system. A convenient one involves picking the basic dynamic variable as a time reparametrization with an action which is the Schwarzian [3, 23]

$$S = -\phi_r \int \{t_P(u), u\} du \quad (2.7)$$

where u is the boundary time. Here we can view $t_P(u)$ as a map between the physical proper time, or boundary time, and the interior Poincare time t_P . We can consider a spacetime with two boundaries, and then we get (2.7) for each of the two boundaries. When we consider this problem, we have an $SL(2)$ symmetry acting as $t_P \rightarrow (at_P + b)/(ct_P + d)$. This symmetry should be treated as a *gauge* symmetry. This means we impose that the associated charges vanish as a gauge constraint¹ [3]. We see that ϕ_r , which is a quantity of dimensions of length, defined via (2.6), sets the strength of the coupling for the gravitational action (2.7).

A simple Lorentzian solution of (2.5) is

$$t_P = \tanh \frac{t_R(u)}{2} = \tanh \frac{\pi u}{\beta}, \quad \text{or} \quad t_R(u) = \frac{2\pi}{\beta} u \quad (2.8)$$

which can be interpreted as a thermal black hole configuration with free energy, energy and entropy given by [3]

$$F = -\frac{\phi_r (2\pi)^2}{2\beta^2}, \quad E = -\phi_r \{t_P, u\} = \frac{\phi_r (2\pi)^2}{2\beta^2}, \quad S = \frac{\phi_r (2\pi)^2}{\beta} \quad (2.9)$$

The full Lorentzian solution has two boundaries and the total gauge $SL(2)$ charges vanish. For this solution, the two boundary trajectories correspond to lines of constant ρ in the Rindler/Thermal coordinates (2.2), and we cannot send signals between the boundaries. See figure (2)(c).

In this paper we are interested in creating a situation where the boundaries correspond to lines of constant σ in the global coordinates (2.1). In this configuration we would have a t -translation invariant dilaton which grows towards both boundaries. There is no solution of this kind in the pure JT gravity with no matter (2.5). Furthermore, there is no solution of this kind if we assume that we have matter which obeys the integrated null energy condition in the bulk. In fact, one of the equations of motion for the metric² implies $(x^\pm = t \pm \sigma)$ [17]

$$-\partial_+(\sin^2 \sigma \partial_+ \phi) = T_{++} \sin^2 \sigma \longrightarrow -2\phi_r = -(\sin^2 \sigma \partial_+ \phi)|_{-\infty}^{+\infty} = \int_{-\infty}^{+\infty} dX^+ T_{X^+ X^+} \quad (2.10)$$

where we have integrated the left expression along a null line, with X^+ being the affine coordinate along the null line, namely $dX^+ = dx^+ / \sin^2 \sigma$. We see that the left hand side is negative if ϕ is growing towards both boundaries as $\frac{\phi_r}{|\sigma - \sigma_{\text{bdy}}|}$. On the other hand the right hand side is non-negative if the integrated null energy condition holds. This problem is a special case of the general topological censorship result [24, 25] that forbids

¹This $SL(2)$ symmetry, which is not broken and is not physical, should not be confused with the physical $SL(2)$ operation on u which is explicitly broken by (2.7) to simply u -translations.

²(2.10) is the two dimensional version of the Raychaudhuri equation.

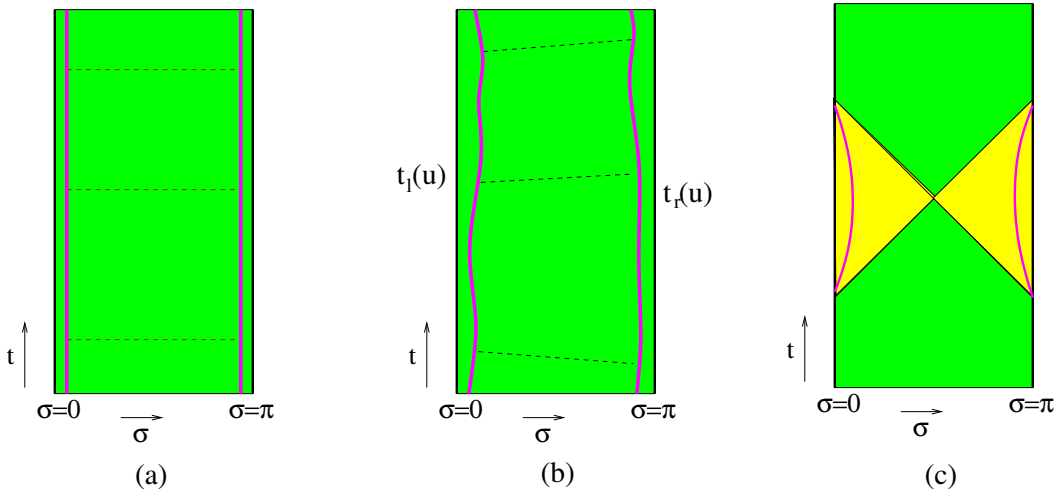


Figure 2: (a) Trajectories of the physical boundaries (in magenta) for the Nearly- AdS_2 geometry with a global time isometry. These trajectories are the lines where the dilaton acquires its boundary value. It can be obtained by introducing an interaction between the two boundaries. (b) We can describe the fluctuations of the boundary trajectories in terms of a pair of functions, $t_l(u)$ and $t_r(u)$, mapping (rescaled) proper time u along the trajectory to the global AdS_2 time coordinate t . The dotted lines can be viewed as insertions of the interaction Hamiltonian. They join points with the same value of u on both boundaries. (c) The physical boundaries for a Nearly- AdS_2 geometry with thermal isometry. Here the two boundary trajectories cover only a finite range of global time and we cannot send a signal between the two trajectories.

traversable wormholes and non-trivial topology in asymptotically flat or AdS_D , $D > 2$, spaces (assuming the integrated null energy condition)³.

This result can be avoided by introducing an interaction that directly couples the two boundaries [5]. Therefore we now add a boundary interaction of the form

$$S_{int} = g \sum_{i=1}^N \int du O_L^i(u) O_R^i(u) \quad (2.11)$$

where O^i are a set of N operators with dimension Δ . We consider a theory with N operators because we will take N to be large so as to enhance the effects of these operators. g has dimensions of $[\text{energy}]^{2\Delta-1}$. The operators are the field operators in the bulk evaluated

³One could imagine the following method for violating the null energy condition. First we consider a bulk CFT in AdS_2 . Since it is a CFT, we get the same results as if we had it on a flat strip. On a flat strip, the energy is negative and equal to $-c/24$ [26]. Nevertheless, when we go back to AdS_2 we have a contribution from the stress tensor from the conformal anomaly that cancels this out, so that we indeed have zero null energy in AdS_2 . This has to be the case since the AdS_2 stress tensor should be $SL(2)$ invariant. See appendix C.1 for more discussion.

at the positions of the boundary. So our bulk theory has at least N matter fields. This is an interaction across the two boundaries, similar to the one considered in [5]. For the reasons explained in [5], this interaction produces negative energy in the bulk, see also [27, 28, 29, 30, 31]. Notice that (2.10) implies that a finite amount of negative energy is enough to resolve the problem. In appendix C.2 we compute this negative energy explicitly for the case of a massless free fermion in the bulk, and in C.3 we compute the profile of the dilaton with this negative energy source. Here we will analyze the same problem using the effective action for the boundary graviton.

When g is sufficiently small, we can approximate the effects of the interaction (2.11) by replacing

$$\langle e^{ig \sum_i \int du O_L^i(u) O_R^i(u)} \rangle \sim e^{ig \sum_i \int dt \langle O_L^i(u) O_R^i(u) \rangle} \quad (2.12)$$

in the path integral. This amounts to resumming a series of ladder type diagrams of the form indicated in figure 2(a). These diagrams dominate in the large N small g limit, with Ng kept fixed. We can further couple this to the gravity modes by performing a reparametrization of the left and right times. These are a map between the proper boundary time u and the global times $t_l(u)$, $t_r(u)$ at the two boundaries (2.3). The system is then described by the effective action

$$S = \int du \left[-\phi_r \left\{ \tan \frac{t_l(u)}{2}, u \right\} - \phi_l \left\{ \tan \frac{t_r(u)}{2}, u \right\} + \frac{gN}{2^{2\Delta}} \left(\frac{t_l'(u)t_r'(u)}{\cos^2 \frac{t_l(u)-t_r(u)}{2}} \right)^\Delta \right] \quad (2.13)$$

where we normalized the correlator for O so that it takes the form $\langle O(t_P^1) O(t_P^2) \rangle = |t_P^1 - t_P^2|^{-2\Delta}$ in Poincare coordinates. We have reparametrized t_P by t_l and t_r indicated in (2.4). This correlator in terms of t_l and t_r has the form we expect for an AdS_2 correlator in global coordinates where t_l and t_r are the boundary global times at the left and right boundaries respectively. This is a way to describe the position of the physical boundary, see figure 2(b).

We postpone the analysis of this action until we obtain the same action from two coupled copies of the SYK model in the next section.

3 Two coupled SYK models

3.1 Review of the SYK model

The SYK model has a Hilbert space generated by N Majorana fermions ψ^i with a Hamiltonian of the form [6, 7]

$$H = (i)^{q/2} \sum_{1 \leq j_1 \leq j_2 \leq \dots \leq j_q} J_{j_1 j_2 \dots j_q} \psi^{j_1} \psi^{j_2} \dots \psi^{j_q},$$

$$\langle J_{j_1 \dots j_q}^2 \rangle = \frac{2^{q-1} \mathcal{J}^2 (q-1)!}{q N^{q-1}} \quad (\text{no sum}) \quad (3.14)$$

where the couplings are drawn from a random gaussian distribution with the mean indicated above. The factor of i is necessary to get a hermitian Hamiltonian when $q/2$ is odd.

At large N the model can be solved by writing an equation for the fermion two point function $G(\tau_1, \tau_2) = \frac{1}{N} \sum_j \langle \psi^j(\tau) \psi^j(0) \rangle$. This equation has the form

$$\partial_{\tau_1} G(\tau_1, \tau_3) - \int d\tau_2 \Sigma(\tau_1, \tau_2) G(\tau_2, \tau_3) = \delta(\tau_{13}) , \quad \Sigma(\tau_1, \tau_2) = \frac{\mathcal{J}^2}{q} [2G(\tau_1, \tau_2)]^{q-1} \quad (3.15)$$

These equations follow from the euclidean action

$$-S_E/N = \log \text{Pf}(\partial_\tau - \Sigma) - \frac{1}{2} \int d\tau_1 d\tau_2 \left[\Sigma(\tau_1, \tau_2) G(\tau_1, \tau_2) - \frac{\mathcal{J}^2}{2q^2} [2G(\tau_1, \tau_2)]^q \right] \quad (3.16)$$

This equations (3.15) can be solved in Euclidean time and can be used to evaluate the free energy using (3.16). In general it is only possible to solve the equations numerically. However, it is possible to solve them analytically at large q . It is also possible to solve them in general at low temperatures, but not too low, $1 \ll \beta \mathcal{J} \ll N$, in terms of a scaling ansatz of the form (for $1 \ll \mathcal{J} \tau_{12} \ll \beta \mathcal{J}$)

$$G(\tau_1, \tau_2) = c_\Delta \text{sgn} \tau_{12} \frac{1}{|\mathcal{J} \tau_{12}|^{2\Delta}} , \quad \Delta = \frac{1}{q} , \quad c_\Delta = \frac{1}{2} \left[(1 - 2\Delta) \frac{\tan \pi \Delta}{\pi \Delta} \right]^\Delta \quad (3.17)$$

At low energies the model has an emergent reparametrization symmetry changing G to $G_f = [f'(u_1) f'(u_2)]^\Delta G(f(u_1), f(u_2))$ were G is given in (3.17). This symmetry is explicitly broken by $1/\mathcal{J}$ effects leading to a Schwarzian action [9, 8].

$$S = -\frac{N\alpha_S}{\mathcal{J}} \int du \{f(u), u\} \quad (3.18)$$

We can then get the thermal correlators and free energy by setting $f = \tan \frac{\pi u}{\beta}$. The coupling constant α_S is determined by four-point function calculation of the SYK model, which goes as $\alpha_S \sim \frac{1}{4q^2}$ in large q limit. (See Ref. [9]).

We are interested in the thermofield double state of the SYK model, which is a state in the Hilbert space of two SYK sites, defined as follows

$$|TFD_\beta\rangle = Z_\beta^{-1/2} e^{-\beta(H_L + H_R)} |I\rangle \quad (3.19)$$

Here Z_β is the thermal partition function at inverse temperature β . $|I\rangle$ is the thermofield double state at infinite temperature, which is a maximally entangled state between two systems. H_L is the SYK Hamiltonian applied to the left system, and H_R is the Hamiltonian of the right system, defined so that $(H_L - H_R) |I\rangle = 0$. For the SYK model with fermions ψ_L^i, ψ_R^i , we can define $|I\rangle$ by

$$(\psi_L^j + i\psi_R^j) |I\rangle = 0, \quad \forall j \quad (3.20)$$

This determines $|I\rangle$ as the ground state of complex fermions with annihilation operators $f_j = \frac{1}{\sqrt{2}} (\psi_L^j + i\psi_R^j)$. With this convention, for the SYK model we obtain $H_R = (-1)^{q/2} H_L$ which describes a SYK model with equal or opposite coupling. The thermofield double state $|TFD_\beta\rangle$ satisfies $(H_L - H_R)|TFD_\beta\rangle = 0$ by construction. The reduced density matrix of each subsystem (left or right) is the thermal density matrix with temperature β^{-1} , and entropy $S_0 + \frac{N(2\pi)^2\alpha_S}{\beta\mathcal{J}}$. S_0 is a constant zero temperature entropy.

3.2 Two coupled SYK models

In this article we concentrate on a model where we start with two decoupled SYK models, both described by same couplings, up to a sign for odd $q/2$, $J_{j_1\dots j_q}^L = (-1)^{q/2} J_{j_1\dots j_q}^R$. A situation like this arises when we consider the thermofield double of the original system. So we denote by ψ_L^i and ψ_R^i the fermions of the two copies the SYK model. But now we introduce a coupling between the two sides of the form

$$H_{\text{total}} = H_{L,\text{SYK}} + H_{R,\text{SYK}} + H_{\text{int}} , \quad H_{\text{int}} = i\mu \sum_j \psi_L^j \psi_R^j \quad (3.21)$$

Note that the state $|I\rangle$, defined in (3.20), is also the ground state of H_{int} . For small μ we expect that the system described by the total Hamiltonian (3.21) can be described as the nearly conformal system associated to two copies of the usual SYK model (3.14) plus a relevant deformation associated to the μ coupling. We expect that the system flows in the IR to a gapped phase described by a ground state $|G\rangle$ of the combined system.

In this paper we will study this gapped phase in detail. We will show that at small coupling μ , or at large q for any coupling, the ground state $|G\rangle$ is very close to the thermofield double state $|TFD\rangle$ of the decoupled system with a particular inverse temperature $\beta(\mu)$, that is determined by the mass μ . For small mass μ , this could be expected for the following reason. We expect that the system will develop an approximate conformal symmetry at energy scales less than \mathcal{J} . Then we can analyze the effects of the coupling as a perturbation to the approximately conformal system. The state that will minimize the interacting Hamiltonian (3.21) will try to maximize the left-right correlations in order to make H_{int} as small as possible. The thermofield double state is a pure state of the combined, but decoupled, left and right systems that has a relatively large value for the left-right correlators. As we decrease the temperature of the TFD, we decrease the expectation value of H_L and H_R , we also decrease H_{int} , but at a different rate. There will be a temperature for the TFD where the energy is minimized. Furthermore, in the conformal approximation we can imagine a conformal map between the circle that prepares the TFD to two parallel lines, which would naively prepare the same state. This is analogous to the usual map between the sphere and the Euclidean cylinder for higher dimensional CFTs. This map is not strictly valid in our case, because the conformal symmetry is not exact, but it leads us to expect that the TFD double could be related to the ground state of a closely related system, whose preparation involves Euclidean time evolution over an infinite time. Furthermore, the interaction term in (3.21) selects a state with relatively large

correlations between the left and right degrees of freedom, as we have in the TFD state. In the rest of the paper we will present precise and detailed arguments for the relationship between $|G\rangle$ and $|TFD\rangle$. Similar phenomena have been studied in $(1+1)$ -d CFTs[32, 33].

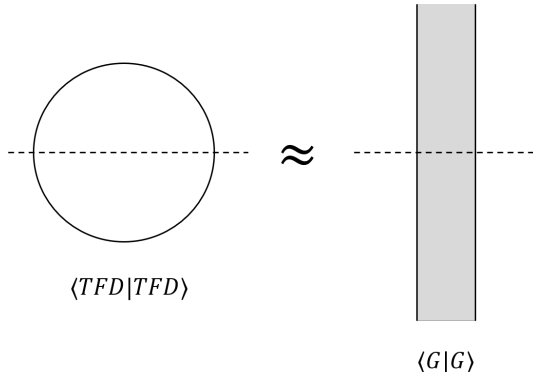


Figure 3: Schematic comparison of the Euclidean path integral that prepares the $|TFD\rangle$ state and the ground state of coupled system $|G\rangle$. The thermal circle is related to two parallel lines by a conformal transformation. The conformal symmetry is weakly broken. The competition of $H_L + H_R$ and H_{int} controls the symmetry breaking and selects the $|TFD\rangle$ with a certain temperature as the ground state.

In the two decoupled systems the $|TFD\rangle$ state undergoes a non-trivial time evolution when we evolve forwards in time for both the left and right times by the same amount. On the other hand $|G\rangle$ is invariant under time evolution by the coupled Hamiltonian (3.21). We had mentioned that the system develops an approximate conformal symmetry that is explicitly broken in the IR. In the case of the decoupled system we preserve a boost-like symmetry corresponding to the usual symmetry of TFD states (forward evolution in t_R and backward in t_L). On the other hand the state $|G\rangle$ preserves a different element of $SL(2)$, which corresponds to forward global time translations on the two times. Moreover, we will see that some features of the spectrum of excitations of the system around the ground state are still governed by the approximate $SL(2)$ symmetry, which is a unique feature of the $(0+1)$ -d case and does not occur in higher dimensional CFT's with a relevant coupling.

3.3 Low energy analysis

In this subsection we find the properties of the ground state when the mass is very small $\mu \ll J$ so that we can use the low energy solution. At leading order, when we ignore the effects of conformal symmetry breaking, we have conformal invariant correlators. If we assume the ground state is close to $|TFD\rangle$, the approximate conformal symmetry allows us to obtain the left-right correlator by reparameterization of the single side conformal

correlator, which takes the form

$$\langle \psi_L(t_l) \psi_R(t_r) \rangle = c_\Delta \frac{i}{[2\mathcal{J} \cos \frac{t_l - t_r}{2}]^{2\Delta}} \quad (3.22)$$

We can get this from (3.17) via a reparametrization $t_P = \tan \frac{t_r}{2}$, $t_P = -1/\tan \frac{t_l}{2}$, with t_P being Lorentzian time, as in (2.3). The i is necessary since the operator $\psi_L(t_l)\psi_R(t_r)$ is antihermitian. Here we are simply choosing a particular time parametrization of the two boundaries. In order to determine whether these correlators are close to a solution, we need to take into account the physics of the reparametrization mode. This can be done by introducing an arbitrary reparametrization $t_l(u)$ and $t_r(u)$ of the above correlator, (3.22). From each single SYK model we get a Schwarzian action for this mode. In addition, the interaction term in (3.21) leads to an additional term. This additional term can be obtained by taking the expectation value of the fields in (3.21), exponentiating as in (2.12), and performing a reparametrization. This implies that we can write down a Lorentzian action of the form

$$S = N \int du \left\{ -\frac{\alpha_S}{\mathcal{J}} \left(\left\{ \tan \frac{t_l(u)}{2}, u \right\} + \left\{ \tan \frac{t_r(u)}{2}, u \right\} \right) + \mu \frac{c_\Delta}{(2\mathcal{J})^{2\Delta}} \left[\frac{t'_l(u)t'_r(u)}{\cos^2 \frac{t_l(u) - t_r(u)}{2}} \right]^\Delta \right\} \quad (3.23)$$

Note that the action has an overall factor of N . This form of the low energy action is the same as what we got in gravity (2.13). So, in the next section we will analyze this low energy action, coupled to conformal matter, and describe several physical consequences.

Let us say a few more words on the rationale behind the approximation (3.23). As we reviewed in (3.16), we can describe the two decoupled systems around the thermofield double state in terms of an effective action. This effective action contains a soft mode, or a low action mode, that can be viewed as pseudo-Goldstone bosons for an spontaneously and explicitly broken reparametrization symmetry [7]. The action in the G, Σ space develops a shallow valley [7]. Motion along the valley is parametrized in terms of the variables in (2.13). The last term in (2.13) is the projection of the the interaction term H_{int} in the coupled Hamiltonian (3.21) to this valley. This extra term modifies the location of the minimum along this valley. When we approximate the dynamics by (2.13) we are neglecting the change of the state along the “hard” directions and taking into account only its change along the “shallow” directions. In other words, we can imagine we have a particle in a shallow valley and we are turning on a small external force. The new equilibrium position will be approximately given by another point in this valley, obtained after evaluating the external potential along the valley. The description of this new “point” is what we will study in detail in the next section.

We should also note that we could have started instead with an interaction Hamiltonian with a more general relevant coupling term, such as $H_{\text{int}} = gN^{1-p}(i\psi_L^j\psi_R^j)^p$. In this case, for $p < q$, we also obtain an effective action like (3.23) but with $\Delta \rightarrow p\Delta$ and a different prefactor for the interaction term.

4 Low energy analysis of the coupled theory

In this section we will study several physical properties that arise both in the case of gravity with the two boundary coupling (2.11) as well as in the case of two coupled SYK models described by (3.21). In both cases, for relatively small interaction strength we get a description that involves the same action (3.23) and (2.13). Just to set notation for this section, let us write it yet once more

$$S = N \int d\tilde{u} \left\{ - \left(\left\{ \tan \frac{t_l(\tilde{u})}{2}, \tilde{u} \right\} + \left\{ \tan \frac{t_r(\tilde{u})}{2}, \tilde{u} \right\} \right) + \eta \left[\frac{t'_l(\tilde{u})t'_r(\tilde{u})}{\cos^2 \frac{t_l(\tilde{u})-t_r(\tilde{u})}{2}} \right]^\Delta \right\} \quad (4.24)$$

The relation between parameters in the two previous actions and (4.24) is

$$\tilde{u} \equiv \frac{\mathcal{J}}{\alpha_S} u = \frac{N}{\phi_r} u, \quad \eta \equiv \frac{\mu\alpha_S}{\mathcal{J}} \frac{c_\Delta}{(2\alpha_S)^{2\Delta}} = \frac{g}{2^{2\Delta}} \left(\frac{N}{\phi_r} \right)^{2\Delta-1} \quad (4.25)$$

We have defined a rescaled time, \tilde{u} . In the SYK model \tilde{u} is basically time measured in units of $1/\mathcal{J}$.

This action should be supplemented by $SL(2)$ constraints stating that the total $SL(2)$ charges vanish [3].

4.1 Classical solution

$N \gg 1$ governs the approach to the classical limit. We imagine that N is larger than any other parameter that appears in the problem. We can first look for a simple solution by making a linear ansatz

$$t_r(\tilde{u}) = t_l(\tilde{u}) = t' \tilde{u}, \quad \text{with} \quad t' \equiv \frac{dt}{d\tilde{u}} = \text{constant} \quad (4.26)$$

Note that we defined t' as a derivative with respect to \tilde{u} . To turn into a derivative with respect to u we have to use (4.25). (4.26) is a solution of the equations of motion for (4.24) for any value of t' . This looks a bit surprising at first since we expected to have a single solution. In these formulas t' is a constant.

We should however recall that the action (4.24) should be supplemented by constraints stating that the total $SL(2)$ charges vanish [9]. Let us explain this in more detail. The action (4.24) has a global $SL(2)$ symmetry generated by

$$\delta t_l = \epsilon^0 + \epsilon^+ e^{it_l} + \epsilon^- e^{-it_l}, \quad \delta t_r = \epsilon^0 - \epsilon^+ e^{it_r} - \epsilon^- e^{-it_r} \quad (4.27)$$

These are simply the $SL(2)$ symmetries of the coordinate X^M expressed in terms of t_l or t_r defined through (2.3). We can compute the associated charges by using the Noether

procedure on (4.24), see appendix B. Here we will quote the answer only for the charge Q_0 evaluated on the configuration (4.26). This gives ⁴

$$Q_0 = -2t' + 2\eta\Delta t'^{2\Delta-1} = 0 \quad (4.28)$$

$$(t')^{2(1-\Delta)} = \eta\Delta, \quad \left(\frac{1}{\mathcal{J}} \frac{dt}{du}\right)^{2(1-\Delta)} = \frac{\mu\Delta}{2\mathcal{J}\alpha_S} \frac{2c_\Delta}{2^{2\Delta}} \quad (4.29)$$

where we imposed that the charge is zero and obtained the value of t' . We have also expressed the answer in terms of SYK parameters and the original time, u . This value determines the relation between the boundary time \tilde{u} and the bulk time t .

The validity of the action, (4.24), as a good approximation to the original SYK requires that

$$t' \ll 1, \quad \eta \ll 1 \quad (4.30)$$

so that the low energy approximation leading to (4.24) is valid. Looking at (4.29) we see that we need $0 < \Delta < 1$. In addition, in order for the classical approximation to (4.24) to be valid we also need

$$Nt' = N(\eta\Delta)^{\frac{1}{2(1-\Delta)}} \gg 1, \quad (4.31)$$

since the inverse of this quantity is the effective dimensionless coupling of the Schwarzian theory. For large enough N we can ensure both (4.31) and (4.30) by taking a small enough η , but not too small.

Once we know t' we can go from the conformal matter correlators to the physical ones⁵

$$\langle \mathcal{O}(t_l)\mathcal{O}(t_r) \rangle = \left[\frac{1}{\cos \frac{t_l - t_r}{2}} \right]^{2\tilde{\Delta}} \longrightarrow \langle \mathcal{O}(\tilde{u}_1)\mathcal{O}(\tilde{u}_2) \rangle = \left[\frac{t'}{\cos \frac{t'(\tilde{u}_1 - \tilde{u}_2)}{2}} \right]^{2\tilde{\Delta}} \quad (4.32)$$

This gives the physical value of left-right correlation functions. In the gravity theory, these can be the two point functions of some matter fields that propagates in the bulk, which could be the same or different, than the matter field that gives rise to the interaction across the boundaries (2.11). In the SYK model it could be the elementary fermion ψ^k or any composite operator that we obtain after taking an operator product of those. For that reason we have indicated that its conformal weight, $\tilde{\Delta}$, need not be the same as that of the fields that give rise to the explicit coupling between the two sides.

The value of t' , (4.29), determines the energy scale of bulk excitations, or equivalently, the energy scale of the conformal excitations of the SYK model. An operator with dimension $\tilde{\Delta}$, or a bulk field with the corresponding mass, has energies $E_t = \tilde{\Delta} + n$ with respect

⁴The expression for the charge can be simply derived from (2.13) by dropping all terms with derivatives higher than the first derivative, since they will not contribute when t' is a constant. Note that $\{\tan \frac{t_l(u)}{2}, u\} = t_l'^2/2$ up to terms with higher derivatives. Then the Noether charge is just simply the usual one associated to t -shifts, the conserved total “momentum” along the t direction.

⁵To get the operators as a function of the unrescaled boundary time u we write $\mathcal{O}(u) = \left(\frac{d\tilde{u}}{du}\right)^\Delta \mathcal{O}(\tilde{u})$ using (4.25).

to global bulk time. This form of the spectrum is fixed by $SL(2)$ symmetry. Then, with respect to (rescaled) boundary time \tilde{u} they have energies

$$E_{\tilde{u}} = t' E_t = t'(\tilde{\Delta} + n) , \quad E_u = \frac{dt}{du}(\tilde{\Delta} + n) \quad (4.33)$$

where the subindex in $E_{\tilde{u}}$ or E_u states whether the energy is conjugate to \tilde{u} or u time translations. The difference is a simple rescaling (4.25). Here $\frac{dt}{du}$ is just a constant, independent of u . Therefore we see that t' sets the scale of the energy gap of the system. More precisely, for the systems we have been describing the energy gap is

$$E_{\text{gap}, \tilde{u}} = t' \Delta , \quad E_{\text{gap}, u} = \frac{\mathcal{J}}{\alpha_S} t' \Delta = \frac{N}{\phi_r} t' \Delta = \frac{dt}{du} \Delta \quad (4.34)$$

This part of the spectrum is invariant under physical $SL(2)$ transformations of boundary time. This is an interesting property. If we looked at the coupled SYK hamiltonian (3.21), we see that the mass term dominates at low energies and we would have expected a generic gapped system, with arbitrary energy spacings. Here we get a pattern of energy spacings that reflect an $SL(2)$ symmetry. This is the type of spectrum we expect from a state/operator correspondence. As we discuss below the gravitational degree of freedom does not follow this pattern.

It is interesting to wonder what all the physical solutions of (4.24) are. In appendix B we show that all solutions of (4.24) with zero Q_{\pm} $SL(2)$ charges can be gauge transformed to solutions where the left and right times are equal. Namely, we can restrict our attention to solutions of the form $t_r(\tilde{u}) = t_r(\tilde{u}) = t(\tilde{u})$, but with a general \tilde{u} dependence. This ansatz sets to zero the Q_{\pm} $SL(2)$ charges, see appendix B. As before, the equations come from demanding that $Q_0 = 0$, which, written in terms of $\varphi = \log t'(\tilde{u})$, reads (see appendix B),

$$0 = Q_0 = 2N e^{-\varphi} [-e^{2\varphi} - \varphi'' + \eta \Delta e^{2\Delta\varphi}] \quad (4.35)$$

We see that this looks like the equations of motion of a non-relativistic particle in a potential with the action

$$S = N \int d\tilde{u} \dot{\varphi}^2 - V(\varphi) , \quad V = e^{2\varphi} - \eta e^{2\Delta\varphi} \quad (4.36)$$

see figure 4. The solution we found in (4.29) corresponds to the minimum of the potential, $e^{2(1-\Delta)\varphi_m} = \eta \Delta$. It is possible to check that solutions of (4.35) also solve the equations of motion, which are simply a time derivative of (4.35). The oscillations around the minimum of the potential give rise to a harmonic oscillator degree of freedom with frequency $\omega_{\tilde{u}} = t' \sqrt{2(1-\Delta)}$, or physical energies

$$E_{\tilde{u}} = t' \sqrt{2(1-\Delta)} \left(n + \frac{1}{2}\right) , \quad E_u = \frac{dt}{du} \sqrt{2(1-\Delta)} \left(n + \frac{1}{2}\right) \quad (4.37)$$

This harmonic oscillator corresponds to the physical gravitational excitations of the system. This single quantum mechanical degree of freedom corresponds to the “boundary

graviton”. It encodes the gravitational dynamics and backreaction of the system. Even though we call it a “boundary graviton” it is a global mode that refers to both boundaries, the left and the right boundary and cannot be associated to just one of them. The fact that we get a minimum and an ordinary harmonic oscillator around the minimum is telling us that the solution we found in (4.29) is stable. Furthermore, the energy scale is also set by t' . These excitations, as opposed to the ones in (4.33) do not organize into an $SL(2)$ multiplet. This is the leading feature of the spectrum associated to the breaking of the $SL(2)$ symmetry. Note also that the energy (4.37) is larger than (4.34) for the range of Δ s that we are considering. This justifies the statement that (4.34) is the actual energy gap of the system.

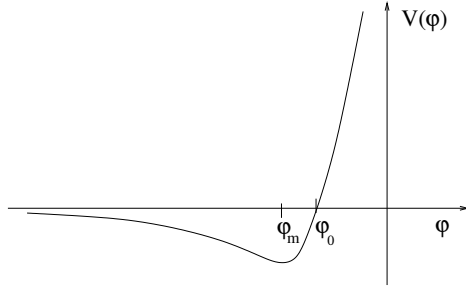


Figure 4: Effective potential for the single degree of freedom associated to the gravitational mode, see (4.36). Here φ_m is the minimum and φ_0 is where it crosses zero.

It is also interesting to compute the conserved energy associated to the lagrangian in (4.24). This is the Noether charge under \tilde{u} translations. We find

$$E_{\tilde{u}}/N = -\left\{\tan \frac{t_l(\tilde{u})}{2}, \tilde{u}\right\} - \left\{\tan \frac{t_r(\tilde{u})}{2}, \tilde{u}\right\} + \eta(2\Delta - 1) \left[\frac{t'_l(\tilde{u})t'_r(\tilde{u})}{\cos \frac{(t_l - t_r)}{2}} \right]^{2\Delta} \quad (4.38)$$

$$= -(2\varphi'' - \varphi'^2 + e^{2\varphi}) - \eta(1 - 2\Delta)e^{2\Delta\varphi} = (\varphi'^2 + e^{2\varphi}) - \eta e^{2\Delta\varphi} \quad (4.39)$$

where we used the equations of motion. This is the energy for a particle in a potential (4.36). In comparing with the SYK Hamiltonian (3.21), we note that only the terms with a $-\eta e^{2\Delta\varphi}$ in (4.38) corresponds to $\langle H_{\text{int}} \rangle$. The rest of the terms corresponds to $\langle H_L + H_R \rangle$. In particular, for the minimum at $e^{2(1-\Delta)\varphi_m} = (t')^{2-2\Delta} = \eta\Delta$, (4.29), we get the energy of the ground state

$$E_{G_{\tilde{u}}}/N = -\frac{(1-\Delta)}{\Delta} e^{2\varphi_m} = -\frac{(1-\Delta)}{\Delta} (\eta\Delta)^{\frac{1}{1-\Delta}}, \quad E_{G_u} = -N \frac{(1-\Delta)}{\Delta} \frac{\alpha_S}{\mathcal{J}} \left(\frac{dt}{du} \right)^2 \quad (4.40)$$

where we have also given the expression in terms of SYK parameters (4.25). The fact that we obtained a single degree of freedom is in agreement with analysis of the standard Rindler-Thermal-whormhole in [34], which found a two dimensional phase space, corresponding to the energy and the relative time shift.

The φ dynamical system (4.36) also has unbounded solutions. An unbounded solution has $\varphi \sim -\gamma\tilde{u}$ for large times, which implies that $t'(u) \propto e^{-\gamma\tilde{u}}$ for large times. This means that the global time t has a maximal range and that the boundary particle trajectory approaches the AdS boundary, since $\sigma = \epsilon t'$. In the gravity case, these solutions develop a horizon. This is also what happens when $\eta = 0$, where we get the solutions corresponding to the TFD (4.49).

What we discussed so far applies to the case where we do not add any further bulk excitations. If we also add bulk particle excitations, then we need to reanalyze the problem, now imposing a different value for the $SL(2)$ charges. In particular if we have a bulk excitation with global energy E_t^{bulk} , and it is at rest in AdS_2 ⁶, then we expect that the charge Q_0 should be set to $Q_0 = E_t^{\text{bulk}}$ instead to zero in (4.35). If we treat the bulk classically, then, if the particle is at rest, then the other charges remain zero, $Q_{\pm} = 0$. When we integrate to get (4.36) we see that we get an extra term in the potential

$$V \rightarrow V + E_t^{\text{bulk}} e^{\varphi}/N \quad (4.41)$$

The extra term is suppressed in the classical limit (for large N). So if the extra added energy is of order one, such as the energy added by the states in (4.33), then we have a small correction. This does not change the physics much. The shift in the minimum of the potential implies that we get an extra energy of order $E_{\tilde{u}} \rightarrow E_{\tilde{u}} + E_t e^{\varphi_m}$ which is the correct, expected new boundary energy, see appendix B. If we add a large amount of energy in the bulk, then we could remove the possibility of having bound states, as we will see in the next section.

4.2 Quantum version

We can consider the quantum version of (4.24). In principle, we should find the right integration measure for our problem, etc. Instead, we notice that the Liouville-type action in (4.36) was already shown to describe correctly the TFD (for $\eta = 0$) [35, 36, 37]. So, to treat our case, we simply add the effects of the new interaction term. Therefore we want to quantize action

$$S = N \int d\tilde{u} [\dot{\varphi}^2 - e^{2\varphi} + \eta e^{2\Delta\varphi}] \quad (4.42)$$

Perhaps a better argument for (4.42) is the following. As argued in appendix (B) any solution of (4.24) that obeys the constraints can be gauge-transformed to a solution of (4.42) and further obeys the gauge condition $t_l(0) = t_r(0) = 0$. We can compute the symplectic form for the original problem (4.24) on this space of solutions. One can check that this symplectic form, at $u = 0$, is the same as the one we get from (4.42).

After shifting $\varphi \rightarrow \tilde{\varphi} = \varphi - \log N$ we get a Schroedinger equation for $\psi(\tilde{\varphi})$ of the form

$$NE_{\tilde{u}}\psi = -\frac{\kappa^2}{4}\psi = -\frac{1}{4}\psi'' + [e^{2\tilde{\varphi}} - \tilde{\eta}e^{2\Delta\tilde{\varphi}}]\psi, \quad \tilde{\eta} \equiv \eta N^{2-2\Delta} \quad (4.43)$$

⁶What we really want is that it is the lowest energy state in the corresponding $SL(2)$ representation.

Exact solution for $\Delta = \frac{1}{2}$

For $\Delta = 1/2$ we can solve this eigenvalue problem and we find the quantization condition⁷

$$\kappa_n = \tilde{\eta} - \frac{1}{2} - n > 0, \quad n = 0, 1, \dots, \hat{N}, \quad \tilde{\eta} = N\eta, \quad \text{for } \Delta = \frac{1}{2} \quad (4.44)$$

which leads to a finite number of states

$$\hat{N}_{\text{bound states}} = \lfloor \tilde{\eta} + \frac{1}{2} \rfloor \sim \eta N \quad (4.45)$$

Note that via (4.31) ηN also controls how classical the system is. In the quantum analysis here we can go to small ηN and we can see that for $\eta N < \frac{1}{2}$ we actually have no bound state, so that we do not have a solution of the kind we are discussing, and we only get the black hole like configurations. The case $\Delta = \frac{1}{2}$ that we are discussing here is such that the boundary coupling g is dimensionless and it is essentially equal to η here, see appendix C.2.

So far we are only discussing the states of the “graviton mode”. If, in addition, we have some extra fields, with their own bulk energy E_t , (and zero q_{\pm} SL(2) charges) then we get an extra term in the potential as in (4.41), which results in an effective shift (for $\Delta = \frac{1}{2}$) $\eta \rightarrow \eta - E_t/N$. This reduces the number of bound states available for the gravity modes.

Approximate discussion for general Δ

For general Δ we could not solve the equation (4.43) exactly, but the fact that we get a finite number of states is also true. For large $\tilde{\eta}$ we can get an estimate on the number of states by a WKB analysis

$$\begin{aligned} \hat{N} &\sim \frac{1}{2\pi} \int pdq = \frac{N4}{2\pi} 4 \int_{-\infty}^{\varphi_0} d\varphi \sqrt{\eta e^{2\Delta\varphi} - e^{2\varphi}} = \frac{2Ne^{\varphi_0}}{\pi} \int_0^1 dz \sqrt{z^{-2(1-\Delta)} - 1} \\ \hat{N} &\sim \frac{N}{\sqrt{\pi}} \frac{\Gamma\left(\frac{\Delta}{2-2\Delta}\right)}{\Gamma\left(\frac{1}{2-2\Delta}\right)} \eta^{\frac{1}{2(1-\Delta)}} = (Nt') \frac{1}{\sqrt{\pi}} \frac{\Gamma\left(\frac{\Delta}{2-2\Delta}\right)}{\Gamma\left(\frac{1}{2-2\Delta}\right) \Delta^{\frac{1}{2-2\Delta}}}, \quad \text{where } e^{2(1-\Delta)\varphi_0} = \eta \end{aligned} \quad (4.46)$$

We see that the number continues to be propotional to the same parameter (Nt') that governs the classicality of the system, playing the role of $1/\hbar$ (4.31).

Comment on the case with a small number of fields in the interaction

In this paper we have mostly concentrated on the case where we have N fields in the bulk, or N operators in the interaction term. If we had a smaller number, say k , then have the same action as in in (4.24) but with the replacement

$$\eta \rightarrow \frac{k}{N}\eta \quad (4.47)$$

⁷The solution that decay at $\varphi \rightarrow \infty$ is $\psi \sim e^{\kappa\varphi - 2e^\varphi} U\left(\frac{1}{2} - \tilde{\eta} + \kappa, 1 + 2\kappa; 4e^\varphi\right)$, with U a confluent hypergeometric function. Imposing that it decays as $\varphi \rightarrow -\infty$ we get (4.44).

We imagine keeping k fixed and of order one as we take N large. This makes η even smaller, which is good in (4.30), but in (4.31) we get now

$$Nt' \propto N^{\frac{1-2\Delta}{2(1-\Delta)}} \quad (4.48)$$

So that for the system to have a classical wormhole, with a large number of bound states, we need that $\Delta < \frac{1}{2}$. In this case the interaction is relevant. In the gravity case, this requires that the bulk fields obey the alternate boundary condition, whether they are bosons [38] or fermions [39]. It would be nice to study this case further, to check the precise regime of validity of such configurations, but we will not do it in this paper.

4.3 Getting the thermofield double from a quench

In this subsection we consider a configuration where we prepare the ground state of the coupled system, with non-zero η , and then, at $\tilde{u} = 0$ we switch off η . So we have $\eta(\tilde{u}) = \eta\theta(-\tilde{u})$. We can view this as a quench where we set the coupling between the two systems to zero at time equal to zero. We argue that the state we get using the low energy approximation (4.24) (with $\eta \rightarrow \eta(\tilde{u})$) is precisely the thermofield double of two decoupled systems.

We will argue that the solution for positive times has the same form as the thermofield double described in (2.8), which in our variables becomes

$$t(\tilde{u}) = 2 \arctan \left[\tanh \left(\frac{\pi \tilde{u}}{\tilde{\beta}} \right) \right], \quad \varphi = \log t' = \log \left[\frac{2\pi}{\tilde{\beta} \cosh \frac{2\pi \tilde{u}}{\tilde{\beta}}} \right], \quad \tilde{u} > 0, \quad (4.49)$$

(see (2.4)). We can check that this is a solution of the theory with $\eta = 0$. At \tilde{u} equal to zero it matches the constant φ solution given by (4.29), which sits at the minimum of the potential in figure 4, provided that

$$t' = \frac{2\pi}{\tilde{\beta}}, \quad \text{or} \quad \frac{dt}{du} = \frac{2\pi}{\beta}, \quad \text{where} \quad \tilde{\beta} = \frac{\mathcal{J}}{\alpha_S} \beta = \frac{N}{\phi_r} \beta, \quad (4.50)$$

where $\tilde{\beta}$ is the rescaled inverse temperature. We have indicated how to translate to SYK or gravity parameters. This also gives a new physical interpretation for t' . Up to a factor of 2π , t' is an effective (rescaled) temperature. It is the temperature of the TFD state that most closely resembles the vacuum of the coupled system. Notice that the physical temperature of the coupled system is zero, when we discuss the ground state of the coupled system, as we are doing here.

In summary, the solution sits at a constant value of φ given by (4.29) for $u < 0$. Immediately after $u = 0$, the η term in the potential (4.36) disappears, φ' is zero, but φ'' is non-zero. This implies that the third derivative of $t(u)$, $t'''(u)$, jumps at $u = 0$, while all lower order derivatives are continuous. This precise value of the jump can also be obtained by analyzing the original equations that come from (4.24) around $\tilde{u} = 0$, with an η that is time dependent. See figure 5(a).

Note that the energy after the transition is

$$E_{\tilde{a}} = Nt'^2 = N \frac{(2\pi)^2}{\tilde{\beta}^2} \quad (4.51)$$

which is equal to the internal energy of the two copies of the thermal state, see (2.9). This is not the same as the energy (4.40), which is measured with respect to a different Hamiltonian, one with $\eta \neq 0$. On the other hand, if we subtract the expectation value of this extra term, we get the same as in (4.51)

$$E_G + gN \langle O_L O_R \rangle = E_G + \eta N t'^{2\Delta} = N t'^2 \quad (4.52)$$

after we use (4.29) and (4.39).

In addition, we can imagine that we take the TFD at inverse temperature $\check{\beta}$ as a variational ansatz for the interacting Hamiltonian. Then the variational energy can be written as the sum of two terms

$$E_{\text{var}}/N = \left(\frac{2\pi}{\check{\beta}} \right)^2 + \langle H_{\text{int}} \rangle = \left(\frac{2\pi}{\check{\beta}} \right)^2 - \eta \left(\frac{2\pi}{\check{\beta}} \right)^{2\Delta} \quad (4.53)$$

The first is the energy of the two decoupled systems, and the second is the expectation value of the interaction term. Minimizing the energy over the choice of $\check{\beta}$ we find that we get the same equations as before, $\check{\beta} = \beta$, (see Eqs. (4.50) and (4.29)). The variational energy (4.53) at the minimum is the same as the ground state energy (4.40).

Notice that this is also saying that the entanglement entropy between the left and right systems, for the ground state of the coupled system, is equal to the entropy in the TFD situation, which is the black hole entropy, or the entropy of a single SYK model at temperature given by (4.50), (2.9).

4.4 Computing the leading correction to the overlap

In this subsection we compute the leading correction to the statement in the previous section. We will see that the state resulting from the quench, resulting from setting the interaction to zero at $\tilde{u} = 0$, is not exactly the TFD. We will do so by computing the leading corrections to the inner product between the ground state of the interacting model and the thermofield double. These go beyond the approximation described by (4.24).

If we denote by $|G\rangle$ the ground state of the coupled system and by $|TFD\rangle$ the usual thermofield double state, then we can compute the overlap between the two states

$$\Omega = \frac{|\langle TFD|G\rangle|^2}{\langle TFD|TFD\rangle \langle G|G\rangle} \quad (4.54)$$

In the approximation where we describe the system using (4.24), and we treat it as in subsection (4.3), we find that the overlap is one, so that the two states are equal. The

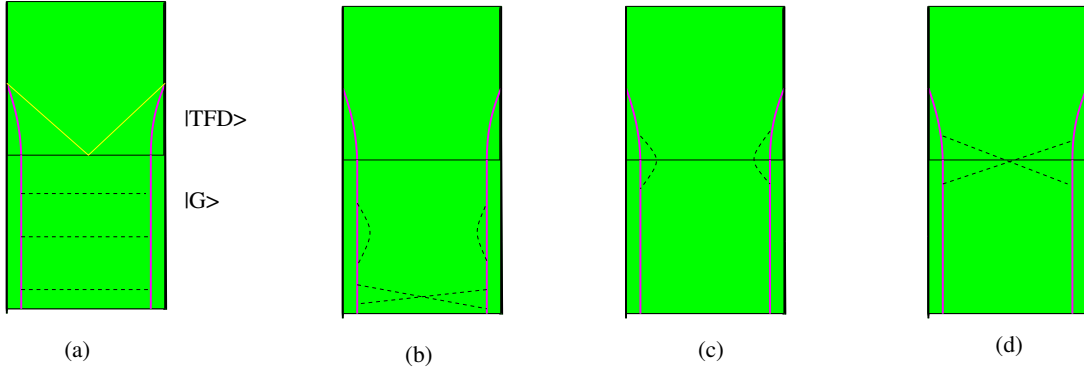


Figure 5: (a) We turn off the interaction hamiltonian at $u = 0$. Then the boundary trajectories look like those of the thermofield double state after that time. We see that at zero time, the ground state of the coupled system is very close to the thermofield double state of the decoupled system. We also display the diagrams that are summed over when we make the approximation in (2.12). (b) some of the diagrams not included in (2.12). (c) and (d) are the two diagrams that compute the leading corrections to the overlap of the two states in section 4.4.

reason is that we have an action that is local in time, and we have a solution which is piecewise the same as the solutions we had for the states in the denominator, therefore we get a cancellation of terms between the numerator and the denominator. In this approximation, we are treating the interaction as in (2.12), which corresponds to summing diagrams like the one in figure 5(a). The treatment in subsection (4.3) corresponded to coupling the gravity modes by performing a reparametrization of these correlation functions. In this approximation we are neglecting the particle creation that occurs when we suddenly turn off the coupling at $u = 0$. We can include these effects by considering the effect of further diagrams, such as the ones in figure 5(b). These diagrams are not local in time, they involve an integral over two times. When we turn off the coupling, some of these diagrams do not cancel between numerator and the denominator in (4.54). In fact, using the overall time translation symmetry, we see that the diagrams that do not cancel are precisely the two diagrams in figure 5(c,d). These diagrams appear in the denominator but not in the numerator. With our interaction involving N fields such as $\sum_i O_L^i O_R^i$, such diagrams give only a single factor of N . Note that the effect of these diagrams is *not* included in the action (4.24), they are higher order effects in the small coupling that couples the two system. Here we simply evaluate those effects. We get a slightly different answer depending on whether the operators that couple the two boundaries are bosons or

fermions. Their final contribution looks like

$$\begin{aligned}
\log \Omega &= -N\eta^2 t'^{4\Delta} \int_0^\infty d\tilde{u} \int_{-\infty}^0 d\tilde{u}' \left[\pm \frac{1}{[\cosh(t'(\tilde{u} - \tilde{u}')/2)]^{4\Delta}} + \frac{1}{[\sinh(t'(\tilde{u} - \tilde{u}')/2)]^{4\Delta}} \right] \\
&= -N\eta^2 t'^{4\Delta-2} h_\pm(\Delta) = -Nt'^2 \frac{h_\pm(\Delta)}{\Delta^2} \\
&\quad \text{where } h_\pm(\Delta) = 4 \int_0^\infty dx x [\pm \cosh^{-4\Delta} x + \sinh^{-4\Delta} x]
\end{aligned} \tag{4.55}$$

where the + corresponds to the case that the operators on each boundary are bosons, while the - corresponds to the case that they are fermions (as in the two coupled SYK models we discussed in section 3). The formula (4.55) includes the effects of particle creation. When we can create particles the probability that we end up with the unexcited TFD state is smaller, and for that reason we get $\Omega < 1$. As η becomes small, this correction becomes smaller. Notice that it is still of order N . The integral in (4.55) converges for $0 < \Delta < \frac{1}{2}$. As $\Delta \rightarrow \frac{1}{2}$ we find that (4.55) diverges. $\Delta = \frac{1}{2}$ corresponds to a conformally coupled field in the bulk and the boundary interaction is marginal. Turning off the coupling suddenly then leads to divergent particle production in the UV. For the case of fermions $h_-(\Delta) \sim 7\zeta(3)\Delta$ as $\Delta \rightarrow 0$, while for bosonic operators $2h_+(\Delta) \sim 1/\Delta^2$ for $\Delta \rightarrow 0$.

4.5 Finite temperature

We can now consider the coupled system at finite temperature. This finite physical temperature should not be confused with the effective temperature of the thermofield double that we discussed above near (4.50). We will denote the physical inverse temperature of the coupled system by $\tilde{\beta}_{ph}$. This is the period of the physical (rescaled as in (4.25)) time \tilde{u} , $\tilde{u} \sim \tilde{u} + \tilde{\beta}_{ph}$.

4.5.1 Lower temperatures

In the AdS_2 picture, we expect that for very low temperatures we should be obtaining a solution with a periodically indentified euclidean AdS_2 , where we indentify the Euclidean AdS_2 global time coordinate, $t \sim t + \beta'$. We will adjust β' momentarily. We imagine that we can impose a similar condition on the conformal solution of the SYK model. We then impose a periodicity condition on the Schwarzian variables

$$t_l(\tilde{u} + \tilde{\beta}_{ph}) = t_l(\tilde{u}) + \beta', \quad t_r(\tilde{u} + \tilde{\beta}_{ph}) = t_r(\tilde{u}) + \beta' \tag{4.56}$$

We continue to consider solutions with $t_l = t_r$ and with constant derivative, which requires $t_l = t_r = \frac{\beta'}{\tilde{\beta}_{ph}} \tilde{u}$. We can evaluate the euclidean action on these solutions to find

$$-S_E/N = \tilde{\beta}_{ph} [-(t')^2 + \eta(t')^{2\Delta}] + \log Z_{\text{bulk}}(\beta'), \quad t' = \frac{\beta'}{\tilde{\beta}_{ph}} \tag{4.57}$$

where the first term comes from the classical Schwarzian action (4.24) and the last term is the partition function of a single bulk field, where we imagine that we have N bulk fields. In the SYK this would be the partition function over the conformal sector obtained as the appropriate sum over representations with the thermal weights given by β' . We can now view β' as a variational parameter and minimize the action (4.57) with respect to β' to obtain the equation

$$0 = -2t' + 2\eta\Delta(t')^{2\Delta-1} - \epsilon(\beta'), \quad \epsilon(\beta') = -\partial_{\beta'} \log Z_{\text{bulk}} \quad (4.58)$$

This is also the equation we would obtain in the Lorentzian theory when we set the $SL(2)$ charge Q_0 to zero. Here $\epsilon(\beta')$ is the finite temperature energy of the bulk fields at inverse temperature β' . At low temperatures, $\Delta\beta' \gg 1$, the energy is approximately $\epsilon \sim \Delta e^{-\Delta\beta'}$, so that

$$0 = -2t' + 2\eta\Delta(t')^{2\Delta-1} - \Delta e^{-\Delta\beta'}, \quad t' = \frac{\beta'}{\tilde{\beta}_{ph}} \quad (4.59)$$

From (4.59) we can solve for β' . The interesting aspect is that there is more than one solution, and that the solution exists only for $\tilde{\beta}_{ph}$ sufficiently large. See figure 6(a).

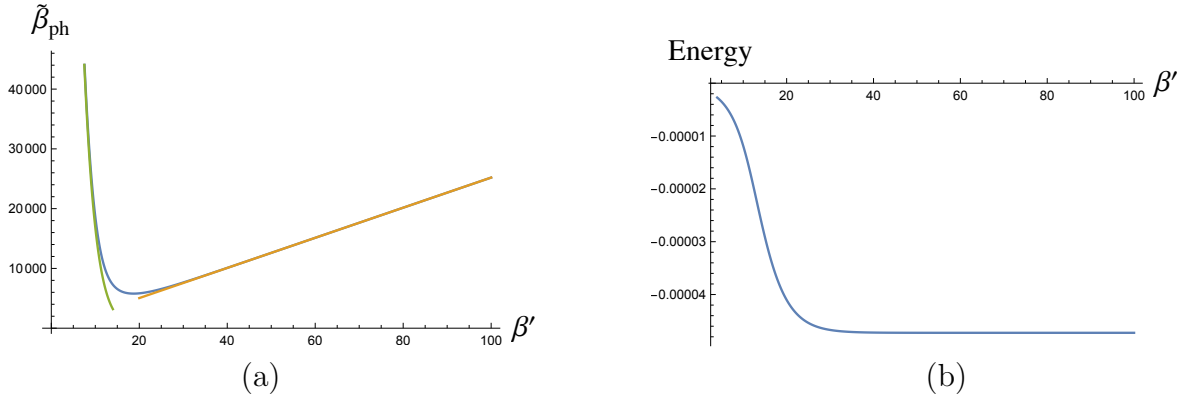


Figure 6: (a) We plot the relation between the physical temperature $\tilde{\beta}_{ph}$ and β' , which is the period of the global euclidean time coordinate t . β' can be viewed as the periodic identification of the global Euclidean time coordinate in the AdS_2 space, in units of the AdS_2 radius. In blue we have the numerical solution of (4.59) for $\Delta = 1/4$ and $\eta = 10^{-3}$. In orange we plot the approximate solution β'_+ (4.60) and in green the approximate solution β'_- (4.61). We see that there exists a minimum value for $\tilde{\beta}_{ph}$ (or maximum value for the temperature) for the solution to exist. For very low values of β' we stop trusting the approximations leading to (4.59). (b) We plot the energy as a function of the parameter β' . Notice that for a given $\tilde{\beta}_{ph}$ we have two values of β' and two energies. The energy increases monotonically as β' decreases. The asymptotic value for large β' is just the zero temperature energy (4.40).

We can find approximate solutions to (4.59) as follows. Here we will analyze only the case with $\Delta < \frac{1}{2}$. We also need small η , (4.30). In the first solution, we neglect the third term in (4.59) and reobtain (4.28) (4.29)

$$(t')^{2(1-\Delta)} = \eta\Delta \longrightarrow \beta'_+ = t' \tilde{\beta}_{ph} = (\eta\Delta)^{\frac{1}{2(1-\Delta)}} \tilde{\beta}_{ph} \quad (4.60)$$

In the second solution we neglect the first term in (4.59) and obtain

$$(2\eta)^{\frac{1}{(1-2\Delta)}} \tilde{\beta}_{ph} = \beta'_- e^{-\Delta\beta'_/(1-2\Delta)} \quad (4.61)$$

We have denoted the two approximate solutions by β'_+ and β'_- . In order to be consistent with the approximations we need $\eta\tilde{\beta}_{ph}^{1-2\Delta} \ll 1$ for the second solution (4.61) and we used this approximation for the second expression. Therefore we have two solutions within the regime

$$\eta^{-\frac{1}{(2-2\Delta)}} \ll \tilde{\beta}_{ph} \ll \eta^{-\frac{1}{(1-2\Delta)}} \quad (4.62)$$

Of course the first solutions (4.60) exists also for arbitrarily large $\tilde{\beta}_{ph}$. The two solutions merge in the lower range of $\tilde{\beta}_{ph}$, but for the precise value we need to consider the full equation and solve it numerically, which is shown in figure 6(a). It can be checked by taking the second derivative of the action (4.57) with respect to β' that that the β'_+ branch is stable and the β'_- in unstable in the canonical ensemble. It is interesting to compute the energy along the whole curve, using (4.38), or $E/N = -t'^2 - \eta(1-2\Delta)t'^{2\Delta}$, with t' obeying (4.59). We find that it varies monotonically, see figure 6. This suggests that if we have an isolated system and we increase the energy in the microcanonical ensemble, then we can explore the solutions with small β' which were unstable in the canonical ensemble.

4.5.2 Higher temperatures

If we consider the coupled system at sufficiently high temperatures, we expect that the Euclidean space solution corresponds to two separate Euclidean black holes. This is *not* described by the action (4.24), but it can still be described using conformal methods applied to the two decoupled black holes. We have the results corresponding to two decoupled thermal systems, each computed using the answers in the nearly conformal approximation. These are corrected to leading order by the diagrams in figure 7(b). We then find

$$\log Z = 2S_0 + N \frac{(2\pi)^2}{\tilde{\beta}_{ph}} + N\eta^2 \tilde{\beta}_{ph}^{2-4\Delta} \int_0^1 dx \left[\frac{\pi}{\sin x\pi} \right]^{4\Delta} + \dots \quad (4.63)$$

where S_0 is the “ground state” entropy of each SYK model or AdS_2 factor. In AdS_2 $S_0 = 2\pi\phi_0$ and it arises from the topological term in (2.5) when the Euclidean solution has the topology of the disk, as in figure 7(b). There is no contribution when the topology is that of a cylinder, as in figure 7(a). We see that the correction in (4.63) is small for small η . On the other hand, the low temperature form of the partition function is dominated by

the ground state energy (4.40) and is of the form

$$\log Z = -N\beta_{ph}E_{Gu} + N \exp\left(-\beta_{ph}\Delta\frac{dt}{du}\right) + \dots \quad (4.64)$$

where we have also included the leading correction from weakly exciting the particles mentioned in (4.33) and we assume that there are N of them, as in the SYK model. Both (4.63) and (4.64) assume that we are at temperatures much smaller than \mathcal{J} . We have also subtracted a common contribution to the ground state energy, which in the SYK model is proportional to $-N\mathcal{J}$.

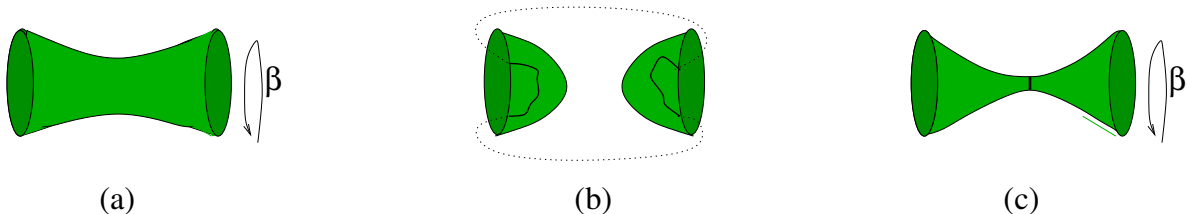


Figure 7: Here we display three branches for a given temperature. The physical temperature is the same for all three, and it is represented by the size of the circle at boundary. (a) In the low temperature phase we have a geometry that connects the two sides. The thermal circle is not contractible, and there are almost no bulk excitations. (b) The high temperature phase contains two separate geometries, each with a contractible euclidean time circle. The leading coupling between two is given by the diagram displayed, which is proportional to μ^2 . The dotted lines indicate that the times are equal. The solid lines indicate two point functions. Finally in (c) we display the phase that is unstable in the canonical ensemble that we discussed in section 4.5.1, which can be interpreted as AdS with global time identified and a small amount of thermal excitations in the bulk. The topology is the same as for (a), but the minimal size of the Euclidean time circle in the interior is smaller, so that we are thermally exciting the bulk modes a bit (represented by the black line at the neck). The physical temperature from the boundary point of view is the same as in (a).

In the canonical ensemble, we expect to get a first order phase transition between these two phases. The most notable aspect of this high temperature phase is its entropy $2S_0$. While in the low temperature phase we have small entropy but we have negative energy (4.40). We expect the transition temperature, T_c , to be approximately given by the equation

$$2S_0 = -E_G/T_c, \quad \beta_c = \frac{2S_0}{-E_G} \quad (4.65)$$

It is possible to check that the temperature we obtain in (4.65) is well within the regime of approximation of both (4.63) and (4.64), at least for Δ not too small⁸. In other words,

⁸This is checked as follows. First to check (4.64) we compute $\tilde{\beta}_c\Delta t' \propto \frac{\Delta^2}{t'}$ which is very large and so

(4.65), is correct in the limit of fixed Δ and very small η . We will see in section 5.4, that for very large q the transition happens beyond the reach of the approximation in (4.63).

Then we conclude that, for small η , we can describe the physics on both sides of the transition by using Schwarzian type variables. It is important to notice that the Schwarzian variables we use at low or high temperatures are not the same! They are based on different underlying conformal states for the rest of the fields. In the gravity description, they are based on different underlying geometries, as figure 7.

On the other hand, we can consider the microcanonical ensemble and start increasing the energy above the vacuum. As we do so, we introduce bulk particles and we need to go beyond the pure gravity, or pure Schwarzian, approximation. This can be done in the SYK model by solving the large N equations of the coupled system. We will discuss this in more detail in section 5.

4.6 Some properties of correlation functions

Here we consider the two point functions of a field \mathcal{O} that propagates in AdS_2 . We can also think of it as one of the fields that we are using in the interaction that produces the solution. In the SYK model we can think of \mathcal{O} as one of the basic fermions, or any other conformal operator with definite conformal dimension in the conformal limit.

The two point functions for this field on the same side and on different sides are given by

$$\langle \mathcal{O}_L(\tilde{u}_1) \mathcal{O}_L(\tilde{u}_2) \rangle = e^{-i\pi\Delta} \left[\frac{t't'}{\sin^2 \frac{t'(u_1 - u_2 - i\epsilon)}{2}} \right]^\Delta, \quad \langle \mathcal{O}_L(\tilde{u}_1) \mathcal{O}_R(\tilde{u}_2) \rangle = \left[\frac{t't'}{\cos^2 \frac{t'(\tilde{u}_1 - \tilde{u}_2)}{2}} \right]^\Delta \quad (4.66)$$

in Lorentzian signature. Note that the left-left correlator has singularities at $t'\tilde{u}_{12} = 0, 2\pi, 4\pi$. While the left right correlator has singularities at $t'\tilde{u}_{12} = \pi, \pi + 2\pi, \dots$. These singularities correspond to the ones expected for light-rays that start from one of the operators and bounce back and forth in AdS_2 , see figure 8(a). They should be regulated by the appropriate $i\epsilon$ prescription. Furthermore, all these singularities, are regulated by UV effects, namely effects that take us away from exact conformal symmetry, already to the leading order in the large N limit. In the SYK model these kick in at values of \tilde{u} which differ by an order one amount (or an order $1/\mathcal{J}$ in u) from the naively singular one. We will see this explicitly when we analyze the SYK model at large q in section 5.3. Finally, gravitational back reaction effects should also smooth out these singularities for the following reason. The singularities arise when we exchange high energy particles. This exchange back-reacts on the gravitational degrees of freedom, which moves the boundary trajectories and smears out the insertion of the other particles. Similar effects were also discussed in the analysis of traversable wormholes in [28].

the exponential corrections in (4.64) are small. Similarly, we can check that $\eta^2 \tilde{\beta}^{2-4\Delta} \propto (t'/\Delta)^{4\Delta}$, which is small if (4.30) holds. For very small Δ this last expression becomes of order one, when we scale parameters as in section 5.3.

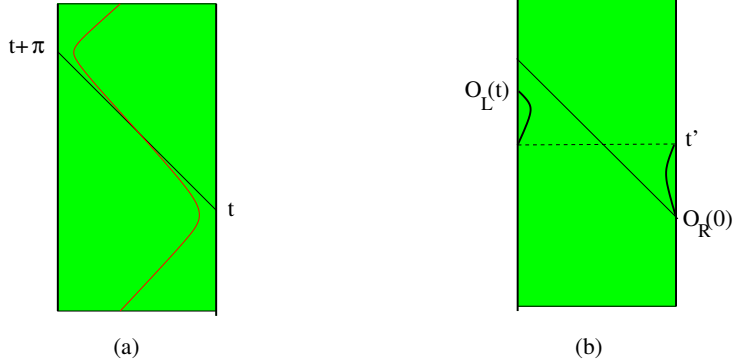


Figure 8: (a) Trajectory of a particle moving in AdS_2 . In the conformal approximation, given by (4.66), there is a singularity at $t_r - t_l = \pi$. (b) Diagram contributing to the commutator between left and right operators before the operator on the left crosses the bulk light cone of the operator on the right. The black lines in the bulk represent propagators. Here we drew AdS diagrams but the same properties hold for the two coupled SYK models.

Notice that the left-right correlators reflect the fact that we can send signals from one system to the other. Of course this is not surprising since we are coupling them. However, as in the traversable wormhole situation, it is interesting how the signal is moving between the boundaries. The interaction is setting up an eternal-traversable wormhole. A particle starts near one boundary, living mostly in the first system and then moves to the other side, living mostly in the second system. This is somewhat reminiscent of two weakly coupled oscillators where the excitation moves between one oscillator to the other, except that here it is doing this through the bulk geometry. Notice that the same property holds in the two coupled SYK models!

Note also the following feature. Let us concentrate on the coupled SYK models in (3.21). Let us first set the SYK couplings to zero, $\mathcal{J} = 0$, but keeping a non-zero mass-like coupling μ . In this case, a fermion on one side will move to the other side after a time of order $\Delta u_0 = 1/\mu$. This is just a simple free fermionic harmonic oscillator. Now, let us turn on a relatively large value of $\mathcal{J} \gg \mu$ so that the low energy discussion in this section applies. Then the time to go across is π in time units measured by t . Via t' , (4.29), this translates into a boundary time of the order of $\Delta u \propto 1/t'$. Comparing this time to the time Δu_0 in the free theory, we get $\frac{\Delta u}{\Delta u_0} \propto (\frac{\mu}{\mathcal{J}})^{\frac{1-2\Delta}{2(1-\Delta)}}$, which vanishes in small μ limit if $\Delta < 1/2$. This means that the self interactions, within each SYK model, accelerate the transfer of information from the left to the right system, relative to the non-interacting system. Of course, for this increase in the information transfer rate we need that the microscopic random couplings of the two models are correlated.

Note that the second correlator in (4.66) is such that the commutator (or anti-commutator, for fermionic operators) between the left and right fields is exactly zero for times $|t'(u - u')| <$

π . In other words,

$$\langle [O_L(\tilde{u}), O_R(0)]_{\pm} \rangle \propto \sin(2\pi\Delta) \left[\frac{t'}{-\cos(\frac{t'\tilde{u}}{2})} \right]^{2\Delta} \theta(t'\tilde{u} - \pi), \quad 0 < t'\tilde{u} < 3\pi, \quad (4.67)$$

This is true to leading order in the η expansion. However, there are some diagrams that contribute to the commutator which are of the form displayed in figure 8(b). This gives an extra term in the commutator (or anticommutator for fermion fields) (for dimensionless times $t < \pi$) of the form

$$\langle [O_L(t), O_R(0)]_{\pm} \rangle \propto \eta t'^{4\Delta-1} (\sin 2\pi\Delta)^2 \int_0^t \frac{d\tau}{[\sin \frac{\tau}{2} \sin \frac{(t-\tau)}{2}]^{2\Delta}}, \quad 0 < t < \pi \quad (4.68)$$

here we assume that \mathcal{O} is one of the fields appearing in the interaction term. We see that there is an extra suppression due to an extra factor relative to (4.67) of $\eta t'^{2\Delta-1} \propto t' \ll 1$ (see (4.30)). However, it is the leading non-zero contribution in the time range in (4.68)

On the other hand, for larger times, we already get a non-zero commutator (4.67).

4.7 The three generators of SL(2)

We have mostly discussed here the “gravitational” degrees of freedom. We have also mentioned “bulk” degrees of freedom that transform in non-trivial representations of SL(2). These are present both in the gravity case and in the SYK situation. These degrees of freedom transform under SL(2) representations with generators q_a that act purely on them. When these degrees of freedom are added to the “gravitational” sector (4.24) we need to modify the constraints so that now they read

$$Q_a + q_a = 0 \quad (4.69)$$

where Q_a are the SL(2) charges of (4.24). We discuss a bit more how this works in appendix B.

We have the time translation symmetry of the full system, generated by the total Hamiltonian $H_{\text{tot}} = H_L + H_R + H_{\text{int}}$ in the coupled SYK systems. This symmetry acts, up to a redshift factor, like the generator q_0 on the conformal degrees of freedom,

$$H_{\text{tot}} - E_{G_u} \sim \frac{dt}{du} q_0 + o(1/N) \quad (4.70)$$

where we have subtracted the ground state energy. It also follows from the discussion in section (4.3), where we matched the ground state to the TFD state, that at $u = 0$ the difference of Hamiltonians

$$H_R - H_L|_{u=0} \sim \frac{dt}{du} \frac{(q_+ + q_-)}{2} + o(1/N) \quad (4.71)$$

acts like the boost generator at $u = 0$. This statement has also corrections due to the particle creation discussed in section (4.4), which we will ignore, assuming that we take a limit of very large N and very small η . The operator on the left is time dependent in the full coupled system. It does not commute with H_{tot} . It turns out that the third $\text{SL}(2)$ generator corresponds to a similar operator but at another time (see appendix B for more details)

$$H_R - H_L \Big|_{u=\frac{\pi}{2} \frac{du}{dt}} = e^{iTH_{\text{tot}}}(H_L - H_R)e^{-iTH_{\text{tot}}} \sim \frac{dt}{du} \frac{(q_+ - q_-)}{2i} + o(1/N), \quad T = \frac{\pi}{2} \frac{du}{dt} \quad (4.72)$$

The time shift corresponds to a shift by $\pi/2$ in the IR time t . Formula (4.72) is derived as follows. We could run the argument leading to (4.71) but at time $t = \pi/2$. The operator on the right hand side is the boost generator around the bulk point $\sigma = 0$, $t = \pi/2$ in coordinates (1). An alternative local expression for the third generator (not equal to (4.72)), arises from taking the commutator between (4.70) and (4.71).

In conclusion, we have identified three operators (4.70), (4.71) and (4.72) that are completely well defined in the boundary theory. We have argued that these operators act like the three generators of $\text{SL}(2)$ on the conformal infrared degrees of freedom of the theory. We have derived this indirectly. It would be nice to derive this more directly in the SYK model. In particular, one would like to understand their commutation relations, and their $1/N$ corrections. However, one can easily verify that in coupled SYK model the microscopic operators $H_{\text{tot}} - E_{Gu}$ and $H_R - H_L$, and their commutator, do not form a closed $\text{SL}(2)$ algebra. This is expected since the $\text{SL}(2)$ symmetry only emerges for low energy states. It would be interesting to learn how to compute the effective commutation relations in the low energy subspace so as to verify the approximate $\text{SL}(2)$ symmetry. We will not do it in this work.

5 The two coupled SYK models beyond the low energy limit

5.1 Large N equations

In this section we study the large N equations for the fermion two point function for the coupled system. We study them in Euclidean time. The effective action with collective variables G and Σ can be easily generalized to the coupled system with Hamiltonian (3.21). One difference is that we now have left-left, left-right, etc, correlators, $G_{LL}(\tau_1, \tau_2)$, $G_{LR}(\tau_1, \tau_2)$, etc. The effective action is

$$\begin{aligned} -S_E/N &= \log \text{Pf}(\partial_\tau \delta_{ab} - \Sigma_{ab}) - \frac{1}{2} \int d\tau_1 d\tau_2 \sum_{a,b} \left[\Sigma_{ab}(\tau_1, \tau_2) G_{ab}(\tau_1, \tau_2) - s_{ab} \frac{\mathcal{J}^2}{2q^2} [2G_{ab}(\tau_1, \tau_2)]^q \right] + \\ &+ \frac{i\mu}{2} \int d\tau_1 [-G_{LR}(\tau_1, \tau_1) + G_{RL}(\tau_1, \tau_1)] \end{aligned} \quad (5.73)$$

Here $a, b = L, R$ denotes the two sides. Note that the functions obey the antisymmetry condition $G_{ab}(\tau_1, \tau_2) = -G_{ba}(\tau_2, \tau_1)$. Here s_{ab} is a sign, $s_{LL} = s_{RR} = 1$, $s_{LR} = s_{RL} = (-1)^{q/2}$, which arises because for odd $q/2$ the signs of the couplings in the left Hamiltonian are the opposite than those on the right Hamiltonian (with the same absolute value). The equations we get from (5.73) are very similar to the ones in (3.15). If we think of the L, R and τ_1, τ_2 indices as one combined index, then the equations have the same structure as in (3.15). The only difference is that there is an additional term, $i\mu\delta(\tau_1 - \tau_2)$ in the expression for the left-right self energy Σ_{LR} . Just to be more explicit, we can write some of the equations

$$\begin{aligned} \partial_{\tau_1} G_{LL} - \Sigma_{LL} * G_{LL} - \Sigma_{LR} * G_{RL} &= \delta \\ \partial_{\tau_1} G_{LR} - \Sigma_{LL} * G_{LR} - \Sigma_{LR} * G_{RR} &= 0 \\ \Sigma_{LL} &= \frac{\mathcal{J}^2}{q} (2G_{LL})^{q-1}, \quad \Sigma_{LR} = (-1)^{q/2} \frac{\mathcal{J}^2}{q} (2G_{LR})^{q-1} - i\mu\delta(\tau_{12}), \end{aligned} \quad (5.74)$$

where $*$ denotes a convolution, as in (3.15). The other equations can be similarly listed. δ in the first equation represents $\delta(\tau_1 - \tau_2)$.

For any solution, the energy can be computed by

$$\frac{E}{N} = \left[\frac{1}{q} \partial_{\tau_1} G_{LL} + \frac{1}{q} \partial_{\tau_1} G_{RR} + i\mu \left(1 - \frac{2}{q} \right) G_{LR} \right]_{\tau_{12}=0^+} \quad (5.75)$$

This formula is derived by noticing that

$$N \partial_{\tau_1} G_{LL} |_{\tau_{12}=0^+} = \sum_i \langle \partial_{\tau} \psi_L^i \psi_L^i \rangle = \sum_i \langle [H, \psi_L^i] \psi_L^i \rangle = \langle qH_L + H_{int} \rangle \quad (5.76)$$

where the operators are all at the same time. The factor of q comes from the fact that a given individual coupling in (3.14) contributes to q terms in the sum over i . We have a similar equation for G_{RR} . We can also express the expectation value of the interaction Hamiltonian in terms of G_{LR} to get to (5.75). Note that (5.75) is an exact formula for the energy when we think of NG as the sum of all the fermion correlators⁹.

In order to solve the equations is it convenient to consider the system at finite temperature. Then the euclidean time is periodic. We can also assume that we have an ansatz where all functions depend only on the difference of times. Then we expect that $G_{LL}(\tau)$ remains positive and is symmetric around $\tau = \beta/2$ and obeys $G_{LL}(0) = \frac{1}{2}$. On the other hand, we expect that $G_{LR}(\tau)$ is purely imaginary and is antisymmetric around $\tau = \beta/2$. This property is consistent with the fact that it should be anti-periodic under $\tau \rightarrow \tau + \beta$. The fact that it is imaginary follows simply the the factors if i in (5.74).

The equations (5.74) can be analyzed numerically or analytically for large q . We discuss some numerical results in the next section.

⁹By ‘‘exact’’, we mean that it is valid for finite N and for definite values of the random couplings of the model.

5.2 Numerical analysis

To gain more intuition, we solve the Schwinger-Dyson equation (5.74) numerically by iteration.¹⁰ For numerical purposes, it is easier to work at finite temperature, where the imaginary time is periodic $\tau = \tau + \beta$. Then τ is discretized as $\tau = \beta \frac{n}{M}$, $n = 0, 1, 2, \dots, M$, where the integer M determines the UV cutoff of frequency $\omega_{\max} = \frac{\pi}{\beta} M$. In our calculation we take $M = 10^5$. To describe correctly the continuous time physics, the discretization time scale $\frac{\beta}{M}$ needs to be much smaller than \mathcal{J}^{-1} and μ^{-1} , which requires $M \gg \beta\mathcal{J}$, $\beta\mu$.

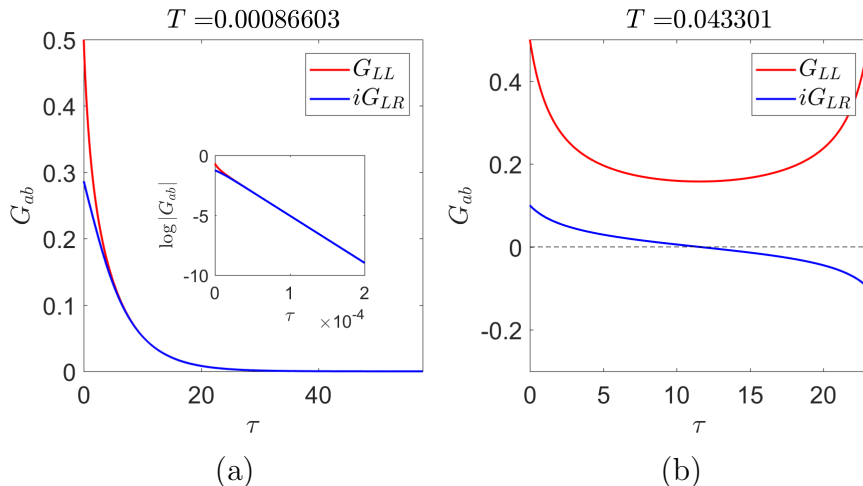


Figure 9: Numerical solution of $G_{ab}(\tau)$ at (a) low temperature and (b) higher temperature. The calculations are done for $\mu = 0.075$, $\mathcal{J} = 1$, $q = 4$. (The low temperature case in (a) is also anti-periodic in imaginary time, but we have only shown the short time part for clarity.) Since G_{LR} is purely imaginary, the imaginary part is plotted. The inset of panel (a) is a log plot of $\log |G_{ab}|$ which shows that the two-point function decays exponentially in time.

The solution of $G_{ab}(\tau)$ for two different temperatures is shown in figure 9. At low temperature, we obtain an exponentially decaying two-point function $G^{ab}(\tau) \propto e^{-E_{\text{gap}}\tau}$ (with the same exponent E_{gap} for both G^{LL} and G^{LR}). This confirms that the coupled SYK model has a gap E_{gap} above the ground state. Figure 10 (a) shows the gap E_{gap} as a function of coupling μ . In the region of small μ , the result is consistent with the dimensional analysis

$$E_{\text{gap}} \propto \mu^{\frac{1}{2-2\Delta}} = \mu^{2/3}, \quad (5.77)$$

which we discussed earlier in Eqs. (4.29) (4.34). For larger μ , we see a cross-over to linear dependence $E_{\text{gap}} \propto \mu + \text{constant}$, which is what we expect when the interaction term in (3.21) dominates.

¹⁰There are numerical subtleties in the iteration procedure, as has been pointed out in Appendix G of Ref. [9]. Here we use the same weighted iteration as in Ref. [9].

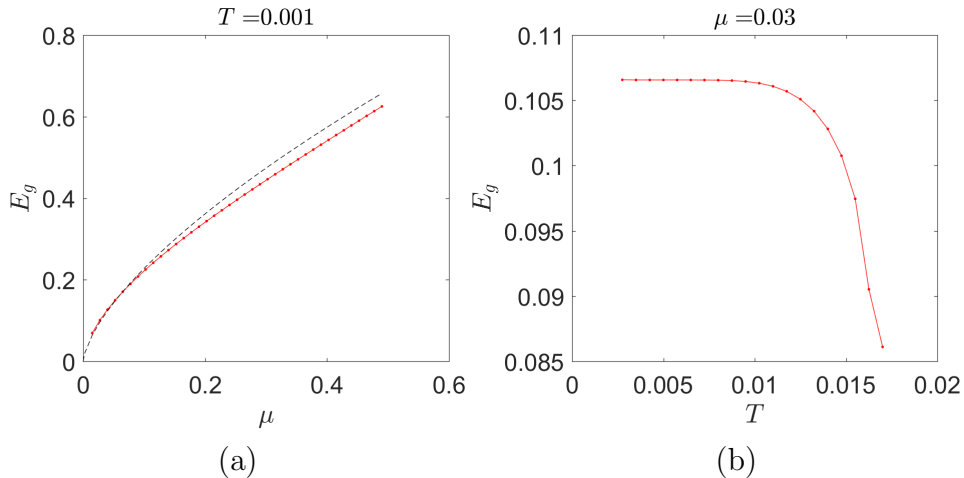


Figure 10: The (effective) energy gap E_{gap} defined by exponential fitting $G_{ab}(\tau) \propto e^{-E_{\text{gap}}\tau}$, as a function of (a) coupling μ and (b) temperature T . The dashed line in (a) shows a fitting to the power law behavior $E_{\text{gap}} \propto \mu^{2/3}$. The calculation is done for $\mathcal{J} = 1$, $q = 4$.

Since the numerics is setup for finite temperature, we can also study the temperature dependence of two-point functions and thermodynamic properties. Figure 10(b) shows how the exponential decaying factor E_{gap} decreases slowly with temperature.¹¹

At higher temperature, for μ that is not too large, we observe a first order phase transition, as can be seen from the behavior of Gibbs free energy, see figure 11(a). To see the phase transition, we start from high temperature and decrease the temperature gradually. We use the solution $G_{ab}(T)$ at temperature T as the initial condition of the iteration for the next step with a lower temperature $T - \Delta T$. When we reach the lowest temperature, we start increasing the temperature and use $G_{ab}(T)$ at each step as the initial condition of next step with temperature $T + \Delta T$. The hysteresis curve we obtain in figure 11(a) suggests that within a range of temperature $T \in [T_{c1}, T_{c2}]$, the free energy has two local minima. The annealing from higher temperature makes the solution stay in the high temperature local minimum, until the minimum almost disappears at temperature T_{c1} and G_{ab} hops to the other minimum. Similarly at temperature T_{c2} the low temperature local minimum disappears. The same features were observed in similar massive deformations of SYK-like models in [13].

The results in figure 11 are in agreement with the general discussion in section 4.5.2. Namely, we see that the low temperature phase has constant energy and the high temperature phase has constant entropy. They cross where those properties still hold.

¹¹At finite temperature, the two-point function at long time is actually a sum of exponentially decaying and exponentially increasing contributions, due to the finite periodicity in time. To obtain the temperature dependence of effective gap E_{gap} we used the long time behavior of G_{ab} , which will be discussed later in Eq. (5.96).

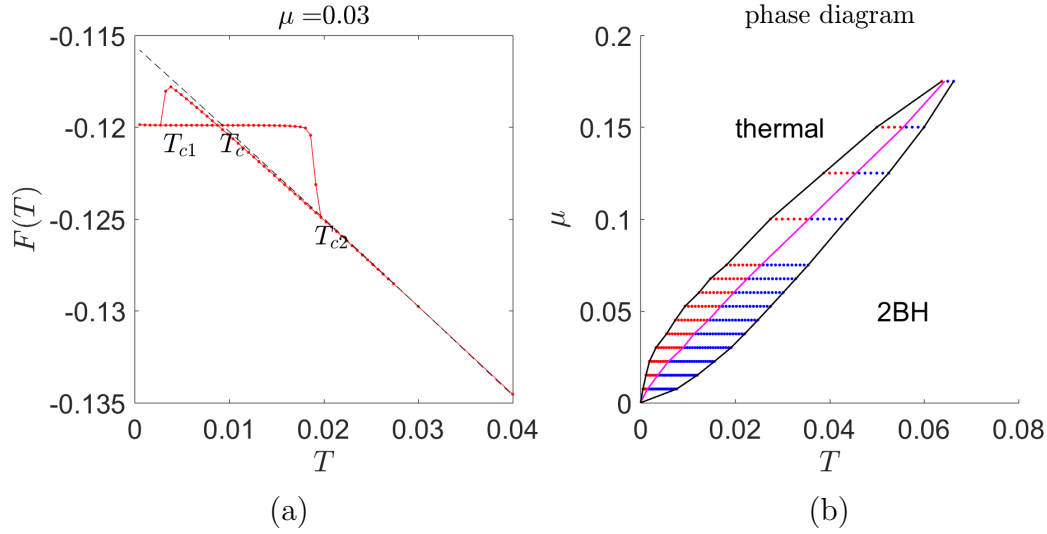


Figure 11: (a) The free energy of the saddle point solution. Starting from the highest temperature, we decrease the temperature to lowest value and then increase it again back to the highest value. The solution at each temperature step is used as the initial condition of the next step. Two saddle points coexist in the region $T \in [T_{c1}, T_{c2}]$, and the free energy of the two saddle points cross each other at some temperature T_c in this region. The black dashed line is the free energy of decoupled two SYK sites, for comparison. (b) The phase diagram in $\mu - T$ plane obtained by calculating the free energy hysteresis curves for different values of μ . The red (blue) dots are data points where the free energy of the high temperature saddle point is higher (lower) than that of the low temperature one. The black solid lines are the lower and upper critical temperatures T_{c1}, T_{c2} , and the pink line is the thermodynamic transition temperature T_c . The calculation is done for $q = 4, \mathcal{J} = 1$.

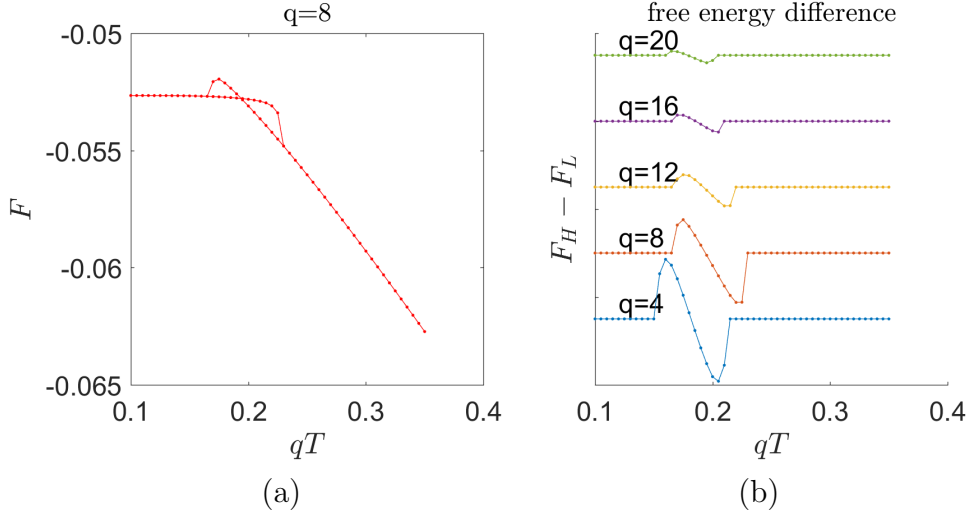


Figure 12: (a) The hysteresis curve for $q = 8$. (b) The difference between the free energy of the two saddle points $\Delta F = F_H - F_L$ for different q . The curves are offset by a constant for clarity. It should be noted that the temperature is rescaled by q since the transition occurs at different temperature region for different q . The calculations are done for $\hat{\mu} = \frac{\mu}{q} = 0.5$.

Varying μ and T leads to a two-dimensional phase diagram, as is shown in figure 11(b). The phase diagram suggests that the first order transition exists for arbitrarily small μ but goes away at large enough μ . The first order phase transition here can be considered as an analog of the Hawking-Page transition[40, 41] between the thermal gas in AdS_2 geometry and the black hole solution. In higher dimensions, the boundary is connected, while in two-dimensions the boundary is disconnected and the black hole solution consists of two AdS_2 black holes, as we have discussed in section 4.5 and figure 7. Compared with the higher temperature Einstein gravity case, the current theory has a large number of bulk fields, of order N . Therefore it was not immediately obvious that a first order phase transition, instead of a smooth crossover, should exist between the two distinct geometries. In fact, as we will discuss later, the two phases are continuously connected in the microcanonical ensemble (at least at large q). It is an interesting question what is the generic physical reason for such phase transition.

The results above are all obtained for $q = 4$, and the generalization to higher q is straightforward. We observe qualitatively the same physics for all q : the exponentially decaying low temperature two-point function, the super-linear growth of gap $E_{\text{gap}}(\mu)$ at small μ , and the first order phase transition for a region of $\mu \in (0, \mu_{\text{max}}]$. As an example, figure 12 shows the hysteresis curve for different q . In the next section, we study the large q limit analytically, which provide further understanding to the form of two-point function, energy gap and phase diagram. We will compare the numerics with analytic results there.

5.3 Large q analysis. Zero temperature

In this section we study the coupled system at large q as in [9]. At large q we write the correlators as

$$G_{LL} = \frac{1}{2} \text{sgn}(\tau) \left(1 + \frac{1}{q} g_{LL} + \dots\right), \quad G_{LR} = \frac{i}{2} \left(1 + \frac{1}{q} g_{LR} + \dots\right) \quad (5.78)$$

It is convenient to scale $\mu = \hat{\mu}/q$, keeping $\hat{\mu}$ fixed when $q \rightarrow \infty$. We can take then derivatives of (5.74) and expand in $1/q$ to obtain

$$\partial_\tau^2 g_{LL} = 2\mathcal{J}^2 e^{g_{LL}}, \quad \text{for } \tau > 0 \quad ; \quad \partial_\tau^2 g_{LR} = -2\mathcal{J}^2 e^{g_{LR}} - 2\hat{\mu}\delta(\tau), \quad \text{for any } \tau \quad (5.79)$$

Surprisingly we see that the two equations decouple. The minus sign in front of $e^{g_{LR}}$ arises from the factors of i in G_{LR} in (5.78)¹². These two functions are related by the boundary conditions, which are

$$g_{LL}(0) = 0, \quad \partial_\tau g_{LR}(0) = -\hat{\mu}, \quad g_{LL} - g_{LR} \rightarrow 0, \quad \text{as } \tau \rightarrow \infty \quad (5.80)$$

The first condition comes from $G_{LL}(0) = \frac{1}{2}$, the second comes from demanding that we reproduce the δ function in (5.79). The last condition applies to the zero temperature situation and is explained in detail in appendix A.

An alternative derivation of the Liouville equations (5.79) is by performing first a large q expansion of the effective action (5.73). One can show that to the order of $\frac{1}{q^2}$ the effective action is equivalent to a Liouville action:

$$\begin{aligned} \frac{1}{N} S_{\text{eff}} &= \frac{1}{4q^2} \int_{\tau_1 > \tau_2} d\tau_1 d\tau_2 (\partial_{\tau_1} g_{LL}(\tau_1, \tau_2) \partial_{\tau_2} g_{LL}(\tau_1, \tau_2) - \partial_{\tau_1} g_{LR}(\tau_1, \tau_2) \partial_{\tau_2} g_{LR}(\tau_1, \tau_2)) \\ &\quad - \frac{\mathcal{J}^2}{q^2} \int_{\tau_1 > \tau_2} d\tau_1 d\tau_2 (e^{g_{LL}(\tau_1, \tau_2)} + e^{g_{LR}(\tau_1, \tau_2)}) - \frac{\hat{\mu}}{q^2} \int d\tau g_{LR}(\tau, \tau) \end{aligned} \quad (5.81)$$

Such effective action for a single SYK model has been discussed in Appendix B of Ref. [42]. For completeness we include the derivation for the coupled model in Appendix D. In writing (5.81) we have neglected possible long-time contributions of the determinants. The Liouville action is defined on a half plane $\tau_1 \geq \tau_2$, with the boundary condition

$$g_{LL}(\tau, \tau) = 0, \quad (\partial_{\tau_1} - \partial_{\tau_2}) g_{LR}(\tau_1, \tau_2)|_{\tau_2=\tau_1} = 2|\hat{\mu}| \quad (5.82)$$

The effective action approach is useful, since it provides a general derivation of the Liouville equations of motion. It applies to different cases such as ground state and finite temperature, and more general situations when the couplings are time-dependent. The different cases are described by the same effective action, with different boundary conditions.

¹²For odd $q/2$, this also includes the extra sign in (5.74).

The solutions of (5.79) are

$$e^{g_{LL}} = \frac{\alpha^2}{\mathcal{J}^2 \sinh^2(\alpha|\tau| + \gamma)}, \quad e^{g_{LR}} = \frac{\tilde{\alpha}^2}{\mathcal{J}^2 \cosh^2(\tilde{\alpha}|\tau| + \tilde{\gamma})} \quad (5.83)$$

Imposing the boundary conditions (5.80) leads to

$$\frac{\alpha}{\mathcal{J} \sinh \gamma} = 1, \quad \hat{\mu} = 2\tilde{\alpha} \tanh \tilde{\gamma}, \quad \tilde{\alpha} = \alpha, \quad \tilde{\gamma} = \gamma, \quad (5.84)$$

$$\alpha = J \sinh \gamma, \quad \tanh^2 \gamma = \frac{\epsilon}{2}(\sqrt{4 + \epsilon^2} - \epsilon), \quad \epsilon = \frac{\hat{\mu}}{2\mathcal{J}} \quad (5.85)$$

Fig. 13 shows a comparison of the analytic solution with direct numerical solution of the large N equations (5.74), which agrees except that the numerical solution is periodic in imaginary time so it is a periodic identification of the zero temperature solution in the low temperature limit. (Finite temperature effects will be discussed in next subsection.)

As an example, we can use these formulas to find an expression for the ground state energy using (5.75) to obtain

$$\frac{E}{N} = \frac{\hat{\mu}}{q^2} \left[-\frac{q}{2} + 1 - \log \tanh \gamma - \frac{1}{\tanh^2 \gamma} \right] \quad (5.86)$$

with $\tanh \gamma$ given by (5.85). When $\mathcal{J} \rightarrow 0$ we get $E = -N\mu/2$ which is indeed the energy for the ground state of H_{int} in (3.21).

In the small ϵ limit, we can compare this answer with the general low energy discussion in section 4. We get agreement once we use the large q expression for $\alpha_S = \frac{1}{4q^2}$, note that $\frac{dt}{du} = 2\alpha$, use (4.29), and take the large q limit of some of the terms. The final large q expression for small $\hat{\mu} \ll \mathcal{J}$ is

$$\frac{dt}{du} = 2\alpha = \sqrt{2\hat{\mu}\mathcal{J}}, \quad \alpha_S = \frac{1}{4q^2}, \quad \text{for } 1 \ll q, \quad \hat{\mu} \ll \mathcal{J} \quad (5.87)$$

Taking the small $\hat{\mu}$ limit of (5.86) we get

$$\frac{E}{N} = -\frac{\hat{\mu}}{2q} + \frac{1}{q^2} \left[-2\mathcal{J} + \frac{\hat{\mu}}{2} \left(1 - \log \frac{\hat{\mu}}{2\mathcal{J}} \right) \right] \quad (5.88)$$

The term linear in \mathcal{J} reflects the ‘‘ground state energy’’ of the two SYK models at large q . This ‘‘ground state energy’’ is not included in (4.24). The rest of the terms agree with the large q (or small Δ) limit of (4.40), after we use use (5.87).

We can continue (5.83) to Lorentzian time to find the left right Lorentzian correlator¹³

$$\langle \psi_L(t) \psi_R(0) \rangle \sim \frac{i}{2} e^{g_{LR}/q} = \frac{i}{2} \left[\frac{\sinh \gamma}{\cos(t\alpha - i\tilde{\gamma})} \right]^{\frac{2}{q}} \quad (5.89)$$

¹³In principle, we can only trust the first term in the $1/q$ expansion of (5.89) and (5.90). We are using this form because the analysis of higher order corrections (for a single SYK) in [43] showed that they are small in the exponential.

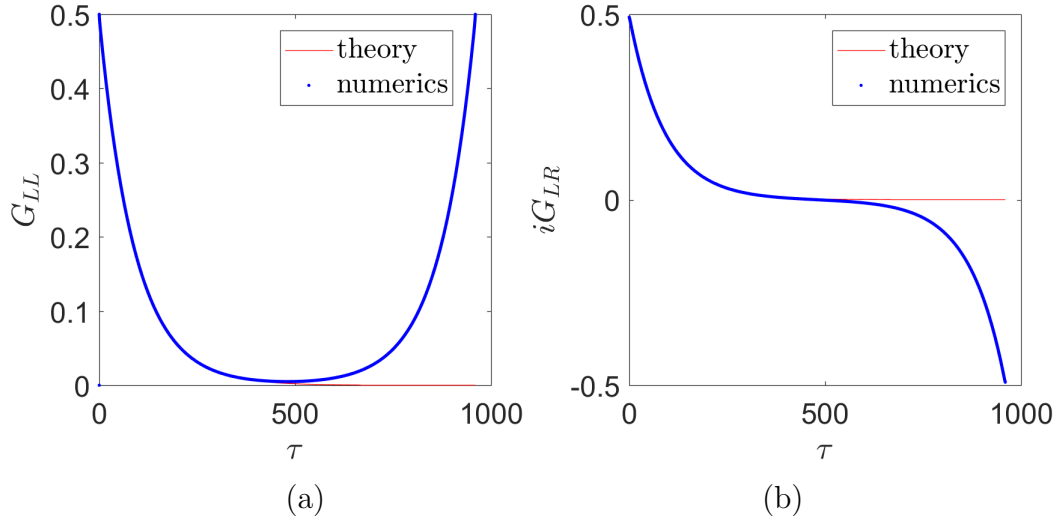


Figure 13: The comparison of analytic solution (5.83) with numerics for $q = 96$ at a low temperature $T = 0.001$. The deviation for $\tau > \frac{\beta}{2}$ is expected because the theoretical formula is for zero temperature, while the numerics at finite temperature is symmetric (for G_{LL} or antisymmetric (for G_{LR}) with respect to $\tau = \frac{\beta}{2}$.

In contrast to (4.66), now the correlator is regular at $t = \pi/(2\alpha)$, with a value of

$$\langle \psi_L(t = \frac{\pi}{2\alpha}) \psi_R(0) \rangle \sim \frac{i}{2} e^{-i\pi/q} \left[\frac{\sinh \gamma}{\sinh \tilde{\gamma}} \right]^{\frac{2}{q}} \quad (5.90)$$

At zero temperature $\tilde{\gamma} = \gamma$ and we get the maximal value we could have for the correlators of such operators. This is saying that we are having a perfect information transfer between the two sides, in this limit. The factor of $e^{-i\pi/q}$ seems related to the proper time experienced by the bulk particles as they go from the left boundary to the right boundary. We can define it in a more physical way by comparing this factor for operators of different dimensions, say replacing $\psi_R^i \rightarrow \psi_R^i(0) \psi_R^j(0)$, and similarly for ψ_L , we get a higher dimension $\tilde{\Delta}$ and a correspondingly extra factor of $e^{-i\pi\tilde{\Delta}}$.

An additional remark is that we can also compute the commutator by using the other operator ordering. The other operator ordering amounts to changing $-i\tilde{\gamma} \rightarrow +i\tilde{\gamma}$. We can then compute the anticommutator

$$\langle \{ \psi_L(t), \psi_R(0) \} \rangle = \frac{i}{2} \left\{ \left[\frac{\sinh \gamma}{\cos(t\alpha - i\tilde{\gamma})} \right]^{\frac{2}{q}} - \left[\frac{\sinh \gamma}{\cos(t\alpha + i\tilde{\gamma})} \right]^{\frac{2}{q}} \right\} \quad (5.91)$$

For small $\tilde{\gamma}$ we see that this commutator is small for $|t| \leq \frac{\pi}{2\alpha}$, but it becomes larger for

larger times, where we lose the extra suppression by $\tilde{\gamma}$. More explicitly

$$\langle \{\psi_L(t), \psi_R(0)\} \rangle \propto \begin{cases} \frac{2\tilde{\gamma}}{q} \tan t\alpha [\cos \alpha t]^{-2/q}, & 0 < t\alpha < \pi/2 \\ \sin \frac{2\pi}{q} [-\cos \alpha t]^{-2/q}, & \pi/2 < t\alpha < 3\pi/2 \end{cases} \quad (5.92)$$

We see that for small $\frac{\hat{\mu}}{\mathcal{J}}$ the anticommutator is suppressed for times less than $\pi/(2\alpha)$ relative to the values it has for later times. This is consistent with what we discussed for the commutator for general q and small $\frac{\hat{\mu}}{\mathcal{J}}$ around (4.67) (4.68).

5.4 Large q at finite temperature

We now consider the coupled system in large q limit at finite temperature. As we have discussed in Sec. 5.2, for $q = 4$ we observed a Hawking-Page type first order phase transition numerically. Physically, the transition is between a low temperature phase of global AdS₂ geometry and a high temperature phase of two black holes. Numerically, we find that the phase transition exists for all q where the computation can be carried, as long as $\hat{\mu}/\mathcal{J}$ is not too large. At large q limit, there is actually an analytic way to understand the phase transition, which we will discuss in this subsection.

Interestingly, the analytic analysis at large q reveals that the two minima of free energy corresponding to the two phases are continuously connected by a saddle point. This continuous connection can be physically explored by considering the theory in the microcanonical ensemble, as opposed to the canonical ensemble. In other words, the theory in the microcanonical ensemble goes continuously between these two phases.

In the following we describe this analysis in more detail, and also analyze other finite temperature properties of the large q problem. For more details see appendix A. We imagine taking q large holding $\hat{\mu} \equiv \mu q$ and \mathcal{J} fixed. Not surprisingly, the particular form of the solution depends on how the temperature scales with q . Notice that the solution in (5.83) is reasonable only at times that are parametrically less than q , otherwise it is not reasonable to expand G as in (5.78). In fact, for very large times we can consider a different approximation to the equations (5.74). For that purpose we notice that Σ_{LL} and Σ_{LR} vary over a relatively short time scale, which is of order one, as compared to the time scale where G varies, which is of order q . Therefore, at very long times, we can approximate the convolutions in (5.74) as follows. First, let us consider the convolution with Σ_{LR} . Up to the overall power of i , this is a positive function with a non-zero integral. Therefore, we can approximate it as a delta function

$$\Sigma_{LR}(\tau) \sim -i\nu\delta(\tau), \quad \nu \equiv i \int_{-\infty}^{\infty} d\tau \Sigma_{LR} = \frac{2\tilde{\alpha}}{q} = \frac{\mu}{\tanh \tilde{\gamma}}, \quad \mu = \frac{\hat{\mu}}{q} \quad (5.93)$$

where we used the short time expression for Σ_{LR} to evaluate the constant ν . Σ_{LL} is an odd function of τ , therefore it leads to a $\delta'(\tau)$, or to a derivative. However the equation (5.74) already contains a $\partial_\tau G$ term, while the term coming from Σ_{LL} has a $1/q$ suppression and

therefore we can ignore it. The conclusion is that, at very long times, the equations (5.74) can be approximated as

$$\partial_\tau G_{LL} + i\nu G_{RL} = 0, \quad \partial_\tau G_{LR} + i\nu G_{RR} = 0 \quad (5.94)$$

and we can use $G_{LL}(\tau) = G_{RR}(\tau)$ and $G_{RL}(\tau) = -G_{LR}(\tau)$ to close the equations. Notice that the equations become local in time. These are the equations for the correlators of a fermionic harmonic oscillator (in Euclidean signature) with solutions $G_{LL} \propto e^{\pm\nu\tau}$. Notice that ν (defined in (5.93)) is setting the long time decay, which can be viewed as the actual energy gap of the system. Notice that it is *not* equal to μ . In fact, it is rescaled by the $1/\tanh\tilde{\gamma}$ factor. So typically, it is larger than μ itself. In the very low temperature solution, and for small μ , this gap actually goes over to $E_{\text{gap}} = \nu \sim \frac{dt}{du} \Delta$, which is what we expect from the low energy analysis (4.33) (5.87). The fact that this goes like $1/q$ means that we start getting deviations from the vacuum at inverse temperatures of order q .

For $\beta = \infty$ we impose that both functions go to zero at large times to obtain the long time solution

$$G_{LL} = -iG_{LR} = Ae^{-\nu\tau}, \quad \text{for} \quad \beta = \infty, \quad \tau \gg 1/\alpha \quad (5.95)$$

This solution was used to set the boundary condition in (5.80) by matching to the short time behavior of (5.95). More generally, we can write

$$G_{LL} = A \cosh[\nu(\beta/2 - \tau)], \quad G_{LR} = iA \sinh[\nu(\beta/2 - \tau)] \quad (5.96)$$

where A should be determined by matching to the shorter time region.

Now we will describe the equations in several consecutive ranges temperature ranges, which display various physical phenomena. We will not discuss the derivation of the formulas. They are derived in appendix A.

Inverse temperatures of order $\beta = q \log q$

In this situation, we can define $\sigma = qe^{-\beta\nu}$, with ν as in (5.93). We take the large q limit while holding σ fixed, such that $\beta = \frac{1}{\nu} \log \frac{q}{\sigma}$. The ansatz for short times is the same as (5.83) and at long times (5.96). Setting the boundary conditions we get

$$\tilde{\alpha} = \alpha, \quad \alpha = \mathcal{J} \sinh \gamma, \quad \tilde{\gamma} = \gamma + \sigma, \quad \hat{\mu} = 2\alpha \tanh \tilde{\gamma}, \quad (5.97)$$

$$\log(q/\sigma) = \frac{\beta\mu}{\tanh \tilde{\gamma}} \quad (5.98)$$

where we also listed the definition of σ .

Eq. (5.97) and (5.98) determines temperature β and parameters α, γ in the solution as functions of σ . The low temperature limit corresponds to $\sigma \rightarrow 0$, in which case Eq. (5.97) reduces to the zero temperature equation (5.84) and (5.85). However, it turns out that the temperature $T(\sigma) = \beta^{-1}(\sigma)$ is not a monotonous function of σ . Fig. 15 shows the relation of the effective energy gap $E_g = \frac{2\alpha}{q}$ and temperature T , together with a comparison with numerical results. Due to the non-monotonicity of T , there is a temperature window

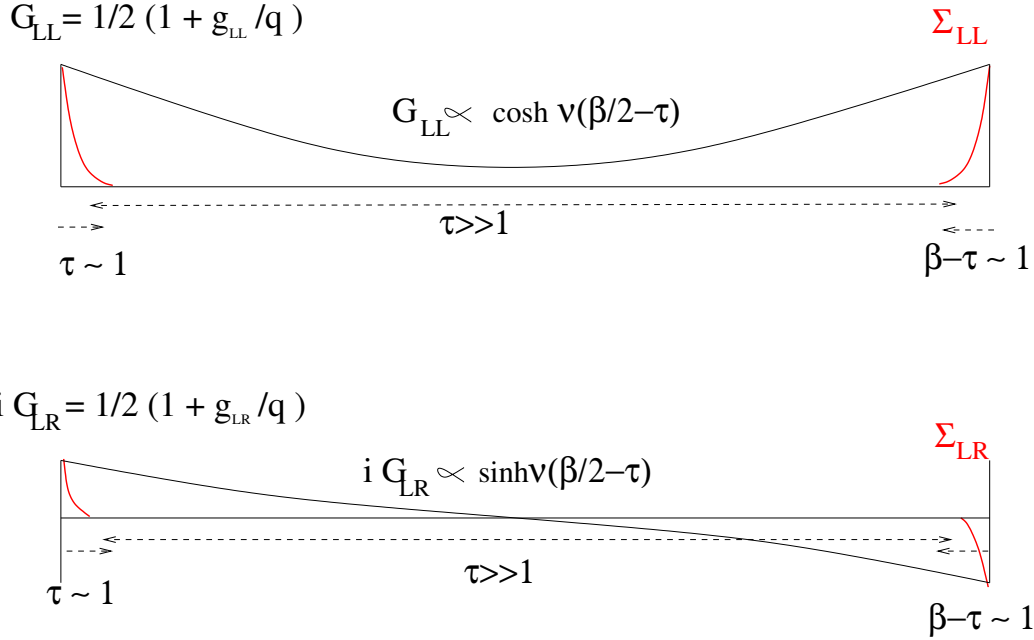


Figure 14: This is a sketch of the Euclidean correlation functions at large q for temperatures of order q . The G_{LL} and G_{LR} correlators vary slowly, they remain close to maximal for relatively short times, but decay at longer times. In contrast the self energies Σ_{LL} and Σ_{LR} decay very quickly, in times of order one and can be completely neglected for times of order q .

$T_1 < T < T_2$ in which there are three solutions with different E_g for a given temperature. They correspond to three saddle points of the free energy, including two minima and one saddle point.

We can compute the energy from (5.75) and also the free energy, see appendix A for a derivation. We find

$$\begin{aligned}
\frac{E}{N} &= \frac{\hat{\mu}}{q^2} \left[-\frac{q}{2} + 1 - \frac{1}{\tanh \gamma \tanh \tilde{\gamma}} - \log \frac{\sinh \gamma}{\cosh \tilde{\gamma}} \right] \\
-\frac{\beta F}{N} &= \frac{\beta \hat{\mu}}{q^2} \left[\frac{q}{2} - 1 + \frac{1}{\tanh \gamma \tanh \tilde{\gamma}} + \log \frac{\sinh \gamma}{\cosh \tilde{\gamma}} + \frac{\sigma}{\tanh \tilde{\gamma}} \right] + \frac{\sigma}{q} \\
\frac{S}{N} &= \frac{\sigma}{q} \left[1 + \log \frac{q}{\sigma} \right] = e^{-\beta \nu} [1 + \beta \nu]
\end{aligned} \tag{5.99}$$

For $\sigma \rightarrow 0$ we recover the zero temperature case, see (5.86). For large σ we are at a relatively high temperature, where it looks like we start exciting the harmonic oscillators with frequency ν , which in this regime is $\nu \sim \mu$. In the intermediate temperature range, the temperature is not a single valued function of σ , so that in the canonical ensemble we have different branches and a first order transition, see figure 15 and figure 16(a). All functions are smooth functions of σ . This can be compared with figure 12(a). On the other hand,

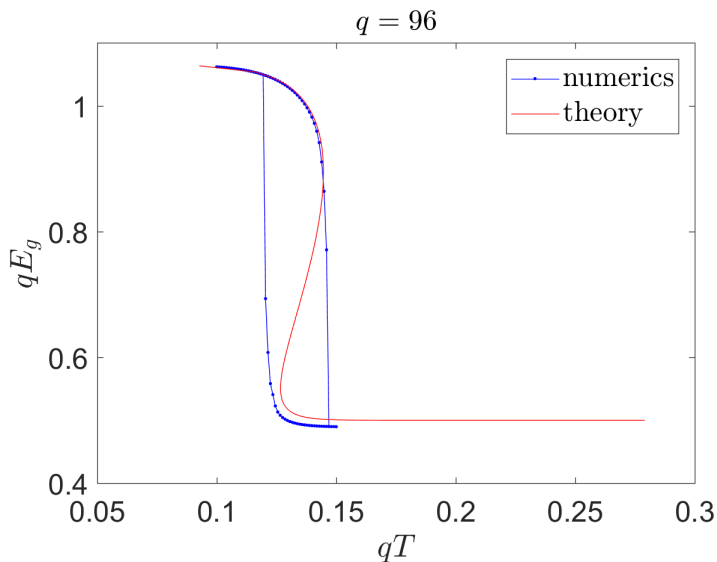


Figure 15: The relation of energy gap and temperature according to the analytic result (5.97) and (5.98) (red line), and the numerical result for $q = 96$ (blue line with dots). Note that the numerics can only find the minima, and jumps between the two minima at critical temperature.

in the microcanonical ensemble we have a monotonous function $S(E)$ displayed in figure 16(b). This shows more explicitly that we go over smoothly from the low temperature to the relatively high¹⁴ temperature. As we increase the energy we encounter a region with negative specific heat, corresponding to the unstable upper curve in figure 16(a). In some physical systems this could lead to phase separation within the system (as in a mixture of water and ice). However, this seems unlikely to happen in the SYK model with its all to all interactions. We have not proven the stability of this region, but we suspect that it is stable in the microcanonical ensemble.

This region was also found in the Schwarzian limit in section 4.5.1. In fact, for small $\hat{\mu}/\mathcal{J}$, we can make contact between the equations (5.97) and the ones in (4.59). We approximate (5.97) as $\frac{\hat{\mu}}{\mathcal{J}} = 2\gamma(\gamma + \sigma)$, with $\gamma, \sigma \ll 1$. These the three terms correspond to the three terms in (4.59), with $\gamma \propto t'$ and $\sigma/q = e^{\frac{-\beta 2J\gamma}{q}}$, after using the equation.

It is interesting to study the Lorentzian correlators in this case. They are given by the analytic continuation of the short time expressions and given by (5.89) (5.90). At finite temperature we have that $\tilde{\gamma} > \gamma$. As $\sigma = \tilde{\gamma} - \gamma$ becomes larger, the left-right correlator decreases, and the energy increases. We also find that the gap $E_{\text{gap}} = \nu$ decreases. We can interpret this as saying that we are producing bulk excitations, or excitations of the

¹⁴We say “relatively high” because it is at the higher end of the $\beta \sim q \log q$ window of temperatures. We still have a few windows to go before we get to really high temperatures!.

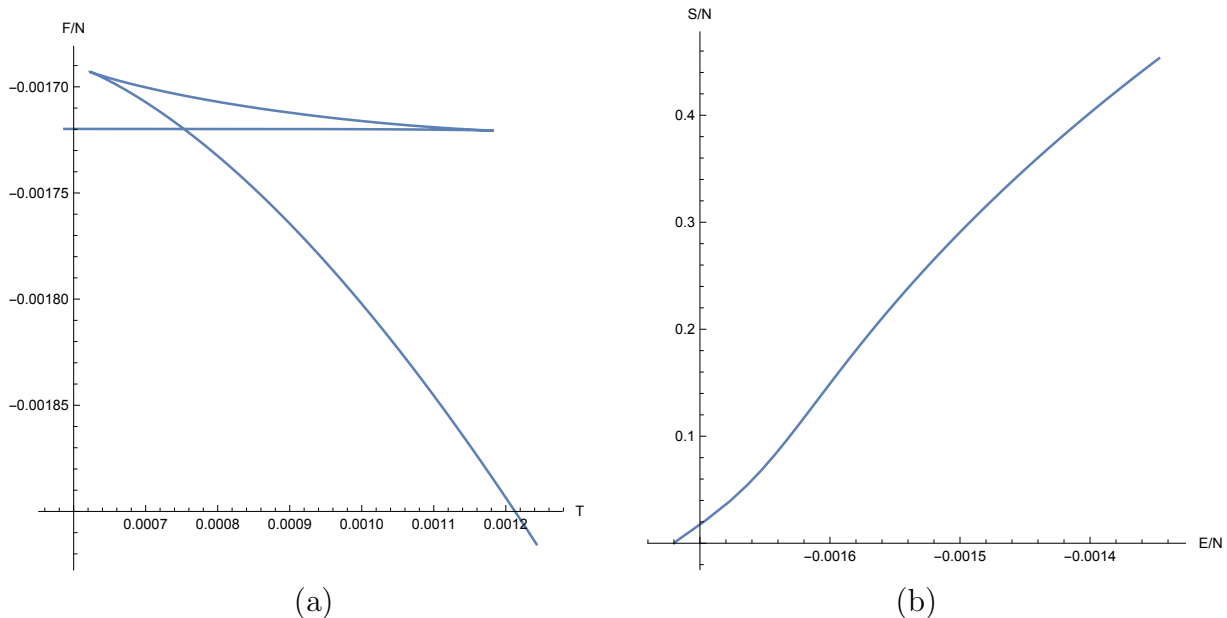


Figure 16: Here we consider a specific case with $q = 50$, $\mathcal{J} = 1$, $\hat{\mu} = .1$ and we plot the free energy as a function of the temperature and the entropy as a function of the energy, according to (5.99). The left plot displays a first order phase transition. The top line is unstable in the canonical ensemble. The right plot shows that in the microcanonical ensemble we have a continuous behavior of the entropy as a function of the energy. The changing slope is related to the change in the temperature as the energy increases, which is displayed more explicitly in figure 17

conformal fields that are hindering the transfer of information from one side to the other. We can also say that the positive energy of these excitations is decreasing the total amount of negative energy available to produce the wormhole, and for this reason the wormhole is deeper.

In this regime as the temperature becomes progressively higher, or more precisely, as the energy becomes higher, we get $\sigma \rightarrow \infty$ and the value of the left right correlator becomes very small. Therefore we see that the wormhole is closing, or at least is not as “transparent” and easy to cross as it was at zero temperature.

The plot in figure 17 holds for $\frac{\hat{\mu}}{\mathcal{J}} \ll 1$. On the other hand, if $\frac{\hat{\mu}}{\mathcal{J}} \gg 1$, we get from (5.97) that $\gamma \gg 1$, which also implies that $\tilde{\gamma} \gg 1$ so that the temperature is approximately given by $\beta\mu \sim \log(q/\sigma)$ which is now a monotonic function of σ . In this regime, there is no phase transition in the canonical ensemble. The precise value where the transition disappears is around $\frac{\hat{\mu}}{\mathcal{J}} \sim 1$. The large q phase diagram is shown in Fig. 18, where the critical temperatures T_1, T_2 are determined by numerically finding the extrema of $T(\sigma)$ curve.

Inverse temperatures of order $\beta \sim q$

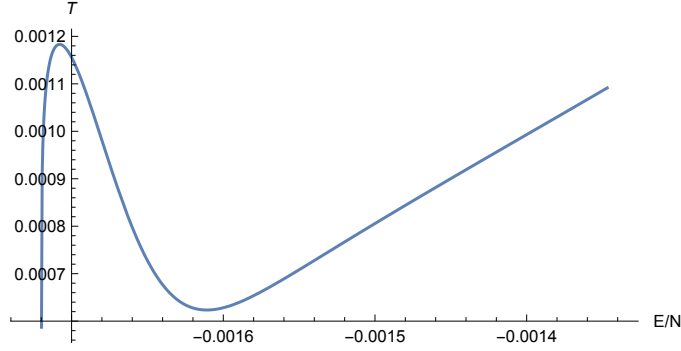


Figure 17: Here we consider a specific case with $q = 50$, $\mathcal{J} = 1$, $\hat{\mu} = .1$ and we plot the temperature as a function of the energy, according to (5.99)

In this regime the function G_{LR} becomes smaller than one everywhere. So we can approximate $G_{LR}^{q-1} = 0$ and Σ_{LR} contains only the μ term. This implies that we can still make the long time ansatz (5.96) but with $\nu = \mu$. Matching to the short time behavior we find

$$2\alpha = \hat{\mu} \tanh \frac{\mu\beta}{2}, \quad \sinh \gamma = \frac{\alpha}{\mathcal{J}} = \frac{\hat{\mu}}{2\mathcal{J}} \tanh \frac{\mu\beta}{2} \quad (5.100)$$

The free energy is now

$$-\frac{\beta F}{N} = \log[2 \cosh \frac{\beta\mu}{2}] + \frac{\beta\mu}{q} \tanh \frac{\beta\mu}{2} \left[\log(2 \sinh \gamma) + \frac{1}{\tanh \gamma} - \gamma - 1 \right] \quad (5.101)$$

As expected, the large $\mu\beta$ limit of this expression matches the high temperature limit of (5.99), so that the two expressions match in their overlapping range. The most notable feature of (5.101) is the first term, which is signalling a rise of the entropy, from the relatively low entropy of (5.99) to the high entropy of order $S \sim N \log 2$ that we find in the limit that $\beta\mu$ becomes small. The excitations responsible for this rise look like the free fermionic oscillators we would have if our Hamiltonian was given only by the interaction term H_{int} in (3.21).

The main phenomenon that happens in this regime is that the entropy rises to close to its maximal value. We can think that in this regime we are creating lots of bulk excitations that make the entropy rise. The final entropy is similar to that of the two separate SYK models.

Inverse temperatures of order $\beta \sim \sqrt{q}$

In this regime we can further approximate G_{LR} as

$$G_{LR} = \frac{i}{2} \mu \left(\frac{\beta}{2} - t \right) \quad (5.102)$$

and this is of order $1/\sqrt{q}$. On the other hand G_{LL} is close to maximal during the whole range of euclidean times. In the equation for G_{LL} we approximate Σ_{LR} by just the $\mu\delta(\tau)$

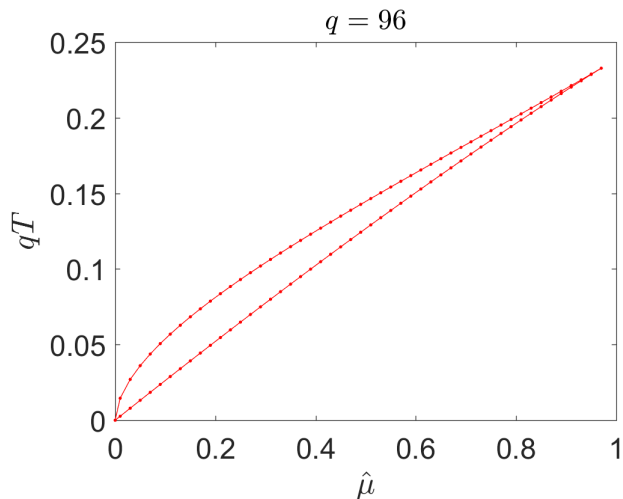


Figure 18: The phase diagram at large q . The vertical axis displays qT and the horizontal one $\hat{\mu}$.

term which then leads to the following equation for the variable g_{LL}

$$\partial_\tau^2 g_{LL} - 2\mathcal{J}^2 e^{g_{LL}} - \frac{\hat{\mu}^2}{q} = 0 \quad (5.103)$$

After a rescaling of time by β we can remove the q dependence and get a simple equation, which is derived and analyzed in the appendix A.3.

The main physical phenomenon that happens within this regime is the growth of the chaos exponent which goes from very small to maximal as the temperature increases within the range we are describing here, see figure 19. See appendix A.3 for details.

The expression for the free energy in this regime is given by

$$-\beta F/N = \log 2 + \frac{(\beta\mu)^2}{8} + \frac{2\beta\mathcal{J}}{q^2} + \frac{(\mu\beta)^2}{2q} \log(\mathcal{J}\beta) + \frac{h[q(\mu\beta)^2]}{q^2} \quad (5.104)$$

where h is a function that we have not determined.

Inverse temperatures of order one

Finally, at temperatures of order one we can set $\mu = 0$ in the computation of g_{LL} and we recover the single copy, large q , SYK result [9]. And the chaos exponent decreases again from the maximal value to $\lambda = 2\mathcal{J}$ for $\beta \rightarrow 0$. The free energy can be written as

$$\frac{F}{N} = \frac{F}{N} \Big|_{\mu=0} - \frac{\beta\mu^2}{8} \quad (5.105)$$

Here the second term is a small correction, and we are in the regime described in general by (4.63). As we hinted after (4.65), and confirmed here, for large q the phase transition does not happen in this regime, it happens at a lower temperature (the regime $\beta \sim q \log q$).

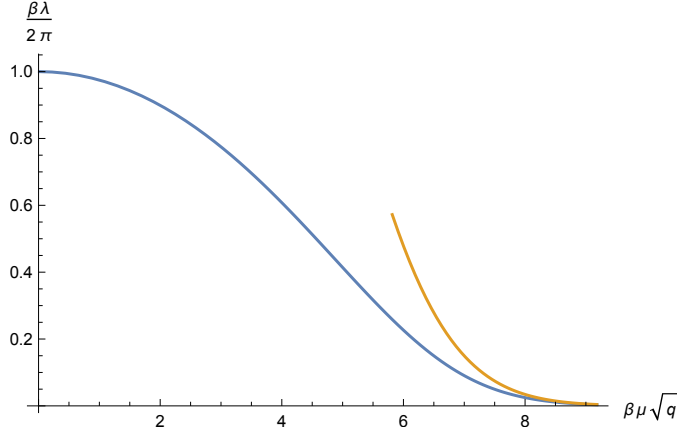


Figure 19: Here we have plotted the ratio of the chaos exponent to the maximal one as a function of $\sqrt{q}\beta\mu$. We see that as the temperature rises we saturate the chaos bound. The orange curve corresponds to the low temperature analytic estimate in (A.155).

5.5 Overlap of the ground state and the TFD at large q

At large q , we can also study the overlap between the coupled ground state and TFD state. The overlap $\langle TFD|G\rangle$ can be computed by an Euclidean path integral. The state $|G\rangle$ can be prepared by $\lim_{\tau\rightarrow+\infty} e^{-\tau H}|0\rangle$ with H the coupled Hamiltonian. The initial state $|0\rangle$ only changes the normalization constant, which we should divide out. Therefore

$$\langle TFD|G\rangle = \langle I|e^{-\frac{\beta}{4}H_0-\tau H}|0\rangle = \langle I|e^{-\frac{\beta}{4}(H_L+H_R)-\tau(H_L+H_R+H_{\text{int}})}|0\rangle \quad (5.106)$$

which can be written as a Euclidean path integral. Carrying out the random average, one obtains a path integral over the collective fields $\Sigma_{ab}(\tau_1, \tau_2)$ and $G_{ab}(\tau_1, \tau_2)$. The effective action has the same form as Eq. (5.73) except that time runs in the range $\tau \in [-\frac{\beta}{4}, +\infty)$, and the bare term in self-energy $\mu\delta(\tau_1 - \tau_2)$ is replaced by a time dependent term

$$\sigma(\tau_1, \tau_2) = \mu\theta(\tau_1)\delta(\tau_1 - \tau_2) \quad (5.107)$$

$\theta(\tau_1)$ is the step function which is 1 for $\tau_1 > 0$ and zero otherwise. Since there is no time translation symmetry, G_{ab} and Σ_{ab} are functions of two time variables $\tau_{1,2}$. At $\tau = -\frac{\beta}{4}$ the two sites L and R are smoothly connected, which leads to the boundary condition

$$\begin{aligned} G_{LL}\left(\tau_1, -\frac{\beta}{4}\right) &= -iG_{LR}\left(\tau_1, -\frac{\beta}{4}\right) \\ \lim_{\tau_2\rightarrow-\frac{\beta}{4}} \partial_{\tau_2} G_{LL}(\tau_1, \tau_2) &= i \lim_{\tau_2\rightarrow-\frac{\beta}{4}} \partial_{\tau_2} G_{LR}(\tau_1, \tau_2) \end{aligned} \quad (5.108)$$

and the same for Σ_{ab} . The boundary condition at $\tau \rightarrow +\infty$ is set by requiring $G_{ab}(\tau_1, \tau_2)$ to approach the ground state solution $G_{ab}(\tau_1 - \tau_2)$ when $\tau_1, \tau_2 \rightarrow \infty$.

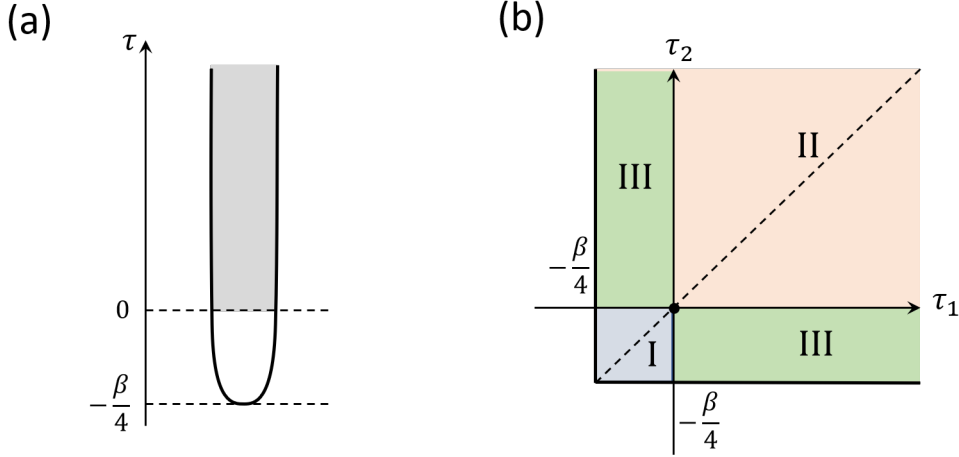


Figure 20: (a) Illustration of the Euclidean time path integral that calculates the overlap $\langle TFD|G\rangle$. The initial state at $\tau = -\frac{\beta}{4}$ is a maximally entangled state $|I\rangle$ of the two sites, and the time evolution in $\tau \in [-\frac{\beta}{4}, 0]$ with decoupled SYK Hamiltonian prepares the TFD state. The backwards time evolution in the interval $\tau \in (0, +\infty)$ with coupled SYK Hamiltonian prepared the coupled ground state $\langle G|$. (b) The τ_1, τ_2 quarter plane on which the two-point functions $G_{ab}(\tau_1, \tau_2)$ is defined. In the large q limit, the Schwinger-Dyson equation is reduced to Liouville equations (5.110) of $g_{ab}(\tau_1, \tau_2)$, with boundary conditions at $\tau_{1,2} = -\frac{\beta}{4}$, $\tau_{1,2} \rightarrow +\infty$ and $\tau_1 = \tau_2$.

In the large q limit, one obtains the same Liouville effective action (5.81) with the boundary condition of g_{LR} changing at $\tau = 0$. Since time translation symmetry is absent, the Green's functions are functions of two time variables:

$$G_{LL}(\tau_1, \tau_2) = \frac{1}{2} \text{sgn}(\tau_1 - \tau_2) \left(1 + \frac{1}{q} g_{LL}(\tau_1, \tau_2) \right), \quad G_{LR}(\tau_1, \tau_2) = \frac{i}{2} \left(1 + \frac{1}{q} g_{LR}(\tau_1, \tau_2) \right) \quad (5.109)$$

g_{LL} and g_{LR} satisfy the Liouville equation similar to Eq. (5.79), but now with two time variables:

$$\frac{\partial^2 g_{LL}}{\partial \tau_1 \partial \tau_2} = -2\mathcal{J}^2 e^{g_{LL}}, \quad \frac{\partial^2 g_{LR}}{\partial \tau_1 \partial \tau_2} = 2\mathcal{J}^2 e^{g_{LR}} \quad (5.110)$$

The equation applies to the quarter plane $\tau_1, \tau_2 \in [-\frac{\beta}{4}, +\infty)$ except the diagonal line $\tau_1 = \tau_2$, where the following boundary condition needs to be imposed:

$$g_{LL}(\tau, \tau) = 0, \quad (\partial_{\tau_1} - \partial_{\tau_2}) g_{LR}(\tau_1, \tau_2)|_{\tau_2 \rightarrow \tau_1} = 2\hat{\mu}\theta(\tau_1) \quad (5.111)$$

Eq. (5.110) has a general solution (see *e.g.* [44])

$$e^{g_{LL}} = \frac{h'_1(\tau_1)h'_2(\tau_2)}{\mathcal{J}^2 (h_1(\tau_1) - h_2(\tau_2))^2}, \quad e^{g_{LR}} = -\frac{f'_1(\tau_1)f'_2(\tau_2)}{\mathcal{J}^2 (f_1(\tau_1) - f_2(\tau_2))^2} \quad (5.112)$$

with functions $h_{1,2}(\tau)$ and $f_{1,2}(\tau)$ determined by the boundary condition.¹⁵ Due to the symmetry $g_{ab}(\tau_1, \tau_2) = g_{ab}(\tau_2, \tau_1)$, we only need to write the solution for the region $\tau_1 > \tau_2$.

In general, the solution g_{LL} and g_{LR} in the overlap calculation is not related to the saddle point solution for $\langle TFD|TFD \rangle$ and $\langle G|G \rangle$. However, we found that a solution can be found by matching the TFD and coupled SYK saddle points when β and μ satisfies a matching condition. This special case maximizes the overlap $\langle TFD|G \rangle$, and the matching condition determines the effective inverse temperature $\beta(\mu)$ for the reduced density matrix of each SYK site in the coupled ground state. In the following we will provide a summary of the solution, and leave more detailed discussion to Appendix E.

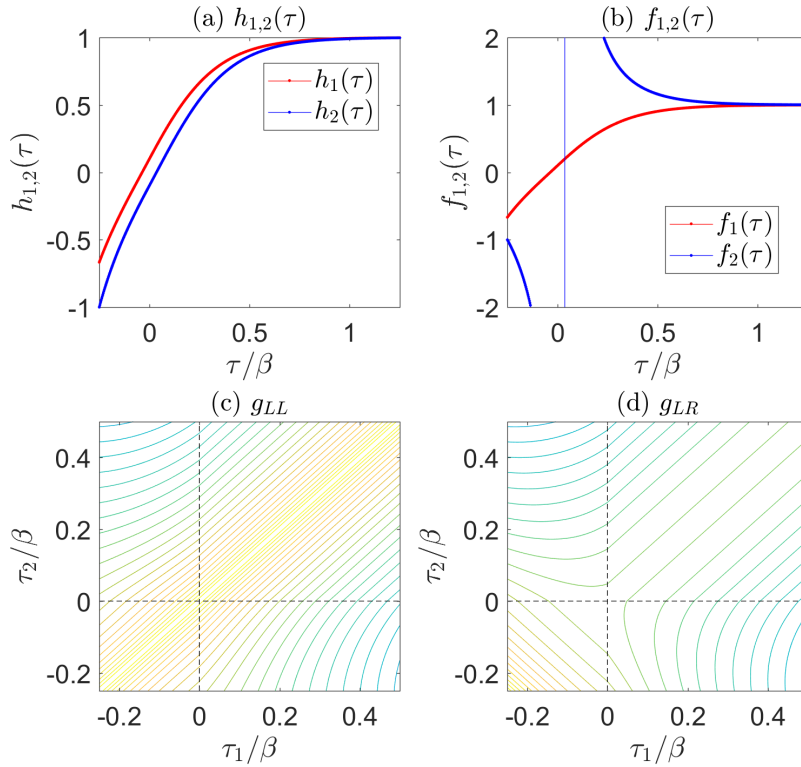


Figure 21: (a) and (b) illustrates the functions $h_{1,2}(\tau)$ and $f_{1,2}(\tau)$ that defines the two-point function solution in Eq. (5.112). (c) and (d) shows the contour plot of corresponding g_{LL}, g_{LR} . From the contour plot one can see that g_{LL} is only a function of $\tau_1 - \tau_2$ in region I and II of Fig. 20 (b), while g_{LR} is only a function of $\tau_1 + \tau_2$ in region I, and a function of $\tau_1 - \tau_2$ in region II. The parameter used in this plot is $\frac{\alpha}{j} = 0.2$.

¹⁵An $SL(2, R)$ transformation $h_{1,2}(\tau) \rightarrow \frac{ah_{1,2}+b}{ch_{1,2}+d}$ (with $ad-bc = 1$) preserves g_{LL} , and similar for f_1, f_2 .

The functions $h_{1,2}$ and $f_{1,2}$ are defined as

$$h_1(\tau) = \begin{cases} \tan(\check{\alpha}\tau + \frac{1}{2}\check{\gamma}), & \tau \in [-\frac{\beta}{4}, 0] \\ \tanh(\alpha\tau + \frac{1}{2}\gamma), & \tau > 0 \end{cases}, \quad h_2(\tau) = \begin{cases} \tan(\check{\alpha}\tau - \frac{1}{2}\check{\gamma}), & \tau \in [-\frac{\beta}{4}, 0] \\ \tanh(\alpha\tau - \frac{1}{2}\gamma), & \tau > 0 \end{cases} \quad (5.113)$$

$$f_1(\tau) = h_1(\tau), \quad f_2(\tau) = \begin{cases} \cot(\check{\alpha}\tau - \frac{1}{2}\check{\gamma}), & \tau \in [-\frac{\beta}{4}, 0] \\ \coth(\alpha\tau - \frac{1}{2}\gamma), & \tau > 0 \end{cases} \quad (5.114)$$

where α and γ are determined by the coupled solution in Eq. (5.85).¹⁶ The solution in the region $\tau_{1,2} \in [-\frac{\beta}{4}, 0]$ is a thermal field double solution if $\check{\alpha}$ and $\check{\gamma}$ satisfy

$$\check{\alpha}\beta + 2\check{\gamma} = \pi \quad (5.115)$$

$\check{\alpha}$ and $\check{\gamma}$ are determined by continuity of g_{ab} and its first derivative at $\tau = 0$, which then determines β through Eq. (5.115). Here we will reserve more details of the derivation to Appendix E, and only write the final result of β as a function of α :

$$\beta = \frac{2}{\alpha} \sqrt{1 + \left(\frac{\alpha}{\mathcal{J}}\right)^2} \arctan \frac{\mathcal{J}}{\alpha} \quad (5.116)$$

In the weak coupling limit $\hat{\mu} \ll \mathcal{J}$, $\alpha \ll \mathcal{J}$, the formula reduces to $\beta \simeq \frac{\pi}{\alpha}$ as expected, see (4.50). For general value of $\hat{\mu}/\mathcal{J}$, the gap α of the coupled SYK model is different from $\frac{\pi}{\beta}$. In the limit $\hat{\mu} \gg \mathcal{J}$, $\alpha \simeq \hat{\mu}/2$, and $\beta \simeq \frac{2}{\alpha} = \frac{4}{\hat{\mu}}$. In the limit $\hat{\mu}/\mathcal{J} \rightarrow \infty$, $\beta \rightarrow 0$, which means the coupled ground state approaches the infinite temperature TFD state, *i.e.* the maximally entangled state $|I\rangle$.

Now we compute the overlap $\langle TFD|G\rangle$ corresponding to this special solution. To the order of $\frac{1}{q^2}$, the overlap is given by the classical saddle point value of the Liouville action (5.81). Denote S as the saddle point action of the overlap solution, and S_{TFD} and S_G as that of the TFD state and the coupled ground state, respectively, the normalized overlap is

$$|\langle TFD|G\rangle| = \exp \left[-N \left(S - \frac{1}{2}S_{TFD} - \frac{1}{2}S_G \right) \right] \quad (5.117)$$

To compute the overlap, we first write the Liouville action (5.81) in dimensionless couplings $\beta\mathcal{J}$ and $\beta\mu$:

$$\begin{aligned} \frac{1}{N}S &= \frac{1}{4q^2} \int_{-\frac{\pi}{2}}^{+\infty} d\theta_1 \int_{\theta_1}^{+\infty} d\theta_2 [\partial_{\theta_1} g_{LL} \partial_{\theta_2} g_{LL} - \partial_{\theta_1} g_{LR} \partial_{\theta_2} g_{LR}] \\ &\quad - \frac{(\beta\mathcal{J})^2}{\pi^2} (e^{g_{LL}} + e^{g_{LR}}) - \frac{\beta\hat{\mu}}{2\pi q^2} \int_{-\frac{\pi}{2}}^{+\infty} d\theta g_{LR}(\theta, \theta) \end{aligned} \quad (5.118)$$

¹⁶ $f_2(\tau)$ has a divergence at $\tau = \tilde{\gamma}/2\check{\alpha}$ but the correlation function stays regular.

with $\theta_{1,2} = 2\pi \frac{\tau_{1,2}}{\beta}$. Now we consider the derivative of S over \mathcal{J} with $\hat{\mu}$ fixed, and $\beta = \beta(\mathcal{J}, \hat{\mu})$ determined by Eq. (5.116).

$$\begin{aligned} \left. \frac{1}{N} \frac{\partial S}{\partial \mathcal{J}} \right|_{\hat{\mu}} &= -\frac{1}{4\pi^2 q^2} \frac{\partial(\beta \mathcal{J})^2}{\partial \mathcal{J}} \int_{-\frac{\pi}{2}}^{+\infty} d\theta_1 \int_{\theta_1}^{+\infty} d\theta_2 (e^{g_{LL}} + e^{g_{LR}}) - \frac{\partial(\beta \hat{\mu})}{\partial \mathcal{J}} \frac{1}{2\pi q^2} \int_{-\frac{\pi}{2}}^{+\infty} d\theta g_{LR}(\theta, \theta) \\ &= \frac{1}{\beta \mathcal{J} q^2} \frac{\partial(\beta \mathcal{J})}{\partial \mathcal{J}} \int_{-\frac{\beta}{4}}^{+\infty} d\tau_1 \int_{\tau_1}^{+\infty} d\tau_2 \partial_1 \partial_2 (g_{LL} - g_{LR}) - \frac{1}{\beta q^2} \frac{\partial(\beta \hat{\mu})}{\partial \mathcal{J}} \int_{-\frac{\beta}{4}}^{+\infty} d\tau g_{LR}(\tau, \tau) \end{aligned} \quad (5.119)$$

In the second equality, we used the Liouville equation.¹⁷ Using the fact $\partial_1(g_{LL} - g_{LR}) \rightarrow 0$ for $\tau_2 \rightarrow +\infty$, we can integrate over τ_2 in the first term and obtain

$$\begin{aligned} \frac{1}{N} \frac{\partial S}{\partial \mathcal{J}} &= -\frac{1}{\beta \mathcal{J} q^2} \frac{\partial(\beta \mathcal{J})}{\partial \mathcal{J}} \int_{-\frac{\beta}{4}}^{+\infty} d\tau_1 (\partial_1 g_{LL}(\tau_1, \tau_2) - \partial_1 g_{LR}(\tau_1, \tau_2)) \Big|_{\tau_2 \rightarrow \tau_1^+} \\ &\quad - \frac{1}{\beta q^2} \frac{\partial(\beta \hat{\mu})}{\partial \mathcal{J}} \int_{-\frac{\beta}{4}}^{+\infty} d\tau g_{LR}(\tau, \tau) \end{aligned} \quad (5.120)$$

The key point of Eq. (5.120) is that the saddle point value of S is transformed into a single integral over τ_1 , and it only depends on the derivative of g_{ab} at the $\tau_1 = \tau_2$ line. Since the solution we construct is identical to the TFD solution in region I and is identical to the ground state solution in region II, we obtain

$$\frac{\partial}{\partial \mathcal{J}} \left[S - \frac{1}{2} (S_{TFD} + S_G) \right] = 0 \quad (5.121)$$

for all \mathcal{J} . For $\mathcal{J} = 0$, one can explicitly verify $|G\rangle_{\mathcal{J}=0} = |TFD\rangle_{\beta=0}$ is the infinite temperature TFD state. Therefore we can integrate the equation above to conclude $|\langle TFD|G\rangle| = 1$ for general \mathcal{J} and $\hat{\mu}$.

Since the Liouville action is only an approximate effective action up to the second order of $\frac{1}{q}$, it is possible that the higher order terms contribute a nontrivial suppression to the overlap. In fact, the computation in (4.55) shows that there is a non-zero correction that goes like $1/q^3$, obtained after analyzing the small Δ limit of (4.55), together with (4.29) (4.25).

As a side remark, we have computed the overlap $\langle TFD|G\rangle$ for small N systems in exact diagonalization. There the temperature β in TFD is tuned to a value $\beta(\mu)$ which makes the SYK energy of each site for the two states the same:

$$\langle TFD|H_L|TFD\rangle = \langle G|H_L|G\rangle \quad (5.122)$$

This is a necessary condition for the two states to be approximately the same. The numerics shows that the overlap is always quite close to 1, although we do not have enough data to do a finite N scaling.

¹⁷Since the term $e^{g_{LL}} + e^{g_{LR}}$ decays in a finite time scale $\sim \alpha$, the Liouville equation of motion is an accurate approximation of the Schwinger Dyson equation.

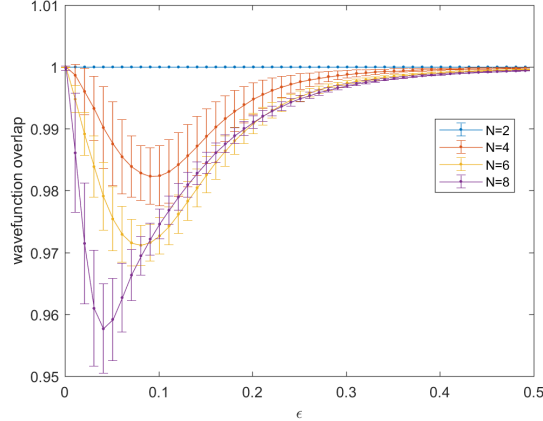


Figure 22: The overlap $|\langle TFD|G\rangle|$ for $N = 4, 8, 12, 16$ Majorana fermions per site.

5.6 Different microscopic couplings

Throughout this paper we have assumed that H_L and H_R have the same couplings, for each random choice of the couplings. We could imagine a different situation where the correlations between the two couplings are not perfect. For example, we could assume that

$$\langle (J_{j_1 \dots j_q}^L)^2 \rangle = \langle (J_{j_1 \dots j_q}^R)^2 \rangle = \frac{\mathcal{J}^2}{\tilde{\mathcal{J}}^2} \langle J_{j_1 \dots j_q}^R J_{j_1 \dots j_q}^L \rangle \quad (5.123)$$

The large N action in this case has the same form as (5.73) but with $\mathcal{J}^2 \rightarrow \tilde{\mathcal{J}}^2$ in the terms involving G_{LR} .

We can easily analyze the equations in the large q limit, where we get the same as in (5.79), but with $\mathcal{J} \rightarrow \tilde{\mathcal{J}}$ in the equation that involves g_{LR} . The solutions are again like the ones in (5.83) but with $\mathcal{J} \rightarrow \tilde{\mathcal{J}}$ in the solution for g_{LR} . The zero temperature equation imposes again the boundary conditions in (5.80) which now imply

$$\frac{\alpha}{\mathcal{J} \sinh \gamma} = 1, \quad \hat{\mu} = 2\tilde{\alpha} \tanh \tilde{\gamma}, \quad \tilde{\alpha} = \alpha, \quad \tilde{\gamma} - \gamma = \sigma = \log \frac{\mathcal{J}}{\tilde{\mathcal{J}}} \quad (5.124)$$

These are similar to (5.84). The only difference is the last equality. In fact, they are the same as the ones we had in (5.97), but with a new definition for σ . We see that if the couplings $J_{j_1 \dots j_q}$ are real, then we always have that $\tilde{\mathcal{J}} \leq \mathcal{J}$. This means that decorrelating the couplings will decrease the physical energy gap, which is

$$\nu = \frac{\hat{\mu}}{q \tanh \tilde{\gamma}} = \frac{\mu}{\tanh \tilde{\gamma}} \quad (5.125)$$

It will also decrease the left-right correlation functions. Curiously, the same sided correlators are not changed drastically, in the sense that they also return to their values at $t = 0$ at the time $t = \pi/\alpha$, in Lorentzian time.

Notice that in the limit that the couplings of the two sides are uncorrelated, we have $\tilde{\mathcal{J}} = 0$. Then σ in (5.124) goes to infinity. In that case the gap (5.125) goes down to the naively expected value equal to μ .

Notice the following point. When discussing of the thermofield double state and its wormhole dual, one might be left with the impression that in order to have a wormhole one needs to have perfectly identical systems and a perfect matching of energy levels. This does not seem necessary. In fact, a model where we change a bit the couplings between the left and right systems will have energy levels that are shifted much more than their spacing. Nevertheless, the system continues to display a whormhole like behavior.

In principle, we could also study this problem with different couplings for finite q . When the couplings are different, even for small μ , we do not expect to be able to approximate the problem using the conformal limit as we did in (4.24). The reason is that the functions G_{LL} and G_{LR} are not given by their conformal field theory limit as a first approximation.

Euclidean wormholes

It is interesting to note that for $\tilde{\mathcal{J}} > \mathcal{J}$, then we can have a solution of (5.124) with $\mu = \tilde{\gamma} = 0$ and $\gamma > 0$. Of course, this is possible only if the couplings J_{ijkl} are complex, so that we can arrange that the correlators between left right couplings are larger than the correlator of left-left or right-right couplings. While complex couplings do not give rise to a sensible Lorentzian theory, they do make sense as a Euclidean theory, in a statistical mechanics context. In this case, the relative (Euclidean) time translation symmetry between the two sides is spontaneously broken, and the configuration would be associated to a geometry looking like a Euclidean wormhole. It would be interesting to study this further and see whether it holds some lessons for Euclidean wormholes in general.

6 Conclusions and discussion

In this paper we analyzed two closely related problems. First we considered the theory of gravity that describes nearly extremal black holes, called nearly- AdS_2 gravity. To this gravity theory we added matter fields with an interaction that looks non-local from the bulk point of view. This interaction connects the two separated boundaries of AdS_2 . The interaction creates negative energy in the bulk and produces a geometry that is closely related to that of global AdS_2 , but with just a global time translation isometry. The second problem involves two copies of SYK models coupled by a simple interaction. The system becomes gapped at leading order in N . Nevertheless it displays natural remnants of the nearly conformal symmetry of a single SYK model. In fact, the spectrum is largely controlled by the broken $SL(2)$ symmetry.

Both systems share a universal subsector described by a common action (4.24). In the gravity side, this subsector encodes the gravitational interactions of the system.

The dynamics of the two coupled SYK systems looks like that of a traversable wormhole. Suppose that we insert excitations on one of the systems. From the point of view of this system, the object becomes more complex, but then, after a while, the simple objects

reassembles on the other side. The dynamics of the simple excitation looks complicated from the boundary point of view but it is simple in the bulk. The object sails smoothly from one side to the other. It goes through a wormhole. This does not violate any causality constraint since we are adding direct interactions between the two sides.

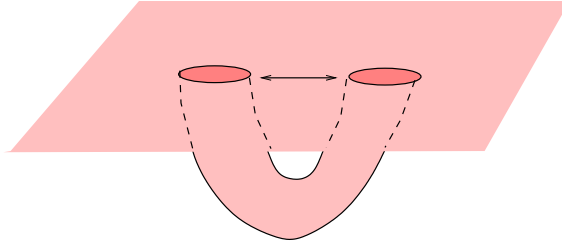


Figure 23: This is a sketch of an idea for producing solutions with non-trivial topology. First we imagine setting up a situation where two near external black holes are close to each other, without falling into each other. This would require background fields holding the black holes in place. Integrating out the fields modes in the ambient space gives rise to an interaction between the fields at the top end of the nearly AdS_2 throats. This interaction can produce a throat that connecting the two sides so that the final geometry is a horizonless eternal traversable wormhole. The throat is supported by negative null energy (energy that contributes negatively to the integrated null energy) produced by quantum effects.

It is interesting to ask whether the interaction we considered in (2.11) could arise from a higher dimensional set up. In fact, we know that nearly- AdS_2 gravity arises universally in the near horizon region of nearly extremal black holes (see e.g. [21]). So, one can imagine a situation where we take two nearly extremal black holes that are relatively near each other, see figure 23. They are far enough that we can think of them as two separate black holes, but close enough that the fields that propagate in that background have correlated fluctuations near the two black holes. Then (2.11) can arise by integrating out the field modes that have energies larger than some small number that is smaller than the inverse distance between the two black holes. If the resulting operator of the form (2.11) has positive sign, then we expect that a traversable wormhole, of the kind discussed here, will form. The full geometry will not contain a horizon, but will have non-trivial topology in the ambient space. There are a few challenges that one has to address. The first is that such near extremal black holes will attract each other by classical forces that are larger than the quantum effects we are discussing. Even if they are orbiting each other, they would be emitting gravitational waves, possibly faster than they can establish the wormhole. Furthermore, the discussion in the present paper was reasonable when the number of fields is large. We can put this large number of fields by hand, but it would be nicer to understand better whether it can be done with a small number of fields. Furthermore, we also need that the fields in the AdS_2 regions should be quantized with alternate boundary conditions, see the end of section 4.2. This should be arranged too.

Another interesting question is the following. Imagine that we couple two systems of this form, which are initially in a mixed thermal state, entangled with other systems (but not with each other). Then initially we expect the energy of the combined system will be positive, relative to the “ground state energy” of the two SYK models. The expectation value of the interaction term in (2.11) or (3.21) is zero because the fields are uncorrelated. By further weakly coupling this to another very cold and large system we can let our system of interest cool down and eventually find its ground state, which will be the wormhole like configuration described here. This is equivalent to saying that we let the black holes evaporate and let them find the ground state. As the system cools down and its energy decreases it will follow the curve of the microcanonical ensemble described in figure 16(b) (for large q). This suggests that the energy decreases smoothly and there is no phase transition between the state containing a pair of black holes vs the state containing the single wormhole. This seems surprising from the geometric point of view, since there is a discrete transition between the two geometries. It seems that one should necessarily go through a non-geometric phase. In fact, the phase diagram in figure 16(a) is reminiscent of what is found for black holes in higher dimensional AdS_D , $D > 3$ [41]. The curve sloping down to the right are the large black holes, the left cusp is the lowest temperature black hole, and the upper curve joining the two cusps is similar to the small black holes in AdS_D . The horizontal curve is similar to global Euclidean AdS_D with an identification of the euclidean time coordinate. In pure gravity the small black hole and the thermal- AdS_D line meet at infinite temperature (in the classical limit). In string theory, they meet at the Hagedorn temperature. In this two dimensional case, the unstable phase corresponds to slight excitations on the the thermal AdS_2 branch, see figure 7(c), rather than a “small” black hole. So the region near the right cusp of figure 16 is described simply, as in section 4.5.1. On the other hand, we do not have a simple picture from the low energy Schwarzian description, or AdS_2 gravity, for the left cusp in figure 16. This would be interesting to find since it seems to involve topology change. Surprisingly, in the SYK model this seems to be a smooth transition (at least at large q). Returning to the higher dimensional case, one could also wonder whether there is a smooth transition between the small black hole and thermal AdS_D . In classical string theory these two solutions have a different order parameter, the expectation value of the winding tachyon field on the thermal circle (or Polyakov loop in the boundary gauge theory description) [41]. Nevertheless it has been suggested that in the microcanonical ensemble, one might have a smooth transition between a gas of strings, or a highly excited string and a small black hole of string size [45].

Notice that the above procedure is a relatively practical and physical way for constructing a pair of SYK models in the thermofield double state. In other words, first we produced the two coupled SYK models and then we let the system cool down to find its ground state. After it has done this, we can turn off the coupling. If the coupling between the two SYK models is small, then the state that we produce is close to the thermofield double, as discussed in section 4.3, 4.4. Note that, due to the comments in section 5.6, the individual couplings do not need to be fine tuned with very high precision.

Acknowledgements

We thank A. Almheiri, Y. Gu, D. Harlow, A. Kitaev, D. Marolf, S. Shenker, D. Stanford, E. Witten, Z. Yang for discussions. J.M. is supported in part by U.S. Department of Energy grant de-sc0009988 and the It from Qubit grant from the Simons foundation. XLQ is supported by the National Science Foundation grant 1720504, and the David and Lucile Packard foundation.

A Thermodynamics of the two coupled SYK models at large q

In this appendix we explore the thermodynamics of the model at large q . Writing $\mu = \hat{\mu}/q$, we are interested in the large q limit for fixed $\hat{\mu}$ and \mathcal{J} . Another parameter is β , the inverse temperature. We can scale the inverse temperature β in various ways with q .

We divide the inverse temperature range into four windows, inverse temperatures of order $q \log q$, q , \sqrt{q} and 1. In each of these temperature ranges we will make different approximations for solving the equations for $G_{ab}(\tau)$, (5.74).

A.1 Inverse temperature of order $q \log q$

Here we make two distinct approximations for the equations. For euclidean times that are small compared to q we approximate G_{LL} and G_{LR} as in (5.78), leading to equations (5.83). On the other hand, at times of order q or larger we approximate the equations as indicated around (5.93) leading to the equations (5.94), with solutions (5.96). For convenience we summarize here the solutions in these two regimes

$$e^{g_{LL}} = \frac{\alpha^2}{\mathcal{J}^2 \sinh^2(\alpha|\tau| + \gamma)}, \quad e^{g_{LR}} = \frac{\tilde{\alpha}^2}{\mathcal{J}^2 \cosh^2(\tilde{\alpha}|\tau| + \tilde{\gamma})}, \quad \tau \ll q \quad (\text{A.126})$$

$$G_{LL} = A \cosh[\nu(\frac{\beta}{2} - \tau)], \quad G_{LR} = iA \sinh[\nu(\frac{\beta}{2} - \tau)], \quad \nu = \frac{\mu}{\tanh \tilde{\gamma}}, \quad 1 \ll \tau \quad (\text{A.127})$$

In this temperature regime we scale the temperature so that

$$\frac{\sigma}{q} = e^{-\beta\nu}, \quad \nu \equiv \frac{\mu}{\tanh \tilde{\gamma}} \quad (\text{A.128})$$

with constant σ .

We now equate the long time expansion of (A.126) to the short time expansion of (A.127) to obtain

$$\begin{aligned} G_{LL} &\sim \frac{1}{2} \left(1 + \frac{g_{LL}}{q}\right) \sim \frac{1}{2} - \frac{1}{q} \left(\log \frac{J}{\alpha} + \gamma + \alpha\tau\right) = A \cosh \frac{\beta\nu}{2} - \tau\nu A \sinh \frac{\beta\nu}{2} \\ -iG_{LR} &\sim \frac{1}{2} \left(1 + \frac{g_{LR}}{q}\right) \sim \frac{1}{2} - \frac{1}{q} \left(\log \frac{J}{\tilde{\alpha}} + \tilde{\gamma} + \tilde{\alpha}\tau\right) = A \sinh \frac{\beta\nu}{2} - \tau\nu A \cosh \frac{\beta\nu}{2} \end{aligned} \quad (\text{A.129})$$

These equations, together with (A.128), imply that

$$\tilde{\alpha} = \alpha , \quad \tilde{\gamma} = \gamma + \sigma \quad (\text{A.130})$$

In addition, from $g_{LL}(0) = 0$ and the proper discontinuity of the derivative of g_{LR} at the origin we get

$$\alpha = \mathcal{J} \sinh \gamma , \quad \hat{\mu} = 2\tilde{\alpha} \tanh \tilde{\gamma} = 2\mathcal{J} \sinh \gamma \tanh \tilde{\gamma} \quad (\text{A.131})$$

These equations, together with (A.128) give us γ and σ as a function of the physical parameters $\hat{\mu}$, \mathcal{J} , β . Alternatively, we can first write

$$\frac{\hat{\mu}}{2\mathcal{J}} = \sinh \gamma \tanh \tilde{\gamma} = \sinh \gamma \tanh(\gamma + \sigma) , \quad \beta\mu = \tanh \tilde{\gamma} \log(q/\sigma) \quad (\text{A.132})$$

and solve the first equation to find $\gamma(\sigma)$ and then use the second equation to find $\beta\mu$ as a function of σ (all for a fixed ratio $\hat{\mu}/\mathcal{J}$). Below we will write expressions for the energy, free energy and entropy, in terms of γ and σ , which can then be viewed as functions of the temperature by solving the equations as indicated here.

We can find the energy using (5.75) to obtain

$$\frac{E}{N} = \frac{\hat{\mu}}{q^2} \left[-\frac{q}{2} + 1 - \frac{1}{\tanh \gamma \tanh \tilde{\gamma}} - \log \left(\frac{\sinh \gamma}{\cosh \tilde{\gamma}} \right) \right] = -\partial_\beta \ell , \quad \ell \equiv \log Z/N \quad (\text{A.133})$$

where we denoted by $\ell = \log Z/N$ the logarithm of the partition function, then we know that $E/N = -\partial_\beta \ell$. In principle, we could integrate this equation to find ℓ . The problem is that this derivative is taken with fixed values of $\hat{\mu}$ and \mathcal{J} .

Instead we will notice that from the effective action (5.73) we can write

$$\begin{aligned} \mathcal{J} \partial_{\mathcal{J}} \ell &= \beta \int_0^\beta d\tau \mathcal{J}^2 (e^{g_{LL}} + e^{g_{LR}}) = \frac{\beta \hat{\mu}}{q^2} \left[\frac{1}{\tanh \gamma \tanh \tilde{\gamma}} - 1 \right] \\ \mu \partial_\mu \ell &= -i\beta\mu G_{LR}(0) = \frac{\beta \hat{\mu}}{q^2} \left[\frac{q}{2} + \log \left(\frac{\sinh \gamma}{\cosh \tilde{\gamma}} \right) \right] \end{aligned} \quad (\text{A.134})$$

where we used that G_{ab} obeys the equations of motion to conclude that only the explicit dependence on J and μ of the action (5.73) contributes to its derivatives. These expressions are consistent with (A.133) being $E/N = -\partial_\beta \ell$, and with ℓ being a function $\ell(\beta\hat{\mu}, \beta\mathcal{J})$ of dimensionless variables. We can use this fact, together with (A.134) to write the derivatives of ℓ with respect to γ and σ , with ℓ viewed as a function of γ and σ . Using (A.132) and (A.128) we can compute

$$\begin{aligned} \frac{\partial_\gamma \mu}{\mu} - \frac{\partial_\gamma \mathcal{J}}{\mathcal{J}} &= \frac{1}{\tanh \gamma} + \frac{1}{\sinh \tilde{\gamma} \cosh \tilde{\gamma}} , & \frac{\partial_\gamma (\beta\mu)}{\beta\mu} &= \frac{1}{\sinh \tilde{\gamma} \cosh \tilde{\gamma}} \\ \frac{\partial_\sigma \mu}{\mu} - \frac{\partial_\sigma \mathcal{J}}{\mathcal{J}} &= \frac{1}{\sinh \tilde{\gamma} \cosh \tilde{\gamma}} , & \partial_\sigma \log(\beta\mu) &= \frac{1}{\sinh \tilde{\gamma} \cosh \tilde{\gamma}} - \frac{1}{\sigma \log(q/\sigma)} \end{aligned} \quad (\text{A.135})$$

We now view ℓ as a function of $\ell(\gamma, \sigma)$ with the physical ratios of parameters $\hat{\mu}$, \mathcal{J} , ∞/β determined as in (A.132). We then write

$$\begin{aligned}\partial_\gamma \ell &= \frac{\partial_\gamma(\beta\hat{\mu})}{\beta\hat{\mu}}\beta\partial_\beta \ell + \left(\frac{\partial_\gamma \mathcal{J}}{\mathcal{J}} - \frac{\partial_\gamma \mu}{\mu}\right)\mathcal{J}\partial_\mathcal{J} \ell \\ \partial_\sigma \ell &= \frac{\partial_\sigma(\beta\hat{\mu})}{\beta\hat{\mu}}\beta\partial_\beta \ell + \left(\frac{\partial_\sigma \mathcal{J}}{\mathcal{J}} - \frac{\partial_\sigma \mu}{\mu}\right)\mathcal{J}\partial_\mathcal{J} \ell\end{aligned}\quad (\text{A.136})$$

where we used that $(\mu\partial_\mu + \mathcal{J}\partial_\mathcal{J} - \beta\partial_\beta)\ell = 0$ by dimensional analysis. Using (A.132), (A.135), (A.133) we can express the right hand sides of (A.136) in terms of σ , γ and then integrate the two equations to find the expression for ℓ quoted in (5.99) and reproduced here for convenience

$$\ell = \frac{\tanh \tilde{\gamma} \log(q/\sigma)}{q} \left[\frac{q}{2} - 1 + \frac{1}{\tanh \gamma \tanh \tilde{\gamma}} + \log \frac{\sinh \gamma}{\cosh \tilde{\gamma}} + \frac{\sigma}{\tanh \tilde{\gamma}} \right] + \frac{\sigma}{q} \quad (\text{A.137})$$

Using the energy (A.133) we can also write the entropy

$$S/N = \ell - \beta\partial_\beta \ell = \frac{\sigma}{q} \left(1 + \log \frac{q}{\sigma} \right) = e^{-\nu\beta}(1 + \beta\nu) \quad (\text{A.138})$$

It is curious that the entropy looks exactly like that of a slightly excited oscillators of energy ν .

In figure 16(a) we plot the resulting free energy as a function of the temperature. We see that we have a first order transition. This is despite the fact that the free energy is a smooth function of σ (for fixed μ/\mathcal{J}). Figure 16(b) shows that in the microcanonical ensemble we have a completely smooth behavior. We also find that the energy is a monotonic function of σ . Finally, in figure 17 we have plotted the temperature as a function of the energy to show how it increases, decreases and then increases again.

When we take the limit $\sigma \rightarrow 0$ we get $\tilde{\gamma} = \gamma$ and reproduce the zero temperature solution (5.85). On the other hand, when $\sigma \rightarrow \infty$, we get that $\tilde{\gamma} \rightarrow \infty$ and

$$\begin{aligned}2\alpha &= \hat{\mu}, \quad \sinh \gamma = \frac{\hat{\mu}}{2\mathcal{J}}, \quad \text{for } \sigma \gg 1 \\ \ell &\sim \frac{\beta\mu}{2} + e^{-\beta\mu} + \frac{\beta\mu}{2} \left[\log(2 \sinh \gamma) + \frac{1}{\tanh \gamma} - \gamma - 1 \right], \quad \sigma \gg 1\end{aligned}\quad (\text{A.139})$$

Note that in this regime ν is becoming independent of the temperature and equal to μ , which is the naively expected gap for the Hamiltonian H_{int} . We also see that since $\tilde{\gamma}$ is becoming large, then $e^{g_{LR}}$ is becoming very small everywhere, a fact that will be important below.

A.2 Inverse temperature of order $\beta \sim q$

We have seen that in the high temperature region of the previous range the function $e^{g_{LR}}$ is becoming very small. What is happening is that $-2iG_{LR}$ is becoming less than one

everywhere, so that we can neglect the term G_{LR}^{q-1} in the expression for the self energy. Therefore, in this regime, the left-right self energy becomes $\Sigma_{LR}(\tau) = -i\mu\delta(\tau)$. This also implies that $\nu = \mu$ in the long time approximation to the functions

$$\begin{aligned} G_{LL} &= \frac{1}{2} \frac{\cosh \mu(\frac{\beta}{2} - \tau)}{\cosh \frac{\mu\beta}{2}} + o(1/q) \\ G_{LR} &= \frac{i}{2} \frac{\sinh \mu(\frac{\beta}{2} - \tau)}{\cosh \frac{\mu\beta}{2}} + o(1/q), \quad \text{for } \tau \gg 1 \end{aligned} \quad (\text{A.140})$$

where we have imposed the appropriate periodicity conditions on the thermal circle. Notice that in this regime $\beta\mu$ and $\beta\tau$ are of order one. We will now consider a short time solution g_{LL} given by the usual expression (5.83). Matching its long time behavior to the short time behavior of (A.140) we obtain

$$2\alpha = \hat{\mu} \tanh \frac{\mu\beta}{2}, \quad \sinh \gamma = \frac{\hat{\mu}}{2\mathcal{J}} \tanh \frac{\mu\beta}{2}, \quad \mu = \frac{\hat{\mu}}{q} \quad (\text{A.141})$$

On the other hand, the short time behavior of G_{LR} is still given by (A.140). Notice that at short times $-2iG_{LR}(0) \sim \tanh \frac{\mu\beta}{2}$ which is less than one in the present regime, consistent with our assumptions. We can now evaluate various derivatives of the free energy in a simple way, as it was done above. We find

$$\begin{aligned} \mathcal{J} \partial_{\mathcal{J}} \ell &= \frac{\beta\mu}{q} \tanh \frac{\beta\mu}{2} \left[\frac{1}{\tanh \gamma} - 1 \right] \\ \mu \partial_{\mu} \ell &= \frac{\beta\mu}{2} \tanh \frac{\mu\beta}{2} + o(1/q) \end{aligned} \quad (\text{A.142})$$

This can be integrated to

$$\ell = \log[2 \cosh \frac{\beta\mu}{2}] + \frac{\beta\mu}{q} \tanh \frac{\beta\mu}{2} \left[\log(2 \sinh \gamma) + \frac{1}{\tanh \gamma} - \gamma - 1 \right] \quad (\text{A.143})$$

where we matched the integration constant by comparing with the expected answer at $\mathcal{J} = 0$ (or $\gamma = \infty$). Notice that the first term in (A.143) is the leading order piece of the free energy and it looks like the partition function of N free fermionic oscillators of frequency μ . The second term is a $1/q$ correction. For relatively low temperature, where $\beta\mu \gg 1$, these expressions match (A.139), which is the high temperature limit of the previous temperature range. It is also interesting to take the large temperature limit of (A.141) and (A.143) to obtain

$$\gamma \sim \frac{(\mu\beta)^2}{4q\mathcal{J}}, \quad \ell \sim \log 2 + \frac{(\beta\mu)^2}{8} + \frac{2\beta\mathcal{J}}{q^2} + \frac{(\beta\mu)^2}{2q} \log \left(\frac{(\mu\beta)^2}{4q\mathcal{J}} \right) + \dots \quad (\text{A.144})$$

One important point about this regime is that when the temperature increases from low to high values within this regime, the entropy rises from close to zero to close to

$\log 2$, which is close to the twice the ground state entropy of two separate SYK systems at large temperature. However, despite the entropy being large, there are still some other properties that are still different from the high temperature regime. For example the Liapunov exponent is still far from maximal. We will discuss this in more detail as we examine the next regime.

A.3 Inverse temperatures of the form $\beta \sim \sqrt{q}$

In this regime we can approximate $G_{LL} = \frac{1}{2}(1 + g_{LL}/q)$ in the whole temperature range. As before, we can approximate $\Sigma_{LR}(\tau) = -i\mu\delta(\tau)$. From (5.74) we get

$$0 = \partial_\tau G_{LR} - \Sigma_{LR} * G_{LR} + i\mu G_{RR} \sim \partial_\tau G_{LR} + i\frac{\mu}{2} \longrightarrow G_{LR} = \frac{i}{2}\mu\left(\frac{\beta}{2} - \tau\right) = -G_{RL} \quad (\text{A.145})$$

where we used that Σ_{LL} goes as $1/q$ and can be neglected, as well as the fact that $G_{RR} = \frac{1}{2}$ to leading order. We have also used the condition that $G_{LR}(\frac{\beta}{2} + x) = -G_{LR}(\frac{\beta}{2} - x)$. This solution also agrees with the large temperature approximation (small $\mu\beta$) of (A.140). We now use this equation and insert it into the time derivative of the first equation in (5.74) to get

$$0 = \partial_\tau [\partial_\tau G_{LL} - \Sigma_{LL} * G_{LL} + i\mu G_{RL}] \longrightarrow 0 = \partial_\tau^2 g_{LL} - 2\mathcal{J}^2 e^{g_{LL}} - q\mu^2 \quad (\text{A.146})$$

where we used (A.145). Now, naively, we could neglect the last term since it goes like $\hat{\mu}^2/q$. However, for large times, of order \sqrt{q} , the first terms are also similar. This can be seen most clearly by defining rescaled variables x and $e^{\hat{g}}$ via

$$x = \frac{\tau - \beta/2}{\beta}, \quad x \in \left[-\frac{1}{2}, \frac{1}{2}\right], \quad e^{\hat{g}} = (\beta\mathcal{J})^2 e^{g_{LL}} \quad (\text{A.147})$$

Now (A.146) becomes

$$\partial_x^2 \hat{g} - 2e^{\hat{g}} - 2k = 0, \quad k \equiv \frac{q\beta^2\mu^2}{2} \quad (\text{A.148})$$

We should then look for solutions to this equation where \hat{g} diverges at $x = \pm\frac{1}{2}$. The first integral of (A.148) is $(\hat{g}')^2 - 4e^{\hat{g}} - 4\hat{g}k = \text{constant}$. We can then further integrate this as

$$2x = \int_{\hat{g}_0}^{\hat{g}} \frac{dg}{\sqrt{e^g - e^{\hat{g}_0} + k(g - \hat{g}_0)}} \quad (\text{A.149})$$

where \hat{g}_0 is the value of \hat{g} at $x = 0$. This is determined by solving the equation

$$1 = \int_{\hat{g}_0}^{\infty} \frac{dg}{\sqrt{e^g - e^{\hat{g}_0} + k(g - \hat{g}_0)}}, \quad \text{or} \quad e^{\hat{g}_0/2} = \int_0^{\infty} \frac{dg}{\sqrt{e^g - 1 + \tilde{k}g}} \quad (\text{A.150})$$

where $\tilde{k} = ke^{-\hat{g}_0}$. The second expression is a bit more useful for numerical evaluations.

When $k = 0$, we have $e^{\hat{g}_0} = \pi^2$, $e^{\hat{g}} = \frac{\pi^2}{\cos^2 \pi x}$. We can then consider the regime when k is very large. One can check numerically that \hat{g}_0 decreases as k increases. At $k = 0$ we have the same equation as for a single copy of a large q SYK model [9], but the boundary conditions we are imposing here are slightly different here due to the way we rescaled the coordinates¹⁸.

The equations discussed here have also appeared in [46], for a closely related problem. The free energy has the form

$$\ell = \log 2 + \frac{(\beta\mu)^2}{8} + \frac{2\beta\mathcal{J}}{q^2} + \frac{(\mu\beta)^2}{2q} \log(\mathcal{J}\beta) + \frac{h[q(\mu\beta)^2]}{q^2} \quad (\text{A.151})$$

We used that

$$-2e^{\hat{g}_0/2} + \int_{\hat{g}_0}^{\infty} dg \left[\frac{e^g}{\sqrt{e^g - e^{\hat{g}_0} + k(g - \hat{g}_0)}} - e^{g/2} \right] = k = \frac{q(\beta\mu)^2}{2} \quad (\text{A.152})$$

thanks to (A.150). Interestingly, the coefficient of the $(\beta\mu)^2$ term in (A.151) is the same as the one in (A.144) throughout the temperature regime of this subsection. In order to determine the logarithmic term in (A.151) we used the expression for $\mathcal{J}\partial_{\mathcal{J}}\ell = \frac{1}{q^2} \int_{-1/2}^{1/2} dx e^{\hat{g}}$, and took into account that the divergence near the end points is regularized and gives a factor of \mathcal{J} , with the rest being \mathcal{J} independent. This method does not determine the μ dependence at this order. For that reason we could not fix the function h in (A.151). The leading μ dependence comes from the expression for the μ derivative, $\partial_{\mu}\ell = -i\beta G_{LR}(0) = \beta^2\mu/4$.

Chaos exponent

We now look at the chaos exponent. This can be done by computing the retarded kernel in the thermofield double configuration. Here we are thinking about the thermofield double of the already doubled physical system. This thermofield double contains four copies of the SYK model. To go to the second side of the thermofield double we can analytically continue after a shift by $\beta/2$ along the Euclidean time direction. The retarded Kernel obeys the equation

$$\partial_{t_1}\partial_{t_2}K(t_1, t_2; t_3, t_4) = 2q\Sigma_{LL}(\beta/2 + it_{34}) \quad (\text{A.153})$$

Here we have neglected $\Sigma_{LR}(\beta/2 + it_{34})$. Here we think of t_1, t_3 as living in the original system while t_2, t_4 live in the second copy of the thermofield double. We are interested in eigenfunctions of this Kernel of the form $K\psi = \psi$, with $\psi = e^{\lambda(t_1+t_2)/2}\chi(t_1 - t_2)$. Then χ obeys the equation

$$-\frac{(\lambda\beta)^2}{4}\chi = [-\partial_y^2 - 2e^{\hat{g}_t}]\chi(y) \quad (\text{A.154})$$

¹⁸Namely, in this subsection we are approximating the boundary condition $e^{\hat{g}(x=\pm 1/2)} = (\mathcal{J}\beta)^2$ by infinity.

where $\hat{g}_l(y) = \hat{g}(iy)$ is the analytic continuation of the Euclidean function $\hat{g}(x)$ (note that $x = 0 = y$ corresponds to $\tau = \beta/2$). $\hat{g}_l(y)$ has a maximum at $y = 0$ and then it decreases as $y \rightarrow \pm\infty$. This implies that (A.154) is a Schroedinger problem with an attractive potential that asymptotes to zero at infinity, and we are looking for its bound states. There is exactly one bound state for the following reason. We can show that $\chi \sim \partial_y \hat{g}_l$ is a zero energy state by taking the ∂_y derivative of the equation that $\hat{g}_l(y)$ obeys (which is the analytic continuation of (A.148)). Furthermore $\partial_y \hat{g}_l$ crosses zero only once. Therefore there is a single state with energy less than zero in the Schroedinger problem (A.154).

We can analyze extreme limits analytically. For $k = 0$ we recover the usual expression $\lambda = 2\pi/\beta$. For large k , $k \gg 1$, the potential can be approximated by a δ function and we can estimate

$$\frac{\lambda\beta}{2\pi} \sim \frac{k^{3/2}e^{-k/4}}{\sqrt{\pi}}, \quad k = \frac{q\mu^2\beta^2}{2} \quad (\text{A.155})$$

which is very small for large k . So we see that as the temperature increases, and we go from large k to small k , the chaos exponent goes from being very small to being maximal.

To study the problem numerically and produce figure 19 we found it convenient to do the following. First we defined a shifted function $\tilde{g} = \hat{g} - \hat{g}_0$ and rescaled variables so that now we have

$$2\tilde{y} = \int_{\tilde{g}}^0 \frac{dg}{\sqrt{1 - e^g - \tilde{k}g}}, \quad \tilde{y} = ye^{\hat{g}_0/2}, \quad \tilde{k} = ke^{-\hat{g}_0} \quad (\text{A.156})$$

The eigenvalue equation now looks

$$-\tilde{\lambda}^2\chi = [-\partial_{\tilde{y}}^2 - 2e^{\tilde{g}}]\chi(\tilde{y}), \quad \tilde{\lambda} = \frac{\lambda\beta}{2}e^{-\hat{g}_0/2} \quad (\text{A.157})$$

Then we changed variables¹⁹ from \tilde{y} to \tilde{g} so that the eigenvalue equation is

$$-\tilde{\lambda}^2\chi = \left[-4(1 - e^{\tilde{g}} - \tilde{k}\tilde{g})\partial_{\tilde{g}}^2 + 2(e^{\tilde{g}} + \tilde{k})\partial_{\tilde{g}} - 2e^{\tilde{g}}\right]\chi \quad (\text{A.158})$$

We want to solve this equation for $g \in [-\infty, 0]$ with the boundary condition that χ is regular at $\tilde{g} = 0$ and that it decays as $\tilde{g} \rightarrow -\infty$. In this way we find $\tilde{\lambda}(\tilde{k})$. We can then find \hat{g}_0 as a function of \tilde{k} from (A.150), and then finally compute $k(\tilde{k})$ and λ from (A.157) (A.148).

A.4 Inverse temperatures of order one

In this regime we can set $k = 0$ in (A.148) and impose $e^{\hat{g}(x=\pm\frac{1}{2})} = (\beta\mathcal{J})^2$. We recover the results we had for the two decoupled SYK models. We will not do this in detail since this was discussed in [9]. The free energy is twice the result in [9]

$$\ell_{\mu=0} = \log 2 + \frac{4}{q^2}\hat{v} \left[\tan \hat{v} - \frac{\hat{v}}{2} \right], \quad \beta\mathcal{J} = \frac{2\hat{v}}{\cos \hat{v}} \quad (\text{A.159})$$

¹⁹We thank Zhenbin Yang for this suggestion.

What we should note is that the leading deviation from the $\mu = 0$ result is

$$\ell = \ell_{\mu=0} + \frac{(\beta\mu)^2}{8} \quad (\text{A.160})$$

This term can be directly computed by using $\partial_\mu \ell = -i\beta G_{LR}(0)$ and the expression (A.145) which continues to be valid in this regime. It is also given by iterating twice the interaction Hamiltonian and using the leading order answer for the correlator

$$\ell - \ell_{\mu=0} = \frac{\mu^2}{2} \int d\tau_1 d\tau_2 G_{LL}(\tau_{12}) G_{RR}(\tau_{12}) = \frac{(\beta\mu)^2}{8} \quad (\text{A.161})$$

The chaos exponent is maximal in the region $\sqrt{q} \ll \beta\mathcal{J} \ll 1$, as we had found in the large temperature range of the previous subsection. It then becomes less than maximal when $\beta\mathcal{J} \sim 1$, becoming $\lambda = 2\mathcal{J}$ at very high temperatures [9].

B SL(2) charges

In this appendix we spell out the general form of the SL(2) charges for the action 4.24. Here we set $N = 1$. Using the Noether procedure for the transformation

$$\delta t_l = \epsilon^0 + \epsilon^+ e^{it_l} + \epsilon^- e^{-it_l}, \quad \delta t_r = \epsilon^0 - \epsilon^+ e^{it_r} - \epsilon^- e^{-it_r} \quad (\text{B.162})$$

we find

$$\begin{aligned} Q_0/N &= Q_0^S[t_l] + Q_0^S[t_r] + \left(\frac{1}{t'_l} + \frac{1}{t'_r}\right) F \\ Q_+/N &= Q_+^S[t_l] - Q_+^S[t_r] + \left(\frac{e^{it_l}}{t'_l} - \frac{e^{it_r}}{t'_r}\right) F \\ Q_-/N &= Q_-^S[t_l] - Q_-^S[t_r] + \left(\frac{e^{-it_l}}{t'_l} - \frac{e^{-it_r}}{t'_r}\right) F \\ F &\equiv \Delta\eta \left[\frac{t'_l t'_r}{\cos^2 \frac{t_l - t_r}{2}} \right]^\Delta \\ Q_0^S[t] &= -t' + \frac{t''^2}{t'^3} - \frac{t'''}{t'^2} \\ Q_+^S[t] &= e^{it} \left(i \frac{t''}{t'} + \frac{t''^2}{t'^3} - \frac{t'''}{t'^2} \right) \\ Q_-^S[t] &= e^{-it} \left(-i \frac{t''}{t'} + \frac{t''^2}{t'^3} - \frac{t'''}{t'^2} \right) \end{aligned} \quad (\text{B.163})$$

We see that if $t_l(\tilde{u}) = t_r(\tilde{u})$, then $Q_\pm = 0$ automatically and Q_0 gives

$$Q_0/N = 2e^{-\varphi} [-\varphi'' - e^{2\varphi} + \eta \Delta e^{2\Delta\varphi}], \quad \text{with } \varphi = \log t' \quad (\text{B.164})$$

Let us imagine we look for solutions with no matter. In this case we need to set the above charges to zero. We now want to argue that any such solution can be gauge transformed to a solution with $t_l(\tilde{u}) = t_r(\tilde{u})$. The argument is the following. First imagine we have a general solution with $t_l(\tilde{u}) \neq t_r(\tilde{u})$. Then, by a global $SL(2)$ transformation we can set the two times and their derivatives equal at $\tilde{u} = 0$, namely $t_l(0) = t_r(0)$ and $t'_l(0) = t'_r(0)$. Then by imposing that $Q_- - Q_+ = 0$ we get that $t''_l(0) = t''_r(0)$. Finally imposing that $Q_- + Q_+ = 0$ we conclude that $t'''_l(0) = t'''_r(0)$. Since the equations of motion are of fourth order, this implies that they are equal for all later times. This shows that solutions obeying the constraints can be gauge transformed to solutions obeying $t_l(\tilde{u}) = t_r(\tilde{u})$.

When we have matter in the bulk (or in the SYK language we excite the approximately conformal invariant degrees of freedom) we have an extra matter contribution, q_a^M to the $SL(2)$ charges.

It is also interesting to compute the expression for the charges, after we expand around the solution we discussed around (4.26) (4.29). We write

$$t_l = t'\tilde{u} + \chi_+(\tilde{u}) + \chi_-(\tilde{u}), \quad t_r = t'\tilde{u} + \chi_+(\tilde{u}) - \chi_-(\tilde{u}) \quad (\text{B.165})$$

The action of the $SL(2)$ gauge transformations (B.162) is

$$\delta\chi_+ = \epsilon^0, \quad \delta\chi_- = \epsilon^+ e^{it} + \epsilon^- e^{-it}, \quad t \equiv t'u \quad (\text{B.166})$$

where we rescaled the time so that now we work in terms of t , which is natural if we are expanding around the vacuum solution. Assuming that t' obeys (4.29) we then find

$$Q_0/N = -2t'd_t[d_t^2 + 2(1 - \Delta)]\chi_+, \quad Q_{\pm}/N = -2t'e^{\pm it}(d_t \mp i)(d_t^2 + 1)\chi_- \quad (\text{B.167})$$

It is also instructive to write down the expression for the total energy (4.38), which is

$$E_{\tilde{u}} = t'^2 N \left[-\frac{1 - \Delta}{\Delta} - 2 \{ d_t^3 \chi_+ + 2(1 - \Delta) d_t \chi_+ \} \right] = -t'^2 N \frac{1 - \Delta}{\Delta} - t' q_0 \quad (\text{B.168})$$

This is the expected expression for the energy at this order in the $1/N$ expansion. Namely, the energy is just given by the bulk energy²⁰ in global time, up to a rescaling factor of t' . Now, here q_a are the charges of the matter theory. We have used the expression for Q_0 in (B.167) and the constraint

$$Q_a + q_a = 0 \quad (\text{B.169})$$

Notice that the \pm components of these constraint equations (B.169) simply determine χ_- from q_{\pm} and we obtain

$$Q_{\pm} + q_{\pm} = 0 \quad \longrightarrow \quad \chi_- = -\frac{1}{8Nt'} (te^{-it}q_+ + te^{it}q_-) \quad (\text{B.170})$$

²⁰The energy is minus the quantity q_0 which is the Noether charge under time translations.

Where we used that q_{\pm} are just constants. We can solve these even as operator equations. The expression for χ is of order $1/N$, for q_{\pm} of order one, so that the small χ approximation was justified. Notice that χ_{\pm} do not appear in the expression for the energy (B.168) to this order in the $1/N$ expansion.

It is also interesting to note that

$$\begin{aligned} H_R - H_L &= \frac{d\tilde{u}}{du} \left[-\left\{ \tan \frac{t_r(\tilde{u})}{2}, \tilde{u} \right\} + \left\{ \tan \frac{t_l(\tilde{u})}{2}, \tilde{u} \right\} \right] = 2N \frac{d\tilde{u}}{u} t'^2 [d_t^2 \chi_- + d_t \chi_-] = \\ &= \frac{dt}{du} \left[\cos t \frac{(q_+ + q_-)}{2} + \sin t \frac{(q_+ - q_-)}{2i} \right] \end{aligned} \quad (\text{B.171})$$

Note that here H_R and H_L should be the Hamiltonians of the right or left SYK models, without the interaction term. In the gravity picture this is the difference of the left and right ADM mass operators. Now, this equation has an interesting interpretation. It is saying that at $t = 0$, the operator $H_R - H_L$ can be identified with $(q_+ + q_-)/2$ which turns out to be the boost generator around the origin in AdS_2 . Finally, the same operator, but at $t = \pi/2$, can be identified as the third generator of the bulk $SL(2)$ transformations. Near the origin of AdS_2 , it acts as a spatial translation. By origin we mean $t = 0$, $\sigma = \pi/2$ in the coordinates in (2.1).

Notice that in the SYK model we can still define the generators q_a as acting on the conformal invariant degrees of freedom, the excitations which are not described by the t_r, t_l variables.

Note that the operator in (B.171) is time dependent. Indeed, this operator is not conserved due to the interaction term in the full Hamiltonian of the coupled system. If we turn off the coupling at $t = 0$, then $H_R - H_L$ will be conserved and equal to the boost generator in the bulk field theory, consistent with the picture in section 4.3.

C Boundary conditions and negative energy for a CFT in the bulk

In this section we imagine we start with AdS_2 and we consider a conformal field theory on AdS_2 . Since it is a conformal field theory, we can forget about the overall scale factor of the metric in (2.1) and consider it on a strip, $ds^2 = -dt^2 + d\sigma^2$. In this appendix we discuss a couple of issues about this. With standard boundary conditions on the strip, we will ask whether this setup gives rise to negative energy or not. Then we will consider the specific case of free fermions and work out the state for various value of the boundary coupling.

C.1 Negative energy on the strip goes to zero energy in AdS_2

It is well known that the energy of a conformal field theory on a strip is given by

$$E = -\frac{c}{24} \frac{\pi}{L}, \quad \text{or} \quad E = -\frac{c}{24}, \quad \text{for } L = \pi \quad (\text{C.172})$$

Here we ask whether this is enough to give rise to negative null energy in the sense discussed around (2.10). The conclusion will be no. We have to realize that we are talking about two different notions of energy. When we think about the flat strip, we imagine renormalizing the energy with a constant cutoff on the flat metric of the strip. When we talk about AdS_2 we imagine doing the same with a cutoff that is constant in AdS_2 proper length. The difference is just a scale factor. We can work out the difference by looking at the general form of the conformal anomaly (in Lorentzian signature)

$$Z[g = e^{2\omega}\hat{g}] = \exp \left\{ i \frac{c}{24\pi} \int d^2x \sqrt{\hat{g}} [\hat{R}\omega + (\hat{\nabla}\omega)^2] \right\} Z[\hat{g}] \quad (C.173)$$

This means that the stress tensor computed by taking derivatives with respect to each metric is given by

$$\begin{aligned} T_{\mu\nu}^g &= T_{\mu\nu}^{\hat{g}} - \frac{c}{12\pi} \left[\partial_\mu\omega\partial_\nu\omega - \frac{1}{2}\hat{g}_{\mu\nu}(\hat{\nabla}\omega)^2 - \hat{\nabla}_\nu\hat{\nabla}_\mu\omega + \hat{g}_{\mu\nu}\hat{\nabla}^2\omega \right] \\ T_{\mu\nu}^g &= T_{\mu\nu}^{\hat{g}} + \frac{c}{24\pi} \begin{pmatrix} 1 & 0 \\ 0 & 1 \end{pmatrix} - \frac{c}{24\pi}g_{\mu\nu} \end{aligned} \quad (C.174)$$

We see that the second term cancels precisely the negative energy we had in $T_{\mu\nu}^{\hat{g}}$. The last term is proportional to $g_{\mu\nu}$ (not $\hat{g}_{\mu\nu}$) and it is the piece that will contribute to the conformal anomaly in AdS_2 , $T_\mu^{g,\mu} = \frac{c}{24}R$.

We conclude that T_{++}^g vanishes. The piece that is proportional to the metric in the stress tensor is a contribution proportional to \sqrt{g} in the action, and it can be absorbed by a shift of the dilaton (and also a shift of the coefficient of the topological term $\phi_0 \int \sqrt{g}R$ in the action).

One comment, is that in a CFT we have various boundary conditions. In this discussion we have assumed that the boundary condition on the left side is the “same” as the one on the right side. By “same” here we mean the CPT conjugate one. It is the one we get by taking a boundary condition along the real line and then mapping the upper half plane to the strip by a conformal transformation. With this pair of boundary conditions we have the minimal energy $E = -\frac{c}{24}$. For other possible combinations we have higher energy, again consistent with the null energy condition in AdS_2 .

C.2 Negative energy for a free fermion AdS_2 plus a boundary interaction

In this subsection we consider a free real fermion theory on a flat strip. We start with the usual boundary conditions

$$\psi_+ = \psi_-|_{\sigma=0}, \quad \psi_+ = -\psi_-|_{\sigma=\pi} \quad \text{for all } t \quad (C.175)$$

After we add the interaction that relates left and right, we end up modifying the boundary conditions to

$$\psi_+|_{\sigma=0} = \cos \pi\epsilon\psi_-|_{\sigma=0} - \sin \pi\epsilon\psi_+|_{\sigma=\pi}, \quad \psi_-|_{\sigma=\pi} = -\cos \pi\epsilon\psi_-|_{\sigma=\pi} - \sin \pi\epsilon\psi_-|_{\sigma=\pi} \quad (C.176)$$

We can get the first relation if we thinking of the reflection and transmission of the incoming fermion. The reflection and transmission factors should be real since the fermion fields are real. In addition, consistency with commutation relations (or unitarity) implies that we can write them as a sine and cosine. We get the second relation in (C.176) by a rotation (or CPT transformation) to the other boundary. Here ϵ is a parameter that is related to the coupling between the left and the right sides. We expect that $\epsilon \propto \eta$, and in comparing with the general discussion, this case corresponds to $\Delta = \frac{1}{2}$. Writing $\psi_+(t) \propto b_\omega e^{-i\omega t}$ and inserting in (C.176) we get the condition

$$\omega = \pm \left[\frac{1}{2} + \epsilon + 2n \right] , \quad \text{or} \quad \cos \pi\omega = -\sin \pi\epsilon \quad (\text{C.177})$$

Assuming $-\frac{1}{2} < \epsilon < \frac{1}{2}$, we see that the positive energies are $\frac{1}{2} + \epsilon + 2n$, $n \geq 0$ and $-\frac{1}{2} - \epsilon + 2n$, $n \geq 1$. For $\epsilon = 0$ these two towers collapse to $\frac{1}{2} + m$, $m \geq 0$. We can compute the ground state energy by adding all the zero point energies of these fermionic oscillators (suitably) regularized to obtain

$$E = -\frac{1}{48} [1 + 12\epsilon(1 - \epsilon)] , \quad -\frac{1}{2} \leq \epsilon \leq \frac{1}{2} \quad (\text{C.178})$$

Special values are

$$E(\epsilon = 0) = -\frac{1}{48} , \quad E(\epsilon = \frac{1}{2}) = -\frac{1}{12} , \quad E(\epsilon = -\frac{1}{2}) = \frac{1}{6} \quad (\text{C.179})$$

In the first case we recover the energy expected from the general formula (C.172), where for a single real fermion we have $c = \frac{1}{2}$. The second case corresponds to a fermion on a circle of length $L = \pi$ with antiperiodic boundary conditions. For a circle the ground state formula analogous to (C.172) is $E = -\frac{c}{12} \frac{2\pi}{L}$, where L is the size of the circle. The last case also corresponds to a fermion on a circle of length π , but with periodic boundary conditions. So we see that (C.178) interpolates between these last two extreme situations.

Notice that, for any *CFT* on the strip, we can couple the two sides such that we end up with “transparent” boundary conditions. Namely, we end up with the boundary conditions for a CFT on a circle of radius π . In such a case, the final energy can be computed in general as $E = -\frac{c}{6}$, which is more negative than the strip result (C.172).

The analysis we made in the bulk of the paper we always assumed that $\eta \propto \epsilon$ was small. For this case, we see we can also take it to be large. However, there is a maximum effective value which is $\epsilon \pm \frac{1}{2}$. If we continue beyond that value we get the same physics (C.177).

C.3 Profile for the bulk dilaton

Here we will compute the profile for the dilaton for the negative energy states discussed above.

In Lorentzian signature, the final form of the stress tensor on the flat strip is then $T_{t\sigma} = 0$, $T_{tt} = T_{\sigma\sigma} = E/\pi$, with E as in (C.178) and $T_{t\sigma} = 0$. When we transform this into an AdS_2 stress tensor, as in (C.174) that still has $T_{t\sigma} = 0$, but now the piece that is not proportional to the metric is

$$\frac{1}{2}(T_{tt}^g + T_{\sigma\sigma}^g) = -\frac{1}{4\pi}\epsilon(1 - \epsilon) \quad (\text{C.180})$$

Comparing this with the contribution to the energy of the interaction Hamiltonian in section 4 we find that they agree if get $\epsilon/4 = \eta$, for small ϵ . We can then make an ansatz $\phi = \phi(\sigma)$ and then from (2.10) we find

$$-\partial_\sigma(\sin^2 \sigma \partial_\sigma \phi) = -\frac{N}{2\pi}\epsilon(1-\epsilon) \sin^2 \sigma \quad \longrightarrow \quad \phi = N \frac{\epsilon(1-\epsilon)}{4\pi} \left[\frac{(\frac{\pi}{2} - \sigma)}{\tan \sigma} + 1 \right] + \frac{c}{24\pi} \quad (\text{C.181})$$

where we have set the integration constants appropriately. Actually, to fix the additive constant we also need to impose the equation for the dilaton that comes from the trace variation of the metric, and use the full stress tensor (C.174). Here N is the total number of Majorana fermions, and $c = N/2$. The additive constant in (C.181) that is proportional to c comes from the term in the stress tensor (C.174) that is proportional to the metric. It is easy to see from the form of the original action (2.5) that such a term can be removed by a shift of the dilaton, up to an overall topological term in the action.

We see that we still get that $\phi \propto 1/\sigma$ near $\sigma = 0$ and similarly near $\sigma = \pi$. Even though the stress tensor components are constant in these coordinates, their invariant values are becoming small. In some sense, the negative stress tensor is concentrated away from the boundaries.

The methods discussed in section 4 reproduce the physics we obtain from the small ϵ limit of this case.

D Derivation of the Liouville effective action

In this appendix, we derive the Liouville effective action from the large q limit of the G, Σ action (5.73).

$$\begin{aligned} -S_E/N &= \frac{1}{2} \text{Tr} \log (\partial_\tau \delta_{ab} - \Sigma_{ab}) - \frac{1}{2} \int d\tau_1 d\tau_2 \sum_{a,b} \left[\Sigma_{ab}(\tau_1, \tau_2) G_{ab}(\tau_1, \tau_2) - s_{ab} \frac{\mathcal{J}^2}{2q^2} [2G_{ab}(\tau_1, \tau_2)]^q \right] + \\ &+ \frac{i\hat{\mu}}{2q} \int d\tau_1 [-G_{LR}(\tau_1, \tau_1) + G_{RL}(\tau_1, \tau_1)] \end{aligned} \quad (\text{D.182})$$

Define

$$G_{ab}(\tau_1, \tau_2) = G_{0ab}(\tau_1, \tau_2) \left(1 + \frac{1}{q} g_{ab}(\tau_1, \tau_2) \right) \quad (\text{D.183})$$

with $G_{0LL}(\tau_1, \tau_2) = \frac{1}{2}\text{sgn}(\tau_1 - \tau_2)$, $G_{0LR} = \frac{i}{2}\text{sgn}(\hat{\mu})$. $[G_0^{-1}]_{ab} = \delta_{ab}\partial_\tau$. G_0 is chosen to be the two-point function of free fermion with a Hamiltonian $H = i\mu \sum_i \chi_{iL}\chi_{iR}$ with $\mu \rightarrow 0$. In large q limit, the self energy at the saddle point also scales with $\frac{1}{q}$, so that we can expand the determinant term as

$$\text{Tr} \log (\partial_\tau \delta_{ab} - \Sigma_{ab}) = \text{Tr} \log (G_0^{-1}) - \text{Tr} (G_0 * \Sigma) - \frac{1}{2} \text{Tr} (G_0 * \Sigma * G_0 * \Sigma) + \dots \quad (\text{D.184})$$

Omitting the constant terms $\text{Tr} \log (G_0^{-1})$ and $G_{0LR} - G_{0RL}$ in the action, we obtain

$$\begin{aligned} \frac{1}{N} S_E &\simeq \frac{1}{4} \text{Tr} (G_0 * \Sigma * G_0 * \Sigma) + \frac{1}{2q} \int d\tau_1 d\tau_2 \sum_{ab} \Sigma_{ab}(\tau_1, \tau_2) G_{0ab}(\tau_1, \tau_2) g_{ab}(\tau_1, \tau_2) \\ &\quad - \frac{\mathcal{J}^2}{4q^2} \int d\tau_1 d\tau_2 e^{g_{ab}(\tau_1, \tau_2)} - \frac{|\hat{\mu}|}{q^2} \int d\tau g_{LR}(\tau, \tau) \end{aligned} \quad (\text{D.185})$$

By integrating out Σ , we will obtain an action of g_{ab} . To do that it is helpful to introduce

$$\Phi_{ab}(\tau_1, \tau_2) = [G_0 * \Sigma(\tau_1, \tau_2)]_{ab} = \int d\tau G_{0ac}(\tau_1, \tau) \Sigma_{cb}(\tau, \tau_2) \quad (\text{D.186})$$

Thus by construction

$$\Sigma_{ab}(\tau_1, \tau_2) = \partial_{\tau_1} \Phi_{ab}(\tau_1, \tau_2) \quad (\text{D.187})$$

The effective action can be written as

$$\begin{aligned} \frac{1}{N} S_E &\simeq \frac{1}{4} \text{Tr} (\Phi * \Phi) + \frac{1}{2q} \int d\tau_1 d\tau_2 \sum_{ab} \partial_{\tau_1} \Phi_{ab}(\tau_1, \tau_2) G_{0ab}(\tau_1, \tau_2) g_{ab}(\tau_1, \tau_2) \\ &\quad - \frac{\mathcal{J}^2}{4q^2} \int d\tau_1 d\tau_2 e^{g_{ab}(\tau_1, \tau_2)} - \frac{|\hat{\mu}|}{q^2} \int d\tau g_{LR}(\tau, \tau) \\ &\simeq \frac{1}{2} \text{Tr} (\Phi * \Phi) - \frac{1}{2q} \int d\tau_1 d\tau_2 \sum_{ab} \Phi_{ab}(\tau_1, \tau_2) \partial_{\tau_1} (G_{0ab}(\tau_1, \tau_2) g_{ab}(\tau_1, \tau_2)) \\ &\quad - \frac{\mathcal{J}^2}{4q^2} \int d\tau_1 d\tau_2 e^{g_{ab}(\tau_1, \tau_2)} - \frac{|\hat{\mu}|}{q^2} \int d\tau g_{LR}(\tau, \tau) \end{aligned} \quad (\text{D.188})$$

where we have done an integration by part in the second term. Integrating over Φ_{ab} we obtain the effective action

$$\begin{aligned} \frac{1}{N} S_{\text{eff}} &= \frac{1}{4q^2} \int d\tau_1 d\tau_2 \sum_{ab} \partial_{\tau_1} (G_{0ab}(\tau_1, \tau_2) g_{ab}(\tau_1, \tau_2)) \partial_{\tau_2} (G_{0ab}(\tau_1, \tau_2) g_{ab}(\tau_1, \tau_2)) \\ &\quad - \frac{\mathcal{J}^2}{4q^2} \int d\tau_1 d\tau_2 \sum_{ab} e^{g_{ab}(\tau_1, \tau_2)} - \frac{|\hat{\mu}|}{q^2} \int d\tau g_{LR}(\tau, \tau) \end{aligned} \quad (\text{D.189})$$

It should be noted that there is a nontrivial Jacobian relating the path integral of Σ_{ab} to that of Φ_{ab} , but the Jacobian is independent from g_{ab} which only contributes a constant term to the effective action.

Since G_{0ab} is a constant except G_{0LL} at $\tau_1 = \tau_2$, and g_{0LL} satisfies the boundary condition $g_{0LL}(\tau_1, \tau_1) = 0$, the effective action can be simplified to

$$\begin{aligned} \frac{1}{N} S_{\text{eff}} &= \frac{1}{8q^2} \int d\tau_1 d\tau_2 (\partial_{\tau_1} g_{LL}(\tau_1, \tau_2) \partial_{\tau_2} g_{LL}(\tau_1, \tau_2) - \partial_{\tau_1} g_{LR}(\tau_1, \tau_2) \partial_{\tau_2} g_{LR}(\tau_1, \tau_2)) \\ &\quad - \frac{\mathcal{J}^2}{2q^2} \int d\tau_1 d\tau_2 (e^{g_{LL}(\tau_1, \tau_2)} + e^{g_{LR}(\tau_1, \tau_2)}) - \frac{|\hat{\mu}|}{q^2} \int d\tau g_{LR}(\tau, \tau) \end{aligned} \quad (\text{D.190})$$

The role of the last term is imposing a boundary condition for g_{LR} at $\tau_1 = \tau_2$. Using the symmetry $g_{ab}(\tau_1, \tau_2) = g_{ab}(\tau_2, \tau_1)$ one can consider the action as the Liouville action defined on the half plane $\tau_1 > \tau_2$:

$$\begin{aligned} \frac{1}{N} S_{\text{eff}} &= \frac{1}{4q^2} \int_{\tau_1 > \tau_2} d\tau_1 d\tau_2 (\partial_{\tau_1} g_{LL}(\tau_1, \tau_2) \partial_{\tau_2} g_{LL}(\tau_1, \tau_2) - \partial_{\tau_1} g_{LR}(\tau_1, \tau_2) \partial_{\tau_2} g_{LR}(\tau_1, \tau_2)) \\ &\quad - \frac{\mathcal{J}^2}{q^2} \int_{\tau_1 > \tau_2} d\tau_1 d\tau_2 (e^{g_{LL}(\tau_1, \tau_2)} + e^{g_{LR}(\tau_1, \tau_2)}) - \frac{|\hat{\mu}|}{q^2} \int d\tau g_{LR}(\tau, \tau) \end{aligned} \quad (\text{D.191})$$

with the boundary condition

$$g_{LL}(\tau, \tau) = 0, \quad (\partial_{\tau_1} - \partial_{\tau_2}) g_{LR}(\tau_1, \tau_2)|_{\tau_2=\tau_1} = 2|\hat{\mu}| \quad (\text{D.192})$$

In addition to the boundary condition at $\tau_1 = \tau_2$ line, other boundary conditions depend on the problem we are considering. For finite temperature thermal ensemble, periodic boundary condition in τ_1, τ_2 are imposed. (In that case, we choose G_0 is anti-periodic in $\tau_1 \rightarrow \tau_1 + \beta$ or $\tau_2 \rightarrow \tau_2 + \beta$, so that g_{ab} is periodic in both directions.)

E The two-time solution

In this appendix we provide more details on finding the interpolating solution we discussed in Sec. 5.5. The starting point is the general solution to Liouville equations (5.112), which we copy here:

$$e^{g_{LL}} = \frac{h'_1(\tau_1) h'_2(\tau_2)}{\mathcal{J}^2 (h_1(\tau_1) - h_2(\tau_2))^2}, \quad e^{g_{LR}} = -\frac{f'_1(\tau_1) f'_2(\tau_2)}{\mathcal{J}^2 (f_1(\tau_1) - f_2(\tau_2))^2} \quad (\text{E.193})$$

We start from the two time-translation-invariant solutions, the TFD solution and the coupled ground state solution. The TFD solution is obtained from the thermal solution of a single SYK site[9]:

$$e^{g(\tau_1, \tau_2)} = \frac{\check{\alpha}^2}{\mathcal{J}^2 \sin^2(\check{\alpha} |\tau_1 - \tau_2| + \check{\gamma})} \quad (\text{E.194})$$

with $\check{\alpha}$ and $\check{\gamma}$ determined by the boundary conditions

$$\check{\alpha} = \mathcal{J} \sin \check{\gamma}, \quad \check{\alpha} \frac{\beta}{2} + \check{\gamma} = \frac{\pi}{2} \quad (\text{E.195})$$

By viewing the thermal circle as a doubled system, we can write the thermal solution above in the form of thermal double solution, with $\tau_1, \tau_2 \in [-\frac{\beta}{4}, \frac{\beta}{4}]$:

$$e^{g_{LL}} = \frac{\check{\alpha}^2}{\mathcal{J}^2 \sin(\check{\alpha}|\tau_1 - \tau_2| + \check{\gamma})^2}, \quad e^{g_{LR}} = \frac{\check{\alpha}^2}{\mathcal{J}^2 \sin(\check{\alpha}(\tau_1 + \tau_2 + \frac{\beta}{2}) + \check{\gamma})^2} \equiv \frac{\check{\alpha}^2}{\mathcal{J}^2 \cos^2(\check{\alpha}(\tau_1 + \tau_2))} \quad (\text{E.196})$$

The boundary condition requires

$$g_{LL}(\tau, -\frac{\beta}{4}) = g_{LR}(\tau, -\frac{\beta}{4}), \quad \lim_{\tau_2 = -\frac{\beta}{4}} \partial_{\tau_2} g_{LL}(\tau_1, \tau_2) = - \lim_{\tau_2 = -\frac{\beta}{4}} \partial_{\tau_2} g_{LR}(\tau_1, \tau_2) \quad (\text{E.197})$$

and similar at $\tau = \frac{\beta}{4}$. This solution can be realized as the general solution (5.112) of Liouville equation, with the choice

$$\begin{aligned} h_1(\tau) &= \tan\left(\check{\alpha}\tau + \frac{\check{\gamma}}{2}\right), \quad h_2(\tau) = \tan\left(\check{\alpha}\tau - \frac{\check{\gamma}}{2}\right), \\ f_1(\tau) &= \tan\left(\check{\alpha}\tau + \frac{\check{\gamma}}{2}\right), \quad f_2(\tau) = \cot\left(\check{\alpha}\tau - \frac{\check{\gamma}}{2}\right) \end{aligned} \quad (\text{E.198})$$

On the other hand, the ground state solution (5.83) corresponds to the choice of functions

$$\begin{aligned} h_1(\tau) &= \tanh\left(\alpha\tau + \frac{\gamma}{2}\right), \quad h_2(\tau) = \tanh\left(\alpha\tau - \frac{\gamma}{2}\right) \\ f_1(\tau) &= \tanh\left(\alpha\tau + \frac{\gamma}{2}\right), \quad f_2(\tau) = \coth\left(\alpha\tau - \frac{\gamma}{2}\right) \end{aligned} \quad (\text{E.199})$$

Now the question is whether we can find a new solution by simply joining the functions in (E.198) and those in (E.199) at $\tau = 1$. To get a solution of Liouville equation, we need $h_{1,2}$, $f_{1,2}$ and $h'_{1,2}$, $f'_{1,2}$ to be continuous.

However, one should remember that there is an $\text{SL}(2, \mathbb{R})$ gauge symmetry for the choice of functions. The solution is invariant under transformations

$$h_1(\tau) \rightarrow \frac{ah_1(\tau) + b}{ch_1(\tau) + d}, \quad h_2(\tau) \rightarrow \frac{ah_2(\tau) + b}{ch_2(\tau) + d}, \quad ad - bc = 1 \quad (\text{E.200})$$

There are two independent $\text{SL}(2, \mathbb{R})$ gauge symmetry, one for $h_{1,2}$ and one for $f_{1,2}$. Therefore when we try to match the two solutions, it is sufficient to find a match up to $\text{SL}(2, \mathbb{R})$ transformation. As a gauge fixing, we could fix the functions (E.199) and carry $\text{SL}(2, \mathbb{R})$ transformation only to the TFD part (E.198). The $\text{SL}(2, \mathbb{R})$ transformed functions can be written as

$$\begin{aligned} h_1(\tau) &= A \tan\left(\check{\alpha}\tau + \frac{\check{\gamma}}{2} + B\right) + C, \quad h_2(\tau) = A \tan\left(\check{\alpha}\tau - \frac{\check{\gamma}}{2} + B\right) + C, \\ f_1(\tau) &= D \tan\left(\check{\alpha}\tau + \frac{\check{\gamma}}{2} + E\right) + F, \quad f_2(\tau) = D \cot\left(\check{\alpha}\tau - \frac{\check{\gamma}}{2} - E\right) + F \end{aligned} \quad (\text{E.201})$$

with arbitrary parameters A, B, C, D, E, F labeling $SL(2, R) \times SL(2, R)$. The matching condition for h_1, h_2 at $\tau = 0$ gives

$$\begin{aligned} A \tan\left(\frac{\check{\gamma}}{2} + B\right) + C &= \tanh\left(\frac{\gamma}{2}\right), \quad A \tan\left(\frac{-\check{\gamma}}{2} + B\right) + C = \tanh\left(-\frac{\gamma}{2}\right), \\ A\check{\alpha} \sec^2\left(\frac{\check{\gamma}}{2} + B\right) &= \alpha \operatorname{sech}^2\left(\frac{\gamma}{2}\right), \quad A\check{\alpha} \sec^2\left(-\frac{\check{\gamma}}{2} + B\right) = \alpha \operatorname{sech}^2\left(-\frac{\gamma}{2}\right) \end{aligned} \quad (\text{E.202})$$

These equations require

$$B = 0, \quad C = 0, \quad A \tan\frac{\check{\gamma}}{2} = \tanh\frac{\gamma}{2}, \quad A\check{\alpha} \left(1 + \tan^2\frac{\check{\gamma}}{2}\right) = \alpha \left(1 - \tanh^2\frac{\gamma}{2}\right) \quad (\text{E.203})$$

Similarly, the equations for f_1, f_2 requires

$$\begin{aligned} D \tan\left(\frac{\check{\gamma}}{2} + E\right) + F &= \tanh\frac{\gamma}{2}, \quad D \cot\left(-\frac{\check{\gamma}}{2} - E\right) + F = -\coth\frac{\gamma}{2}, \\ D\check{\alpha} \sec^2\left(\frac{\check{\gamma}}{2} + E\right) &= \alpha \operatorname{sech}^2\frac{\gamma}{2}, \quad -D\check{\alpha} \csc^2\left(\frac{\check{\gamma}}{2} + E\right) = -\alpha \operatorname{csch}^2\frac{\gamma}{2} \end{aligned} \quad (\text{E.204})$$

From the second line we get

$$\tan^2\left(\frac{\check{\gamma}}{2} + E\right) = \tanh^2\frac{\gamma}{2} \quad (\text{E.205})$$

Using this equation in Eq. (E.204) we obtain

$$D = 1, \quad F = 0, \quad \check{\alpha} = \frac{\alpha}{\cosh\gamma} \quad (\text{E.206})$$

In addition, from Eq. (E.203) and Eq. (E.204) we see that

$$\frac{\tan\frac{\check{\gamma}}{2}}{\sec^2\frac{\check{\gamma}}{2}} = \frac{\tan\left(\frac{\check{\gamma}}{2} + E\right)}{\sec^2\left(\frac{\check{\gamma}}{2} + E\right)} = \frac{\check{\alpha} \tanh\frac{\gamma}{2}}{\alpha \operatorname{sech}^2\frac{\gamma}{2}} \Rightarrow E = 0, \quad A = 1 \quad (\text{E.207})$$

In summary, we obtain the following matching condition:

$$\begin{aligned} A = 1, \quad B = 0, \quad C = 0, \quad D = 1, \quad E = 0, \quad F = 0 \\ \tan\frac{\check{\gamma}}{2} = \tanh\frac{\gamma}{2}, \quad \check{\alpha} = \frac{\alpha}{\cosh\gamma} \end{aligned} \quad (\text{E.208})$$

Note that Eq. (E.208) is consistent with the thermal boundary condition (E.195) since

$$\alpha = \mathcal{J} \sinh\gamma, \quad \check{\alpha} = \frac{\alpha}{\cosh\gamma} = \mathcal{J} \tanh\gamma = \mathcal{J} \frac{2 \tanh\frac{\gamma}{2}}{1 + \tanh^2\frac{\gamma}{2}} = \mathcal{J} \sin\check{\gamma} \quad (\text{E.209})$$

This consistency is because $e^g \rightarrow 1$ in the $\tau_1 - \tau_2 \rightarrow 0$ limit in both regions. The temperature that matches the ground state solution is determined by the boundary condition (E.195). β can be expressed as a function of α :

$$\beta = \frac{2}{\check{\alpha}} \left(\frac{\pi}{2} - \check{\gamma}\right) = \frac{2}{\alpha} \sqrt{\alpha^2 + 1} \arctan\frac{\mathcal{J}}{\alpha} \quad (\text{E.210})$$

References

- [1] A. Almheiri and J. Polchinski, “Models of AdS₂ backreaction and holography,” *JHEP* **11** (2015) 014, arXiv:1402.6334 [hep-th].
- [2] K. Jensen, “Chaos and hydrodynamics near AdS₂,” arXiv:1605.06098 [hep-th].
- [3] J. Maldacena, D. Stanford, and Z. Yang, “Conformal symmetry and its breaking in two dimensional Nearly Anti-de-Sitter space,” *PTEP* **2016** no. 12, (2016) 12C104, arXiv:1606.01857 [hep-th].
- [4] J. Engelsy, T. G. Mertens, and H. Verlinde, “An investigation of AdS₂ backreaction and holography,” *JHEP* **07** (2016) 139, arXiv:1606.03438 [hep-th].
- [5] P. Gao, D. L. Jafferis, and A. Wall, “Traversable Wormholes via a Double Trace Deformation,” arXiv:1608.05687 [hep-th].
- [6] S. Sachdev and J. Ye, “Gapless spin fluid ground state in a random, quantum Heisenberg magnet,” *Phys. Rev. Lett.* **70** (1993) 3339, arXiv:cond-mat/9212030 [cond-mat].
- [7] A. Kitaev, “A simple model of quantum holography.” <http://online.kitp.ucsb.edu/online/entangled15/kitaev/>, <http://online.kitp.ucsb.edu/online/entangled15/kitaev2/>. Talks at KITP, April 7, 2015 and May 27, 2015.
- [8] A. Kitaev and S. J. Suh, “The soft mode in the Sachdev-Ye-Kitaev model and its gravity dual,” arXiv:1711.08467 [hep-th].
- [9] J. Maldacena and D. Stanford, “Remarks on the Sachdev-Ye-Kitaev model,” *Phys. Rev.* **D94** no. 10, (2016) 106002, arXiv:1604.07818 [hep-th].
- [10] A. Jevicki and K. Suzuki, “Bi-Local Holography in the SYK Model: Perturbations,” *JHEP* **11** (2016) 046, arXiv:1608.07567 [hep-th].
- [11] S. Banerjee and E. Altman, “Solvable model for a dynamical quantum phase transition from fast to slow scrambling,” *Physical Review B* **95** no. 13, (2017) 134302.
- [12] X. Chen, R. Fan, Y. Chen, H. Zhai, and P. Zhang, “Competition between chaotic and nonchaotic phases in a quadratically coupled sachdev-ye-kitaev model,” *Physical review letters* **119** no. 20, (2017) 207603.
- [13] T. Azeyanagi, F. Ferrari, and F. I. Schaposnik Massolo, “Phase Diagram of Planar Matrix Quantum Mechanics, Tensor, and Sachdev-Ye-Kitaev Models,” *Phys. Rev. Lett.* **120** no. 6, (2018) 061602, arXiv:1707.03431 [hep-th].

- [14] X.-Y. Song, C.-M. Jian, and L. Balents, “Strongly correlated metal built from sachdev-ye-kitaev models,” *Physical review letters* **119** no. 21, (2017) 216601.
- [15] D. Chowdhury, Y. Werman, E. Berg, and T. Senthil, “Translationally invariant non-fermi liquid metals with critical fermi-surfaces: Solvable models,” *arXiv preprint arXiv:1801.06178* (2018) .
- [16] C. Bachas and I. Lavdas, “Quantum Gates to other Universes,” *Fortsch. Phys.* **66** no. 2, (2018) 1700096, [arXiv:1711.11372 \[hep-th\]](#).
- [17] J. M. Maldacena, J. Michelson, and A. Strominger, “Anti-de Sitter fragmentation,” *JHEP* **02** (1999) 011, [arXiv:hep-th/9812073 \[hep-th\]](#).
- [18] G. J. Galloway and M. Graf, “Rigidity of asymptotically $AdS_2 \times S^2$ spacetimes,” [arXiv:1803.10529 \[gr-qc\]](#).
- [19] R. Jackiw, “Lower Dimensional Gravity,” *Nucl. Phys.* **B252** (1985) 343–356.
- [20] C. Teitelboim, “Gravitation and Hamiltonian Structure in Two Space-Time Dimensions,” *Phys. Lett.* **B126** (1983) 41–45.
- [21] P. Nayak, A. Shukla, R. M. Soni, S. P. Trivedi, and V. Vishal, “On the Dynamics of Near-Extremal Black Holes,” [arXiv:1802.09547 \[hep-th\]](#).
- [22] K. S. Kolekar and K. Narayan, “ AdS_2 dilaton gravity from reductions of some nonrelativistic theories,” [arXiv:1803.06827 \[hep-th\]](#).
- [23] A. Kitaev. Talk given IAS chaos workshop, Oct. 18, 2016.
- [24] G. J. Galloway, K. Schleich, D. M. Witt, and E. Woolgar, “Topological censorship and higher genus black holes,” *Phys. Rev.* **D60** (1999) 104039, [arXiv:gr-qc/9902061 \[gr-qc\]](#).
- [25] G. J. Galloway, K. Schleich, D. Witt, and E. Woolgar, “The AdS / CFT correspondence conjecture and topological censorship,” *Phys. Lett.* **B505** (2001) 255–262, [arXiv:hep-th/9912119 \[hep-th\]](#).
- [26] H. W. J. Bloete, J. L. Cardy, and M. P. Nightingale, “Conformal Invariance, the Central Charge, and Universal Finite Size Amplitudes at Criticality,” *Phys. Rev. Lett.* **56** (1986) 742–745.
- [27] L. Susskind, “ER=EPR, GHZ, and the consistency of quantum measurements,” *Fortsch. Phys.* **64** (2016) 72–83, [arXiv:1412.8483 \[hep-th\]](#).
- [28] J. Maldacena, D. Stanford, and Z. Yang, “Diving into traversable wormholes,” *Fortsch. Phys.* **65** no. 5, (2017) 1700034, [arXiv:1704.05333 \[hep-th\]](#).

- [29] L. Susskind and Y. Zhao, “Teleportation Through the Wormhole,” [arXiv:1707.04354 \[hep-th\]](#).
- [30] I. Kourkoulou and J. Maldacena, “Pure states in the SYK model and nearly- AdS_2 gravity,” [arXiv:1707.02325 \[hep-th\]](#).
- [31] A. Almheiri, A. Mousatov, and M. Shyani, “Escaping the Interiors of Pure Boundary-State Black Holes,” [arXiv:1803.04434 \[hep-th\]](#).
- [32] H. Li and F. D. M. Haldane, “Entanglement spectrum as a generalization of entanglement entropy: Identification of topological order in non-abelian fractional quantum hall effect states,” *Physical review letters* **101** no. 1, (2008) 010504.
- [33] X.-L. Qi, H. Katsura, and A. W. Ludwig, “General relationship between the entanglement spectrum and the edge state spectrum of topological quantum states,” *Physical review letters* **108** no. 19, (2012) 196402.
- [34] K. V. Kuchar, “Geometrodynamics of Schwarzschild black holes,” *Phys. Rev.* **D50** (1994) 3961–3981, [arXiv:gr-qc/9403003 \[gr-qc\]](#).
- [35] D. Bagrets, A. Altland, and A. Kamenev, “SachdevYeKitaev model as Liouville quantum mechanics,” *Nucl. Phys.* **B911** (2016) 191–205, [arXiv:1607.00694 \[cond-mat.str-el\]](#).
- [36] D. Bagrets, A. Altland, and A. Kamenev, “Power-law out of time order correlation functions in the SYK model,” *Nucl. Phys.* **B921** (2017) 727–752, [arXiv:1702.08902 \[cond-mat.str-el\]](#).
- [37] D. Stanford and E. Witten, “Fermionic Localization of the Schwarzian Theory,” *JHEP* **10** (2017) 008, [arXiv:1703.04612 \[hep-th\]](#).
- [38] I. R. Klebanov and E. Witten, “AdS / CFT correspondence and symmetry breaking,” *Nucl. Phys.* **B556** (1999) 89–114, [arXiv:hep-th/9905104 \[hep-th\]](#).
- [39] G. Cacciapaglia, G. Marandella, and J. Terning, “Dimensions of Supersymmetric Operators from AdS/CFT,” *JHEP* **06** (2009) 027, [arXiv:0802.2946 \[hep-th\]](#).
- [40] S. W. Hawking and D. N. Page, “Thermodynamics of Black Holes in anti-De Sitter Space,” *Commun. Math. Phys.* **87** (1983) 577.
- [41] E. Witten, “Anti-de Sitter space, thermal phase transition, and confinement in gauge theories,” *Adv. Theor. Math. Phys.* **2** (1998) 505–532, [arXiv:hep-th/9803131 \[hep-th\]](#).
- [42] J. S. Cotler, G. Gur-Ari, M. Hanada, J. Polchinski, P. Saad, S. H. Shenker, D. Stanford, A. Streicher, and M. Tezuka, “Black holes and random matrices,” *Journal of High Energy Physics* **2017** no. 5, (2017) 118.

- [43] G. Tarnopolsky, “On large q expansion in the Sachdev-Ye-Kitaev model,” [arXiv:1801.06871 \[hep-th\]](#).
- [44] A. Eberlein, V. Kasper, S. Sachdev, and J. Steinberg, “Quantum quench of the sachdev-ye-kitaev model,” *Physical Review B* **96** no. 20, (2017) 205123.
- [45] G. T. Horowitz and J. Polchinski, “Selfgravitating fundamental strings,” *Phys. Rev.* **D57** (1998) 2557–2563, [arXiv:hep-th/9707170 \[hep-th\]](#).
- [46] A. M. García-García, B. Loureiro, A. Romero-Bermúdez, and M. Tezuka, “Stability of chaos in a generalised Sachdev-Ye-Kitaev model,” [arXiv:1707.02197 \[hep-th\]](#).